

3. SITE 319

The Shipboard Scientific Party¹

SITE DATA

Location: Bauer Deep
Dates Occupied: 4-16 January 1974
Time on Site: 284.5 hours (11.85 days)
Position: 13°01.04'S; 101°31.46'W
Water Depth: 4296 meters (drill pipe)
Penetration:
Hole 319: 116.5 meters
Hole 319A: 157 meters
Number of Cores:
Hole 319: 14
Hole 319A: 7
Total Length of Cored Section: 175.5 meters
Total Core Recovered: 99.33 meters
Percentage Core Recovery: 57%
Oldest Sediment Cored:
Depth below sea floor: 110 meters
Nature: Metalliferous nannofossil ooze
Age: Early Miocene (N8)
Velocity: 1.57 km/sec
Basement:
Depth subbottom:
Hole 319: 110 meters
Hole 319A: 98 meters
Nature: Basalt
Velocity: 6.0 km/sec
Principal Results: Four meters of Quaternary metalliferous calcareous clay and ooze at the surface overlie 22 meters of Miocene-Pliocene metalliferous calcareous clay and ooze, 50 meters of middle Miocene light nanno ooze, and 34 meters of middle and early Miocene metalliferous ooze. The oldest sediments above basalt are in foram Zone N8. The basalt is relatively fresh, as evidenced by high velocity and low water content. Three cooling units in Hole 319 are probably pillows, with glass recovered only from the base of the uppermost unit. Hole 319A reached basalt 12 meters higher than Hole 319 and cored 59 meters of basalt in at least five cooling units.

BACKGROUND AND OBJECTIVES

Geologic Setting

The Bauer Deep is the depression between the active East Pacific Rise on the west and the extinct Galapagos Rise on the east (Figure 1; Heath et al., 1973; Herron, 1972). The East Pacific Rise at 11°S consists of a north-northeast-trending central topographic block 15-20 km wide and 300 meters high rising to an average depth of 2700 meters; this is flanked by block-faulted ridges aligned parallel to the rise crest (Figure 2). Magnetic anomalies indicate a spreading whole-rate of 16.0 cm/yr (Rea, 1975).

This rugged terrain, which contains very little sediment, increases in depth eastward to an abrupt scarp at 104°20'W, 13°S. At this scarp, the terrain changes from an average depth of 3700-3900 meters to low, rolling hills at 4200 meters; some troughs in this area are as deep as 4600 meters. To the east, the terrain is higher and more rugged, rising onto the west flank of the fossil Galapagos Rise.

Magnetic data in much of this region are difficult to interpret due to large diurnal variations and proximity to the magnetic equator. Estimates of age are based on scattered magnetic data together with the suggestion of Sclater et al. (1971) that depth is a function of age. Information from the present East Pacific Rise indicates that it emerged on the west flank of the old Galapagos Rise 6-8 m.y. ago (Anderson and Halunen, 1974; Rea, 1975). The Galapagos Rise probably became inoperative at about this same time. According to the Sclater age-depth curve, the age of crust at Site 319 is estimated as 20-25 m.y.

Crust in the Nazca plate is somewhat thinner than in other Pacific areas, with higher velocities (Hussong et al., 1972; Johnson et al., 1973). A sub-Moho layer with velocities approaching 9 km/sec at depths less than 15 km is found throughout most of the northern part of the plate (Hussong et al., 1973). Refraction data show that, for crust older than 2 m.y., crustal velocities decrease with increasing age, but mantle velocities increase. The plate appears to be in isostatic compensation except at the Peru-Chile Trench (Rose and Couch, 1973).

Both the East Pacific Rise crest and the Bauer Deep contain metalliferous sediments. These are characterized by (a) high transition metal to aluminum ratios (Dymond et al., 1973); (b) mineralogy dominated by goethite, nontronite, and manganese hydroxyoxides (Eklund, 1974); (c) sulfur, uranium, and oxygen isotopic compositions consistent with formation from seawater at low temperature (Dymond et al., 1973; Bender et al., 1971); (d) Sr-isotopic compositions suggesting equilibration with seawater (Dasch et al., 1971; Bender et al., 1971); (e) Pb-isotopic compositions similar to those of

¹Robert S. Yeats, Ohio University, Athens, Ohio (Co-Chief Scientist); Stanley R. Hart, Carnegie Institution of Washington, Washington, D.C. (Co-Chief Scientist); James M. Ade-Hall, Dalhousie University, Halifax, Nova Scotia; Manuel N. Bass, Carnegie Institution of Washington, Washington, D.C.; William E. Benson, National Science Foundation, Washington, D.C.; Roger A. Hart, Physical Research Laboratory, Ahmedabad, India; Patrick G. Quilty, West Australian Petroleum Party Ltd., Perth, West Australia; Harvey M. Sachs, Case Western Reserve University, Cleveland, Ohio; Matthew H. Salisbury, National Science Foundation, Washington, D.C.; T.L. Vallier, University of California at San Diego, La Jolla, California. Additional contribution by G. Blechschmidt, University of Washington, Seattle, Washington.

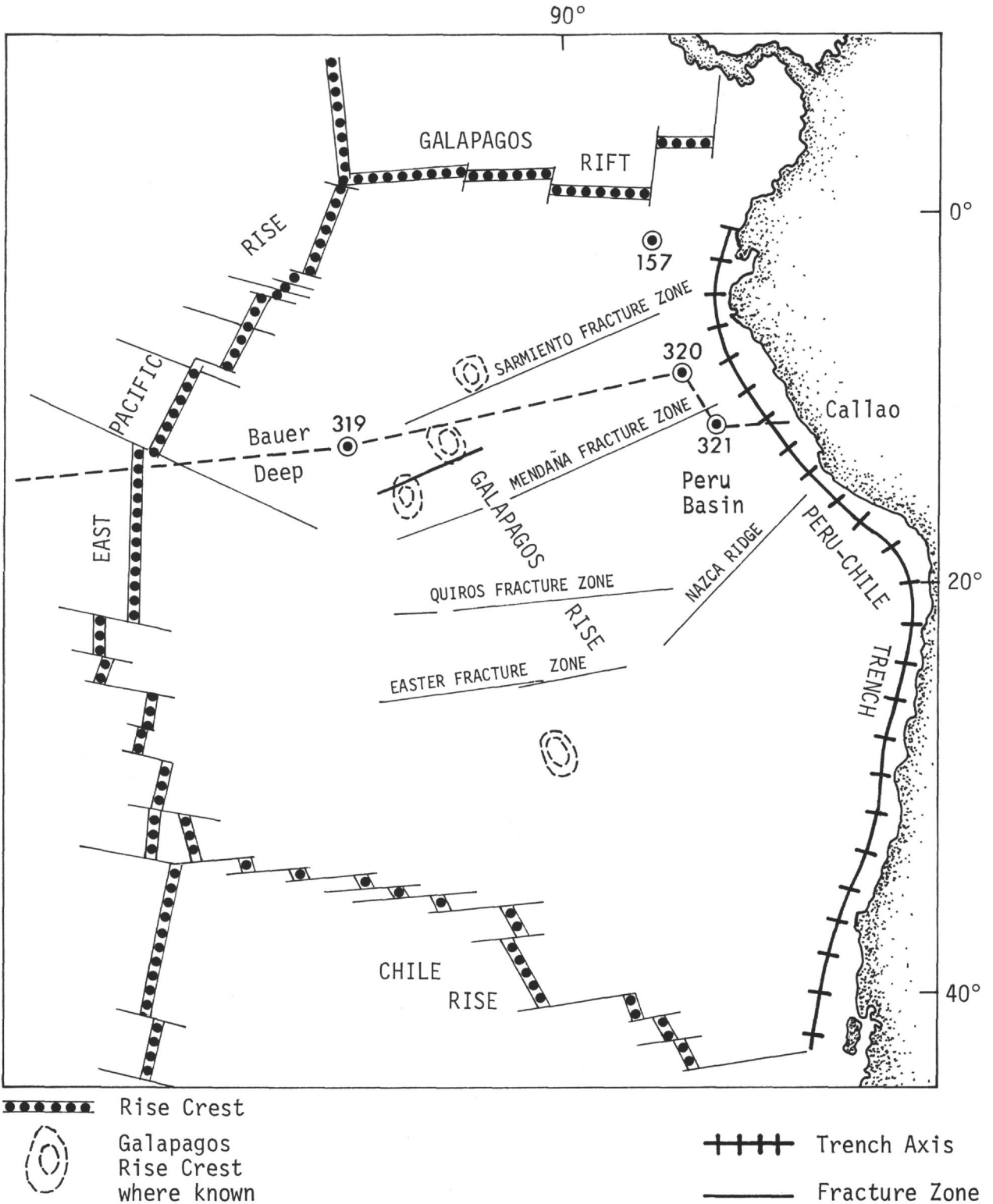


Figure 1. Location map of sites drilled during Leg 34.

mid-ocean ridge tholeiites (Dasch et al., 1971); and (f) REE patterns like those of seawater (Bender et al., 1971; Dymond et al., 1973; Corliss et al., 1972). Bauer Deep samples differ from East Pacific Rise samples by having

(a) lower Fe/Al and Mn/Al ratios, (b) higher Si and Ni contents, (c) greater abundance of poorly crystallized iron-rich montmorillonite, and (d) higher Ni:Fe ratios (Dymond et al., 1973). Dymond and Veeh (in press)

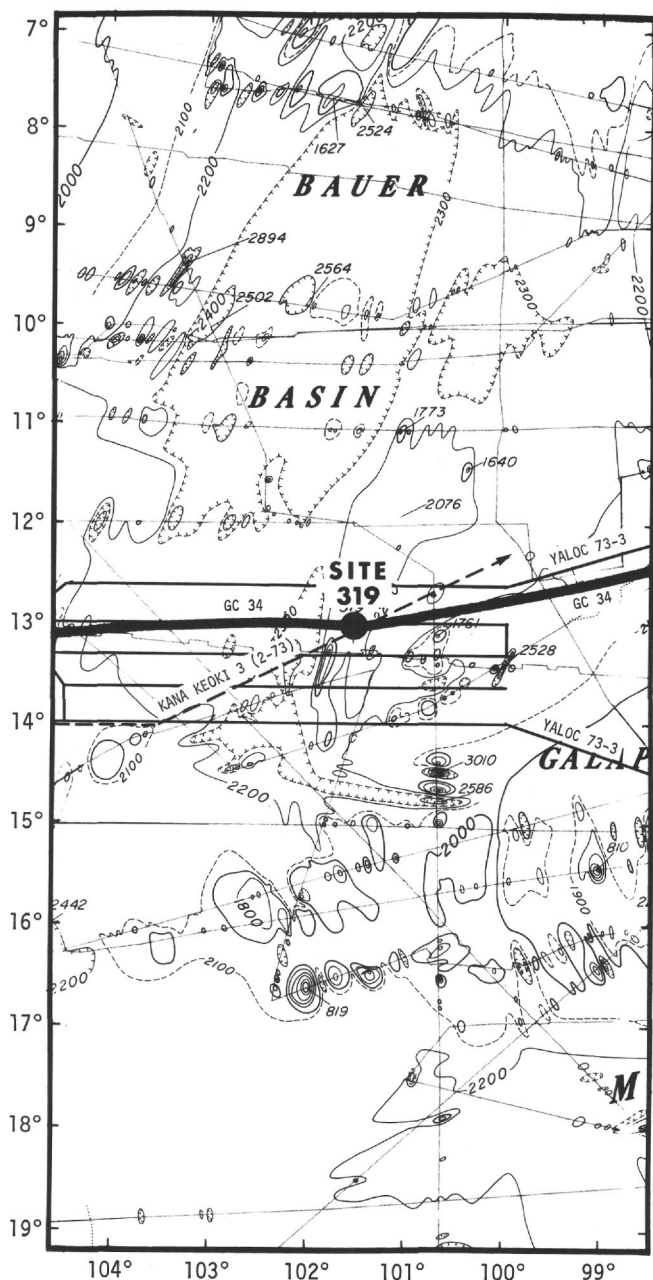


Figure 2. Regional setting of Site 319 based on bathymetry of Mammerickx et al. (1975).

ascribe the chemical differences largely to the higher content of iron-rich montmorillonite in the Bauer Deep samples. They consider that the similarities far outweigh the differences, that the differences are due to transport and/or local diagenetic conditions, and that the deposits of both areas have a common origin.

These observations are compatible with the precipitation of metals in the form of authigenic ferromanganese coatings and micronodules. The depletion of cerium and the volcanic character of the lead isotope ratios in the metalliferous sediments distinguish them from typical ferromanganese nodules. It has been suggested that the metalliferous sediments are precipitated from volcanic or hydrothermal emanations resulting from the interaction of seawater with new oceanic crust forming at the rise crest (Corliss, 1971). Metal enrichment in the Bauer

Deep may be due to transport of these metals from the rise crest; the longer time spent in seawater could account for the differences between Bauer Deep and East Pacific Rise metalliferous sediments.

The Bauer Deep is presently below the CCD. The shallowest piston cores with metalliferous sediments were taken at 4090 meters at Site 319; thus, the CCD is now above that depth. Some of the piston cores in the Bauer Deep recovered yellow-brown calcareous clay beneath the surficial metalliferous sediments.

The selection of Site 319 was based on a detailed survey of the Bauer Basin during *Yaloc-73*, Leg 3. It is in a basin about 8 km wide (east-west) at 13°00.8'S, which is part of a broadly faulted zone on the low western flank of the Galapagos Rise. Basins in the area are bounded by faults with vertical separations of 200-500 meters; seamounts up to 2000 meters above the general terrain level are locally present. The *Yaloc-73* survey shows about 0.12 sec (100 m) of sediment; 0.02 sec of nearly transparent sediment overlies thinly layered sediment, which itself overlies nearly transparent sediment.

Objectives

The objectives of Site 319 were (1) to determine the history of sedimentation and particularly of metalliferous sedimentation in the Bauer Deep, (2) to determine the geochemistry of metalliferous sediments below the surface and compare it with that of metalliferous sediments from the rise crest, and (3) to penetrate basement as deeply as possible using the re-entry cone.

OPERATIONS

Site Survey

Site 319 was selected from the *Yaloc 73-3* detailed survey of the Bauer Deep from 12°50' to 14°S and 100° to 105°W (Figures 3, 4, and 5). It is the largest basin in this survey area containing a sediment sequence thick enough to support the bottom-hole assembly for coring basalt. The site was crossed on an easterly heading, and a box survey was made around the site in order to determine the size and orientation of the basin.

Like the *Yaloc 73-3* profile, the *Glomar Challenger* profile shows a series of closely spaced reflectors near the surface of the basin, underlain by a transparent, homogeneous sequence, which lies on a basement surface of moderate topographic relief. Based on the airgun profiles, total sediment thickness is 0.11 sec at the site and over most of the basin, which would be 110 meters at $V_p = 2.0$ km/sec and 90 meters if $V_p = 1.6$ km/sec. Mudline depth below sea level based on PDR was estimated at 4290 meters (corrected, using Matthews tables, Area 41), as compared to 4311 meters (corrected) from the *Glomar Challenger* airgun profile and 4313 meters (corrected) from the sonobuoy record. Apparently, the mudline consists of sediments which reflect weakly if at all at airgun frequencies. For more details concerning the Site 319 area, see Yeats and Heath (this volume).

A sonobuoy was launched at 1937 hr (local time) on 5 January, and 4 hr 36 min of sonobuoy records were obtained. During this period, the sonobuoy drifted 3.173 km from the ship at a heading of 275°.

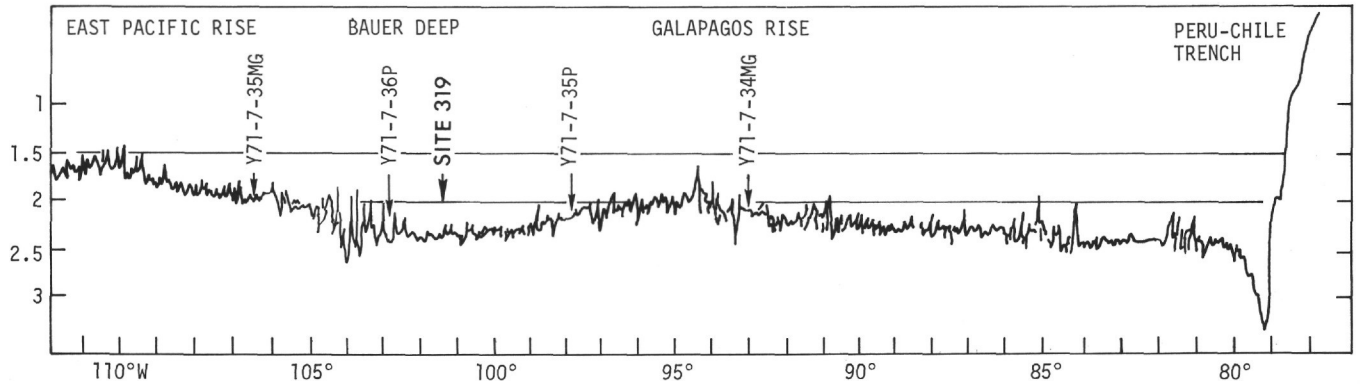


Figure 3. Bathymetric profile of the Nazca plate from the crest of the East Pacific Rise to the Peru-Chile Trench at 10°-11°S. Depth scale is in thousands of fathoms, assuming velocity of sound in seawater of 800 fm/sec (after Heath et al., 1973).

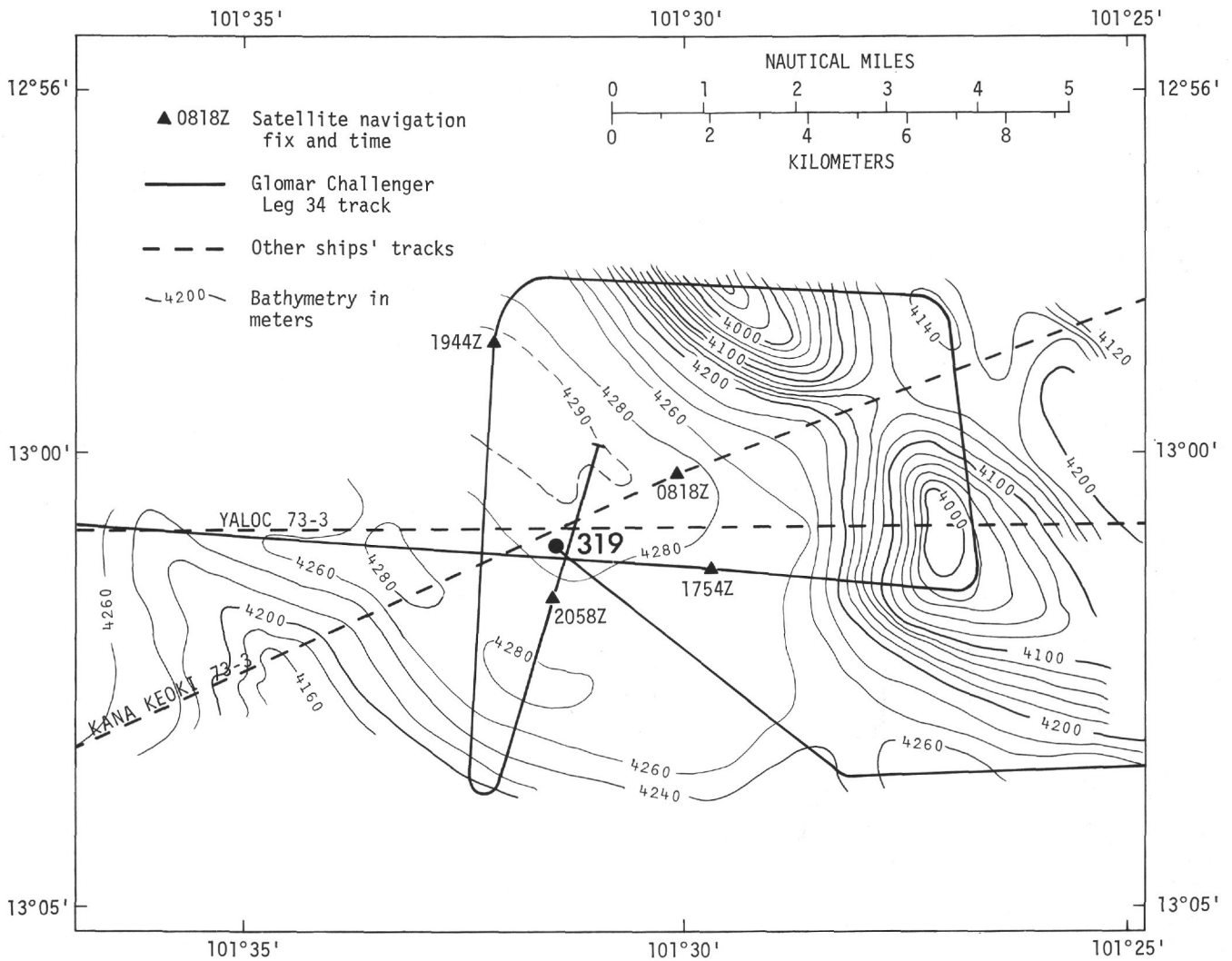


Figure 4. Bathymetry around Site 319 based on the tracks of Yaloc-73, Leg 3, Kana Keoki-73, Leg 3, and Glomar Challenger, Leg 34. Depths are in meters, corrected by using Matthews tables, Area 41.

Drilling Program

Hole 319

Drill pipe was run to the mudline at 4296 meters, the heave compensator installed in the passive mode, and

the hole spudded at 0900 hr (local time) on 5 January. Fourteen cores were taken (summarized in Table 1). Ship's heave during coring was 2 to 5 feet, as seen on the heave compensator. Despite the heave compensator and calm seas, the sediment cores were highly disturbed.

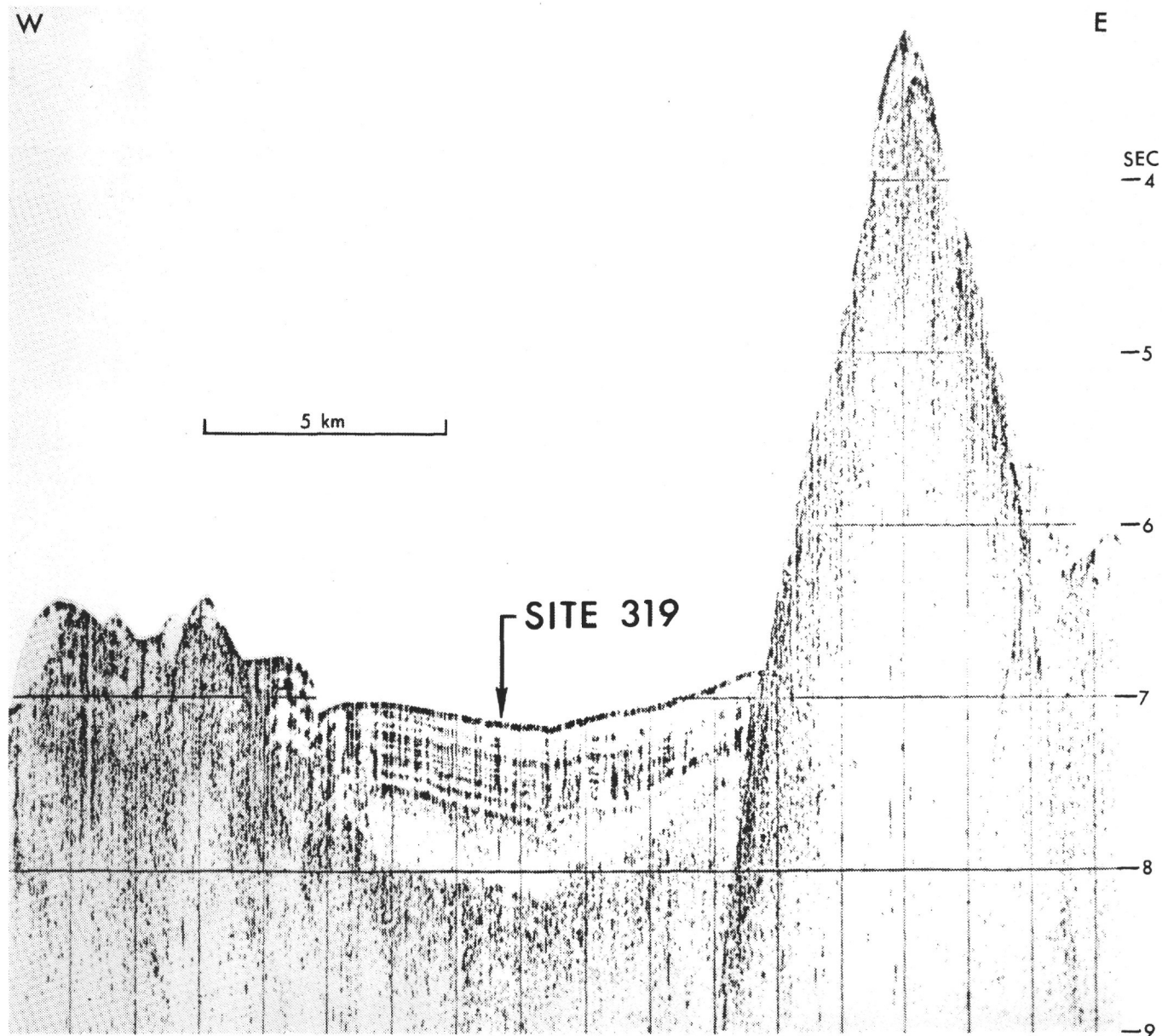


Figure 5. 3.5-kHz reflection profile across Site 319 made during Yaloc-73, Leg 3.

Heat-flow measurements were taken at 4343.5 and 4372 meters. The first heat-flow probe gave the better data. The second run showed a continuous rise in temperature which may have been friction induced because the bit was lowered frequently to maintain thermal contact between the probe and the sediments.

The top of the basalt is best placed at 4406 meters; the hard drilling in the last 1.5 meters of Core 12 is assumed to be basalt. Light bit weight (10,000 to 15,000 lb), slow rotation, and low pump pressure were used to try to recover the sediment-basalt contact in Core 12, but recovery was 3.5 meters sediment and no basalt. Core 13 in basalt was taken with 20,000 lb bit weight, 40 rpm rotary, and 5-6 rpm pump, but drilling was slow with high torque, as on Core 12, and the barrel was pulled after 3 meters. It was obvious from the cylindrical shape

of the core than a rat-hole into the basalt had been made. Core 14 was taken with the oriented core barrel. The core orientation photographic device worked satisfactorily, but recovery was poor, and the scribe marks could not be found on the core. The hole reached total depth (TD) at 2030 hr (local time) 6 January.

Hole 319A

The drill string was pulled and the re-entry cone and mud-cross assembly keelhailed. The mud cross was a new device designed to prevent cuttings from building up inside the cone during drilling. The ability to remove cuttings from the hole is a function of pump pressure (which controls fluid flow rate in the annulus between the drill collars and the hole), fluid viscosity (drilling mud is more effective than salt water), and cross-

TABLE 1
Coring Summary, Site 319

Core	Time on Deck	Depth From Derrick Floor (m)	Depth Below Mudline (m)	Depth Below Top Basalt (m)	Recovery (m) (%)	Remarks
Hole 319						
1	1015 (5 Jan)	4296.0-4305.5	0-9.5		9.4 99	Top of core took weight
2	1145	4305.5-4315.0	9.5-19.0		5.5 58	Full heave comp., no pump or rotation
3	1305	4315.0-4324.5	19.0-28.5		3.5 37	No heave comp., no rotation or pump
4	1434	4324.5-4334.0	28.5-38.0		9.3 98	Full heave comp., rotation, pump last 4 meters
5	1618	4334.0-4343.5	38.0-47.5		8.0 84	Heave comp., rotation, pump last 2 meters
6	0100 (6 Jan)	4343.5-4353.0	47.5-57.0		8.6 91	Heave comp., rotated and pumped
7	0230	4353.0-4363.5	57.0-66.5		9.2 97	Heave comp., rotated and pumped
8	0410	4362.5-4372.0	66.5-76.0		6.5 68	Heave comp., rotated and pumped
9	0830	4372.0-4381.5	76.0-85.5		4.2 44	Heave comp., rotated and pumped
10	1015	4381.5-4391.0	85.5-95.0		6.9 73	Heave comp., rotated and pumped
11	1145	4391.0-4400.5	95.0-104.5		9.3 98	Heave comp., rotated and pumped
12	1347	4400.5-4407.5	104.5-111.5	0-1.5	3.5 50	Last 1.5 meters slow and hard; no basalt recovery
13	1744	4407.5-4410.5	111.5-114.5	1.5-4.5	0.8 27	1 hr 40 min to drill 3 meters full heave comp.
14	2130	4410.5-4412.5	114.5-116.5	4.5-6.5	0.1 5	5-meter barrel with core orientation; heave comp.
Hole 319A						
1	1700 (9 Jan)	4394.0-4403.5	98.0-107.5	0-9.5	1.1 12	Heave comp. on
2	0130 (10 Jan)	4403.5-4413.0	107.5-117.0	9.5-19.0	2.9 26	Tight hole after cutting core
3	0740	4413.0-4422.5	117.0-126.5	19.0-28.5	7.3 77	Changed bits after cutting core
4	1432 (13 Jan)	4422.5-4424.5	126.5-128.5	28.5-30.5	0.6 30	1 hr reaming hole
5	0200 (14 Jan)	4424.5-4434.0	128.5-138.0	30.5-40.0	1.1 12	30 min reaming hole; 5 hr. 20 min repairing Bowen power sub
6	0745	4434.0-4443.5	138.0-147.5	40.0-49.5	0.5 5	45 min reaming hole
7	1150	4443.5-4453.0	147.5-157.0	49.5-59.0	1.0 11	35 min reaming hole; 1 hr 45 min rotating time on core

sectional area. As the cuttings emerge from the casing into the larger cross-section of the cone, fluid carrying capacity decreases, raising the possibility that cuttings would build up within the cone and cause fill in the hole. The mud cross was intended, in effect, to extend the small cross-sectional area to the top of the cone, where three conductor pipes would carry the cuttings outside the cone.

After a day spent keelhauling the cone and mud cross and running casing, Hole 319A was spudded at 0030 hr (local time) 9 January and the 13-3/8 in. casing was washed in from 4296 to 4362.5 meters. The hole was drilled to basalt at 4394 meters, 12 meters higher than in Hole 319. A coring summary is shown in Table 1.

After cutting Core 2, the pipe became stuck and had to be worked free. After cutting Core 3, one of the cables securing the mud cross to the moon pool broke, and it was decided to come out of the hole after 14 hr coring time on the bit. The ship moved 1000 feet west of station to jettison the mud cross.

Re-entry was accomplished after considerable operational difficulties which took over 2 days. These difficulties were mainly due to (1) hangup of the EDO scanning tool due to small clearance between the tool and the bit throat, (2) failure of some of the circuits within the scanning tool, and (3) poor video on the 45° scanner (although video on the 8° scanner was good).

Drill pipe was run to 4383 meters. It was necessary to wash in from 4383 to 4413 meters and to ream to bottom at 442.5 meters. Cores 4 through 7 were cut and retrieved, with considerable problems due to a tight hole and stuck pipe, despite circulating the hole with mud. The Bowen power sub motor had to be replaced after Core 5. Core barrel 8 was dropped, and while working the pipe to bottom, the motor and transmission on the Bowen power sub froze again when the pipe stuck. The pipe was worked free and the Bowen sub repaired. The core barrel was retrieved (with a considerable amount of basalt drill cuttings and a punch core presumably from the base of the sediments), and a center bit run. The hole was washed and reamed from 4366 to 4453 meters and circulated clean with mud. The core barrel was dropped, but the pipe became stuck again, and the decision to abandon the hole was made. The pipe was worked free and the drill string retrieved, and the site was abandoned at 1210 hr (local time) 16 January.

Best coring was found in the massive basalt in Core 2 and 3. Below this, the basalt was finer grained and highly fractured, so that the core consisted of small rounded joint blocks of basalt. Drusy vugs and zones of alteration along fractures and the tendency of cores to break along fractures suggest that the fractures were zones of weakness which permitted pieces of basalt to fill in the hole and become wedged against the drill

collars. The drill cuttings consisted predominantly of fine-grained, altered basalt and basalt glass; glass was only rarely found in the cores themselves. Apparently, the small joint blocks of fine-grained basalt, together with the glassy selvages, comprised most of the material that fell into the hole. Open fractures which constitute zones of weakness probably remain open in part due to the low lithostatic pressure imposed by the small thickness of sediment overburden, and in part due to insufficient time to seal the old and any newly formed cracks with vein deposits.

Slow coring rates were also due to the relative freshness of the basalt, among the freshest materials yet drilled during the Deep Sea Drilling Project. Basalts which are overlain by a thick sediment cover and are more highly altered should allow faster penetration rates.

LITHOLOGY

Description of Units: Sediments

The sedimentary section in Hole 319 has been divided into four major lithostratigraphic units (Table 2, Figure 6), with no major gaps apparent. The sediment units, which overlie basalt (Unit 5), are described from top to bottom.

Unit 1: Iron-rich Brown Clay (Core 1, 0-4 m)

The top 4 meters of Core 1 consist of dark reddish-brown (5YR 2.5/2) ferruginous clay. Carbonate content is generally less than 10% and consists largely of angular grains of calcite and sparse coccoliths which show dissolution effects. Zeolite crystals (probably phillipsite) are common and make up from 3% to 10% of the material. Other than the zeolites and the larger of the ferruginous grains, the coarse fraction is apparently from a volcanic source and comprises 1% to 3% of the unit. It consists of plagioclase, a few grains of pitted quartz, fish teeth, minor glass, and a sparse suite of heavy minerals, chiefly biotite with very small amounts of colorless clinopyroxene and orthopyroxene. The clay is colorless to yellow-brown smectite.

The most striking feature of the unit is the ferruginous grains that constitute 10% to 15% of the core. They are

yellow-brown to dark reddish-brown, isotropic, and apparently amorphous, ranging in size from a few microns to more than 100 microns. The larger grains appear to be aggregates. Although similar material has been described in other marine sections, these ferruginous grains lack an accepted name. For convenience in this report we call them "red brown semiopaque oxides" ("RSOs"). RSOs are essentially free of Fe^{+2} and are thought not to be responsible for the magnetization of sediments.

Unit 2: Iron-bearing Calcareous Brown Clay and Clayey Nanno Ooze (Cores 1 to 3, 4-28.5 m)

Unit 2 is essentially a 24-meter-thick transition unit between the ferruginous clays of Unit 1 and the clay-poor nanno ooze of Unit 3. Individual beds consist of: (a) iron-rich brown clay similar to Unit 1; (b) iron-bearing calcareous brown clay with an RSO content of 5% to 10% and a carbonate content greater than 30%; and (c) yellow-brown clay-rich nanno ooze with an RSO content of 1% to 4%. In general, clay and RSO contents decrease and carbonate increases with depth, but numerous reversals of these trends occur.

Unit 3: Nanno Ooze (Cores 3 to 8, 28.5-76 m)

Near the base of Core 3 the clayey ooze grades into nanno ooze, which, despite its color (various shades of light to medium yellow browns), is remarkably pure. Clay content reaches 15% in a few beds, especially in the upper 10 meters, but is generally 10% or less. The coloring is caused largely by a few percent of the RSOs, which are omnipresent, although in much smaller amounts than in the other units.

Unit 4: Iron-bearing Nanno Ooze (Cores 8 to 12, 76-110 m)

The bottom 34 meters of Hole 319 consists of a low-clay nanno ooze, similar to that of Unit 3 except the colors are darker and the RSO content is higher, generally 5% to 10%. The color values correlate directly with the RSO content, which is as low as 3% in the lightest and as much as 15% in the darkest beds. The darkest colors and highest RSO concentrations are between 76 and 85 meters and between 95 and 104

TABLE 2
Lithostratigraphic Summary, Site 319

Unit	Subbottom Depth (m)	Lithology	Core	Age
1	0-4	Iron-rich brown clay	1	Quaternary and Pliocene
2	4-28.5	Iron-bearing calcareous brown clay, clay-rich nanno ooze, and minor iron-rich brown clay	1-3	Pliocene to middle Miocene
3	28.5-76	Nanno ooze and foram-rich nanno ooze	3-8	Middle Miocene
4	76-110	Iron-bearing nanno ooze	9-12	Early and middle Miocene
5	110-116.5	Basalt	12-14	?

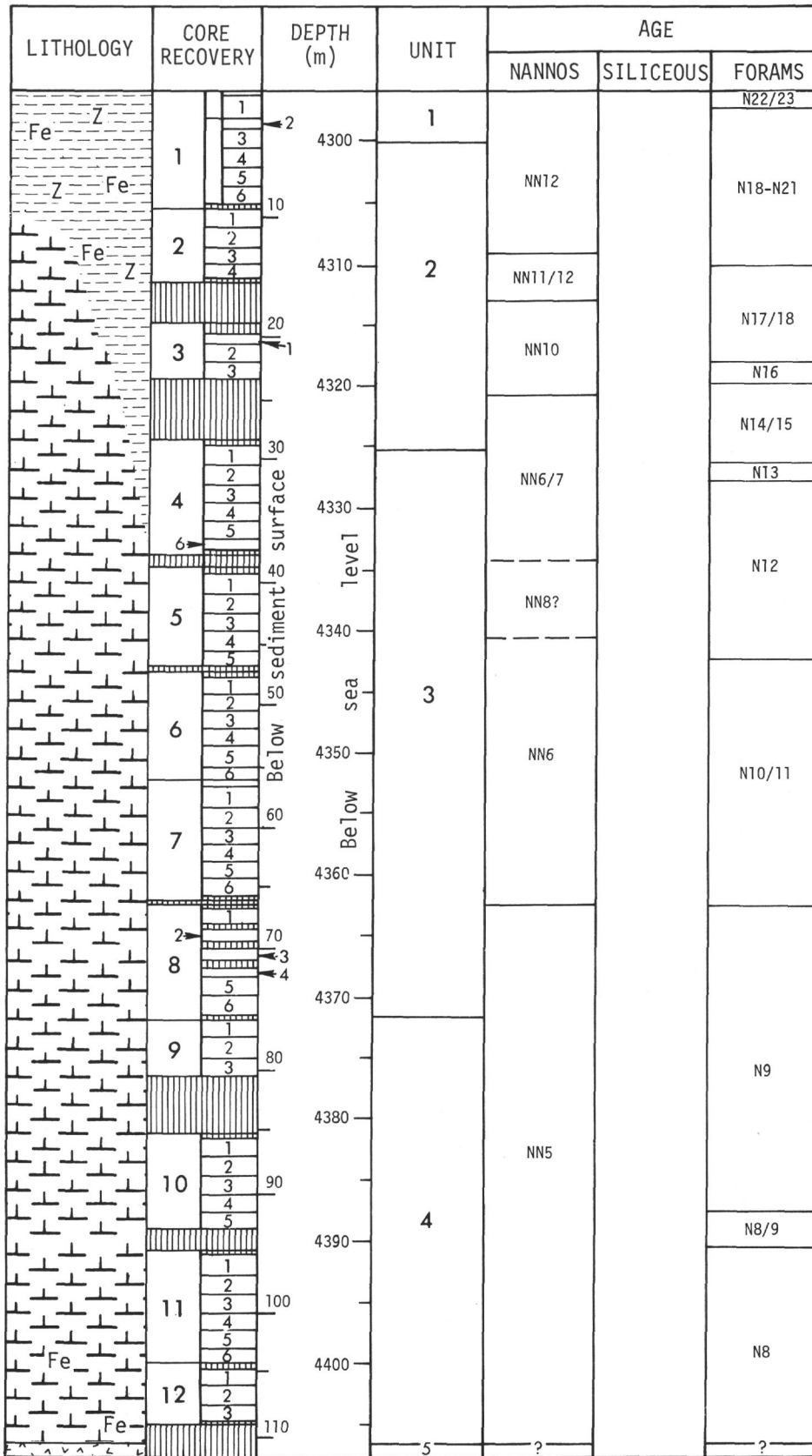


Figure 6. Stratigraphic column, Hole 319.

meters. There is no apparent increase in RSO content in the bottom 6 meters.

Discussion of Sediments

Three features of the sediments of Site 319 are noteworthy. These are:

1) Exogenous volcanic minerals: As noted above, 1% to 3% of Unit 1 is a coarse fraction, apparently from a volcanic source, that consists of plagioclase, some potassium feldspar, a colorless clinopyroxene, orthopyroxene, biotite which may be partly altered to smectite, clear, high-silica glass, and quartz. The minerals are fresh except for some of the biotite. The same assemblage is present in Units 2-4 in reduced amounts. The percentage of these volcanic materials seems to be inversely related to sedimentation rates, indicating a nearly constant sedimentation rate for these volcanic constituents alone. The composition of the suite suggests andesitic or dacitic derivation, and the small but steady supply of the materials suggests a large and fairly distant source area. As Site 319 lies in the belt of southeast trade winds, the andesitic volcanoes of the Andes chain would seem the likely parents, although some mid-ocean center such as Easter Island cannot be ruled out.

2) Dissolution effects and the absence of opaline silica: The forams and nannofossils show strong dissolution effects in Unit 1 and some such effects in Unit 2. Evidently the site passed through the lysocline at about the time of deposition of Unit 2. It cannot be determined whether this was due to sinking of the Bauer Deep or to raising of the CCD.

The virtual absence of opaline silica, except for a very few robust, corroded diatoms and rads, is noteworthy. A few calcified specimens of what seem to be Radiolaria were seen in the nanno ooze of Unit 3. We infer that rads and diatoms were present in the original biota, but that depositional or postdepositional conditions promoted the dissolution of silica during most of the sedimentary history of the Bauer Deep.

3) Metalliferous sediments of the Bauer Deep: All the sediments cored at Site 319 contain at least traces of metalliferous particles (RSOs). For a thorough discussion see Boström et al. and Dymond et al. (this volume). They reach high concentrations in the upper 26 meters and lower 34 meters, but no sample was devoid of them; even the middle 50 meters of lighter colored ooze averages 1% or 2% (visual estimates).

The three types of RSOs distinguished in this volume are as follows:

1) Red semi-opaques. These are yellow-red to red-brown, translucent to opaque, mostly isotropic, but locally birefringent. They tend to be equidimensional with irregular edges and variable in size with the mean between 10μ and 15μ .

2) Yellow flakes and spherules. These are light yellow, reddish-yellow, and yellow-brown in color and are all translucent. The spherules are invariably isotropic; some of the flakes are isotropic, although some show slight birefringence. Size range is from about 10μ down to the limit of resolution ($\sim 2\mu$). In general, the darker colors are characteristic of the larger grains, and they seem to form a continuous series with type 1.

At least the lighter colored flakes are probably similar to the "smectite" of Dasch et al. (1971).

3) Aggregates. These are dark red to black in color and semi-opaque to completely opaque. They range in size from less than 20μ to more than 100μ . Dark colors and opacity vary directly with size, and the darkness of the larger particles may be due to size alone or may result from higher concentrations of iron and manganese oxides. They correspond, at least in part, to the aggregates of Cronan et al. (1971) and von der Borch et al. (1971) and are probably the micronodules of Dasch et al. (1971).

Although all three types of RSOs occur throughout the section, they are not distributed uniformly. The aggregates dominate Unit 1 and parts of Unit 2. They decrease rapidly downward from the top of Unit 3 and are present only in trace amounts in the entire bottom half of the core, even in the darker iron-bearing oozes of Unit 4. The red semi-opaques and the yellow flakes are common in both the upper (Units 1 and 2) and lower (Unit 4) parts of the section; they are rare in the middle. Yellow spherules are more abundant in Unit 5 than in the upper units. Finally, as noted in the lithologic description, there is no relative basal enrichment just above the basalt. RSOs are abundant throughout Unit 4 and reach their highest concentrations in beds between 76 and 85 meters and between 95 and 104 meters.

The greater abundance of RSOs in Unit 4 as compared with Unit 3 must be due to a relatively high primary supply of these grains. Both Units 3 and 4 are nanno ooze and have approximately the same high sedimentation rate of 3 meters to 4 meters per million years. If RSOs are of hydrothermal origin, their abundance in Unit 4 probably reflects the proximity of an active ridge crest.

The concentration of RSOs in Units 1 and 2 may be accounted for by changes in the rates of sedimentation. From very low concentrations in most of Unit 3, the RSOs and the clay content increase rather sharply near the top of the unit; the RSO increase is about an order of magnitude. This increase coincides with an abrupt drop in the sedimentation rate to about 0.23 m/m.y. (an order of magnitude lower than in the lower units). As most of the lower part of Unit 2 was evidently deposited above the CCD, this change in rate would appear to be caused by a sudden decrease in carbonate productivity. Whatever the cause, the change in rate alone could account for the apparent tenfold increase in RSOs between Unit 3 and Unit 2. Similarly, the still higher RSO content of Unit 1 coincides with the zone of carbonate dissolution, after the Bauer Deep passed through the CCD. On the other hand, we note also that the RSOs of the upper units tend to be dominated by what we call the "aggregates," which virtually overwhelm the other types in the upper meter or so. This would imply either that the RSOs of the upper part of the section were from a new source, or, more likely, that the aggregates are the result of diagenetic changes due to increasing length of exposure time before burial.

Description of Units: Basalt

Hole 319 bottomed in relatively fresh basalt, based on high sonic velocity and low water content. Three cooling

units, probably pillows, were encountered, with glass found only at the base of the uppermost unit. Hole 319A reached basalt 12 meters higher than Hole 319. Fifty-nine meters of basalt were cored in Hole 319A, comprising at least five cooling units up to 15.6 meters thick. Core recovery was best in massive basalt with widely spaced joints and veins, and poorest at cooling unit contacts and in thin cooling units where textures change abruptly and joints are closely spaced. Only two glass selvages were recovered, although drill cuttings in core catches suggest that glass selvages probably are common.

The basement surface rocks in Holes 319 and 319A are microphyric basalts with both plagioclase and olivine phenocrysts and clinopyroxene microphenocrysts. Despite the proximity of the two holes, it is not possible to correlate the uppermost units. Hole 319 sampled three cooling units in a cored distance of 6-7 meters, whereas the uppermost unit recovered at Hole 319A was a single cooling unit approximately 7 meters thick. The mineralogies and textures of rocks from the two holes are essentially identical, however, and the basement surface is probably a relatively uneven and laterally complex series of related flows and pillows. Irregularities in the basement surface are indicated by the 12-meter difference in basement depth at the two holes.

Joint spacing varies widely and was a major factor in core recovery and the sizes of individual core pieces. Evidence that the fractures are true joints (extension fractures probably related to cooling) and not faults (shear fractures) includes the presence of drusy crystals on fracture surfaces and the absence of slickensides or minor offset along fractures. The small joint blocks were probably fragments of pillows and marginal portions of thicker units. Their size on recovery was approximately their in situ size, as indicated by the correspondence of internal weathering zones with external shape. In the interiors of the thicker units, the joint spacing is wider, up to 15-30 cm, resulting in better core recovery and smoother drilling conditions.

The primary mineralogy of the rocks consists of olivine, clinopyroxene, plagioclase, titanomagnetite, sulfide, ilmenite, and rare chromian spinel. Olivine occurs as phenocrysts and microphenocrysts in the coarser grained rocks. Opaque minerals occur only rarely in the olivine, suggesting that the olivine grew in a fractionated magma in which chromian spinel was no longer crystallizing and in which the titanomagnetite had not yet started crystallizing. Persistence of olivine crystallization into the groundmass of these tholeiitic rocks confirms that chemically they lay initially on the olivine-plagioclase cotectic and progressed during crystallization to the three-phase olivine-plagioclase-augite cotectic. Clinopyroxene ranges from metastable (?) pigeonite in spherulites of quenched marginal rocks to normal augite in the more slowly cooled interior rocks. In the coarse rocks, the late, small grains in or near quenched groundmass appear optically to include pigeonite and subcalcic augite. The augite is light brown, and commonly shows wavy extinction, hourglass sector zoning, or a remarkable zoning in

which radially oriented sectors extinguish step-wise or continuously (depending on the fineness of the sectors) in such a manner that an extinction band sweeps fan-like across the grain. Such sector zoning is probably in part of compositional origin, but may also have evolved by filling-in of early spherulites. If so, the zoning indicates rapid cooling and may provide a criterion that the rocks are from flows rather than sills in which such metastable textures would have been annealed. In some rocks augite occurs as microphenocrysts, showing that the magmas had reached the three-phase olivine-plagioclase-pyroxene cotectic prior to eruption. Plagioclase occurs as phenocrysts showing weak or oscillatory zoning, with strong normal zoning at the very edges. The composition of the earliest plagioclase ranges from An_{60} to An_{80} . The phenocrysts near the top of the thicker flow units tend to be more sodic, suggesting sinking of early formed crystals and later growth of more sodic phenocrysts after emplacement. The groundmass plagioclase occurs as normally zoned laths, which are typically skeletal, not only in quenched rocks but also in the mesostases of coarser grained rocks. Such quenching of late liquid in the most slowly cooled portions of the units sampled again supports an origin as flows or shallow sills rather than deeply intruded sills.

Titanomagnetite and its oxidized equivalents are always the dominant opaque phase in the Site 319 basalts. Titanomagnetite usually shows skeletal form, indicating rapid cooling. In the massive basalts, subhedral grains also occur. Grain sizes range from $1/4\mu$ to 100μ . Ilmenite occurs sporadically in the massive basalts, amounting to a maximum of 40% of the magnetite volume. Sulfides are ubiquitous but are always a minor opaque constituent in terms of abundance. Pyrite and pyrrhotite are the commonest sulfides, with rarer chalcopyrite and cupriferrous pyrrhotite.

Both high and low temperature alteration processes have affected the opaque phases. Mild high temperature (deuteric) oxidation of titanomagnetite led to ilmenite exsolution from magnetite in two massive basalt samples. Rather common partial high temperature oxidation of pyrrhotite globules has led to a degree of replacement of pyrrhotite by pyrite, together with the formation of magnetite rims around the globules.

The most widespread alteration process is the low-temperature oxidation of titanomagnetite, leading to the formation of the cation-deficient phases collectively known as titanomaghemite. All pillow basalt samples have highly cation-deficient oxide phases while some massive basalts have also experienced this alteration process. Slight cation deficiency causes the mild development of volume change cracks. With cation deficiency in excess of 0.6 on a 0 to 1 scale, color lightening, increased reflectivity, expulsion of surplus iron into surrounding silicates, and the replacement of the oxide by a dull gray silicate phase all become apparent. The calibration of alteration states observed with the microscope has been achieved by comparison with rock magnetism measurements on the same samples.

Many of the textures in the cooling units of Site 319 are those commonly observed in submarine basalts: glass, grading through a zone of isolated spherulites,

then to coalesced spherulites which coarsen inward to a variolitic texture and, ultimately, in the coarser units, to ophitic and subophitic textures. Several unusual and interesting textures were also noted. One is a reverse quenching phenomenon observed in the pyroxenes, wherein the early, rapidly quenched crystallites of pyroxene spherulites coarsen outwards to nonskeletal, intergranular pyroxene with a "slower-growth" appearance. The second is the recurrence of quench spherulitic pyroxene in the mesostases of even the coarsest parts of the thickest diabasic units. The spherulites, which appear to be essentially identical to those in the glass selvages, indicate a late return to conditions of severe undercooling, high viscosity, or both. Three causes may be suggested: a late acceleration of cooling as the latent heat of crystallization of the small, rapidly decreasing amount of residual magma failed to compensate heat losses from the margins of a cooling unit; an increase of viscosity due to desiccation of the residual hydrous magma due to crystallization of late magmatic biotite (and amphibole ?); and quenching due to an influx of seawater into cooling cracks that penetrated deeply into the rigid crystal network in which the late magma pockets were encased. The desiccation cause is self-reinforcing, so that, once started, it could trigger the formation of quench smectite of the type so commonly seen experimentally in hydrous basalt systems. The late spherulites, like the strongly zoned pyroxenes, and the late highly skeletal plagioclase and titanomagnetite, strongly support the inference that the rocks from Site 319 are from flows, not sills.

While the basalts at Site 319 are among the freshest reported by the Deep Sea Drilling Project, they do record an interesting and complex history of low temperature alteration. The most consistently altered material is the mesostasis of all rocks, both fine and coarse grained, which is typically replaced by extremely fine grained smectite (part of which is conceivably of quench origin in coarse-grained rocks). Palagonite rinds are common on glass surfaces, and the olivines are normally altered to a coarser grained smectite, which has in the past been frequently misidentified as chlorite or serpentine. Low temperature oxidation of titanomagnetite produces cation-deficient phases known collectively as titanomaghemite. Pyroxene and plagioclase are essentially unaltered throughout the units.

Two environments of alteration can be distinguished, in addition to that in which the early palagonite formed by direct exposure to seawater. A nonoxidizing environment resulted in the alteration of mesostasis and olivine to green to blue smectite. Simultaneously, smectite, pyrite, and marcasite were deposited as veins in which the carbonate was largely in the form of aragonite and relatively high-Mg calcite. An oxidizing environment, which affected rock previously altered by the nonoxidizing processes, resulted in the alteration of any remnant olivine to Fe-oxide pseudomorphs and of previously formed green smectites to red, yellow, and brown smectites which now appear to be essentially colorless smectite spotted in varying degrees with dusty Fe-oxide. Secondary micas are probably celadonites formed during the oxidizing alteration. The late oxidizing episode

also led to the formation of very fine grained, Fe-stained veins of low-Mg calcite. While both alteration facies are believed to have been initiated early, before any significant thickness of sediment was deposited, they are nonetheless thought to be of low temperature and not deuteric origin, i.e., not related to the initial cooling of the units.

BIOSTRATIGRAPHY

Benthonic Faunas

All samples from core catchers contain benthonic faunas, including calcareous foraminifera, echinoid spines, and rare ostracodes. It is thus possible that all sediments accumulated above the CCD and that the sediments were later depressed to their present position after deposition.

Samples from sediments above Core 1, Section 3 have virtually all of the useful calcareous fossils removed. The only benthonic element consists of a few agglutinated foraminifera.

Planktonic Faunas

Throughout the sediments of Leg 34, the warm water planktonic foraminiferal zonation of Blow (1969) is applicable and the details are given in more depth by Quilty (this volume). Faunas in most cores are well preserved and abundant, but some evidence of dissolution and reworking is present at several levels.

The top three sections (0, 1, 2) of Core 1 are barren of planktonic foraminifera. Sections 3-6 and the core catcher contain reduced faunas due to obvious dissolution effects. Faunas are late Miocene to early Pliocene in age but do not allow greater differentiation at the time of writing. Cores 3 and 4 (Sections 1 and 2 only) contain an apparently condensed N13-N17/18 sequence, without many species of zonal index significance. Ages are based mainly on gross faunal characteristics.

All deeper cores are early or middle Miocene in age with zone index species common. N12 encompasses Core 4, Section 3 to Core 6, Section 6. The *Globorotalia fohsi* series is well represented. N10/11 (undifferentiated) is present in Sample 6, CC to Core 7 (all sections). The *Orbulina* datum is in Core 10, Section 4 and marks the base of N9. *Globigerinatella insueta*, *Globigerinoides sicanus*, and *Praeorbulina glomerosa curva* establish the N8 age of sediments below Core 10, Section 4.

Calcareous Nannoplankton

Sections 1 and 2 of Core 1 are barren of calcareous nannofossils. A moderately well preserved late Miocene assemblage including *Ceratolithus tricorniculatus*, *Discoaster brouweri*, and *Discoaster pentaradiatus* appears in Section 3 of Core 1. This assemblage was also found in Core 2. Core 3 yielded late Miocene calcareous nannofossils which are characteristic of the *Discoaster calcaris* Zone (NN10). Nannofossils in this core and in the remainder of the cores are abundant, moderately well preserved, and dominated by solution-resistant taxa. Discoasters are generally overcalcified, thereby making identification difficult. Cores 4, 5, 6, and 7 contain middle Miocene nannofossils including *Discoaster*

exilis. Cores 5 and 6 show signs of reworking with some elements of the *Sphenolithus heteromorphus* Zone (NN5) appearing in an assemblage dominated by taxa characteristic of the *Discoaster exilis* Zone (NN6). Cores 8 through 12 contain early to middle Miocene nanofossils including abundant *Sphenolithus heteromorphus* and a few discoasters of the "*Discoaster deflandre* group."

SEDIMENTATION RATES

Deposition at Site 319 appears to have been continuous since late in the early Miocene (N8) until the Recent (N23), although no faunas younger than N18 were identified. Stratigraphic control in the early and middle Miocene indicates that calcareous ooze accumulated at a rate of 30-40 m/m.y. (Figure 7).

Calcareous benthonic faunas (echinoids, foraminifera) and planktonic foraminifera are common into the Pliocene (e.g., 319-1-4) indicating that the apparent marked decrease in sedimentation rate (which coincides with a marked reduction in carbonate percentages) may be due wholly or in part to carbonate dissolution effects. The time at which the area was depressed into a carbonate dissolution regime is not known with certainty but would be approximately late Pliocene-Pleistocene.

There is no evidence from any "nearby" holes (e.g., Leg 33 holes) to suggest a diminution in the rate of organic productivity in the vicinity. If this is true, the approximately 35 meters of late Miocene and younger metalliferous clays, which accumulated slowly, may represent the condensed section of up to 350 meters original section of similar composition to the early and middle Miocene ooze of Cores 4-12.

GEOCHEMICAL MEASUREMENTS

Geochemical measurements on sediments and interstitial waters (pH, alkalinity, salinity, and calcium carbonate) are made routinely on *Glomar Challenger*. For the first time, during Leg 34, measurements of water and calcium carbonate contents were made on basalt samples. Data not reported here are available from the Deep Sea Drilling Project.

A total of 10 "mini-cores" was taken at subbottom depths ranging from 3.0 to 107.5 meters. The pH values (electrode technique) ranged from 7.48 at 6 meters to 7.57 at 107.5 meters, compared with a surface seawater pH of 8.15. Surface water alkalinity was 2.39 meq/kg. Alkalinity of the interstitial water was higher, beginning with 2.91 meq/kg at 3 meters, jumping to 3.22 meq/kg at 6 meters, then decreasing to 2.6 meq/kg at 46 meters, rising to 2.87 meq/kg at 64.4 meters and then staying around 2.8 meq/kg to the bottom of the sediments. Surface seawater salinity is 35.2 ‰. The interstitial water salinity is 34.4 ‰ in the surface sediments. Below 22 meters it increases to a high of 34.9 ‰ at 64.4 meters and then decreased to 34.4 ‰ at 97.9 meters.

Calcium carbonate contents measured on the ship by the "carbonate bomb" method are comparable to those obtained at the DSDP shore laboratory (see the core forms in this site report chapter and Cameron, this volume) and are not reproduced here.

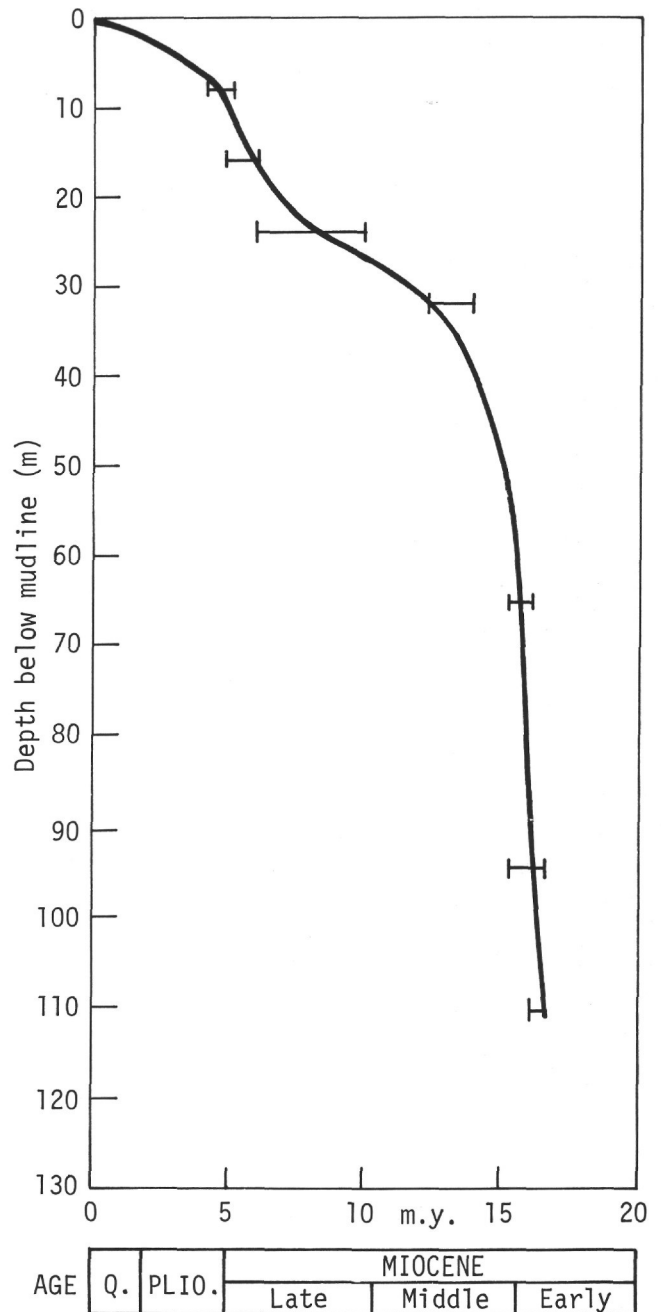


Figure 7. Sedimentation rate diagram, Hole 319.

Thirty-four analyses of H₂O and CaCO₃ were made on basalts from Site 319. Twenty-six samples were subsequently analyzed on shore (Table 3). Compared to H₂O values on other DSDP cores, values on Site 319 basalts are lower than normal. In fact, a number compare favorably with fresh rocks dredged from oceanic ridges (Hart, 1973).

PHYSICAL PROPERTIES

Measurements of wet-bulk density, porosity, sonic velocity, and thermal conductivity were made at closely spaced intervals in the recovered sediment column. These properties, together with electrical resistivity and

TABLE 3
H₂O and CO₂ Contents of Site 319 Basalts

Sample (Interval in cm)	CO ₂ (%)	H ₂ O Total (%)
Hole 319		
13-1, 59-64	0.07	0.30
13-1, 77-78	0.26	0.54
13-1, 140-143	0.25	0.91
Hole 319A		
1-1, 48-51	0.26	0.84
1-1, 139-142	0.22	0.55
2-1, 27-30	0.11	0.44
2-1, 111-114	0.20	1.34
2-2, 114-117	0.27	1.36
2-3, 86-89	0.08	1.42
2-3, CC	0.25	1.37
3-1, 78-81	0.21	0.97
3-2, 14-17	0.27	0.81
3-2, 127-130	0.34	1.04
3-3, 36-39	0.30	0.97
3-3, 106-109	0.30	1.18
3-4, 18-21	0.31	0.92
3-4, 100-103	0.29	0.91
3-5, 37-41	0.34	0.88
3-5, 75-78	0.25	0.96
4-1, 129-132	0.30	1.09
5-1, 20-22	0.39	1.59
5-1, 76-79	0.26	1.11
6-1, 84-89	0.16	0.88
6-1, 93-98	0.15	1.03
7-1, 119-122	0.34	1.30
7-1, 121-124	0.29	1.10

with the exception of thermal conductivity, were measured on the basalt. Magnetic studies were conducted on both sediment and basement samples. Compilations of these data, given with the subsequent core descriptions, present a remarkably simple column which reflects the lithology and geophysics at the site.

The upper 35 meters of sediment displays a steady increase in wet-bulk density, sonic velocity, and thermal conductivity (from 1.14 to 1.64 g/cc, 1.51 to 1.53 km/sec, and 1.53 to 2.51 mcal/cm sec°C, respectively) which is largely controlled by a decrease in porosity in this interval from 91 to 61 volume percent. Though it is possible that the high porosities measured in samples from this level were imparted by drilling disturbance, it is felt from geophysical evidence that similarly high porosities exist in situ at this site. A steady change in lithology from Fe-rich metalliferous clays at the mudline through calcareous nanno oozes toward the base of the interval exerts a secondary control on sonic velocities, the steady increase in CaCO₃ content contributing to the observed increase in velocity with depth. Acoustic impedance increases with depth at Site 319 in response to increasing wet-bulk density and velocity.

From 35 meters to basement, the measured physical properties are for the most part monotonously uniform with wet-bulk density, porosity, sonic velocity, and thermal conductivity averaging 1.72 g/cc, 58%, 1.57 km/sec, and 2.77 mcal/cm sec°C, respectively.

The underlying basalts at Holes 319 and 319A are remarkable in several respects. Their high average density, 2.92 g/cc, ranks them among the densest basalts

reported during the DSDP program to date. Furthermore, no change in density is observed with depth. The scatter in measured densities (2.84-3.01 g/cc) is rather small and fails to show correlation with any other feature, even with obvious discoloration features associated with fractures and joints. Consistent with this, measured seismic velocities are high (averaging 6.0 km/sec) even at atmospheric confining pressure. These observations all suggest that submarine alteration has not proceeded beyond an early stage, a finding consistent with the density-age relation of Salisbury and Christensen (1973) and the age of the site (15-17 m.y.) as determined from the oldest overlying sediments.

Fifty-nine sediment thermal conductivity measurements and two in-hole temperature determinations were made for Hole 319. Thermal conductivity was measured with the shipboard digitized system which allows measurements to be made concurrently at up to five different positions. Generally, four of the available positions were used for sediment measurements and the fifth for a conductivity standard having a conductivity of 2.84 ± 0.10 mcal/cm sec°C. Conductivity values range from 1.61 to 4.00 mcal/cm sec°C, with 36 of the values between 2.00 and 2.99 mcal/cm sec°C, and the arithmetic mean is 2.72 mcal/cm sec°C. There is a rise from a mean value of close to 2.0 units, characterizing the top 35 meters of the section, to about 2.7 units that characterizes most of the rest of the section. The thermal conductivity increase with depth is explained by the decrease of porosity with depth, based on the inverse relationship between porosity and conductivity.

Two in-hole temperature measurements were attempted, one at 47.5 meters and the other at 76 meters (subbottom depths). In each case, the down-hole instrument was fitted with a 19-in. (48.26 cm) extender and a 2-3/4-in. (7.0 cm) probe. A major difficulty encountered during the measurement period was the inability of the very soft sediments to maintain the weight of the drill string after lowering to bottom. In order to maintain thermal contact with undisturbed sediments the bit was lowered slightly once during the measurement cycle at 47.5 meters and 12 times during the cycle at 76.0 meters. Essentially complete temperature recordings, including good mud line temperatures, were obtained on both runs.

The only means available for estimating heat flow at the site is by comparing the mud line and 47.5-meter temperatures. The mud line temperature is well defined at 1.8°C giving a temperature difference of 1.6°C over 47.5 meters. The harmonic mean thermal conductivity over the topmost 47.5 meters of the sediment section is 2.22 mcal/cm sec°C giving an apparent heat flow over this interval of 0.80 mcal/cm²sec. This value is significantly less than the average of 1.54 HFU for the 5° × 5° region which includes the site, as given by Langseth and von Herzen (1971). However, inclusion of some high East Pacific Rise values in an average is likely to make their figure a doubtful guide to Bauer Deep heat flow.

MAGNETISM OF THE BASALT AND SEDIMENTS

The paleomagnetic properties of 15 vertically oriented samples of basalt from this site were measured in a

program combining shipboard and shore-based laboratory work (see Ade-Hall and Johnson, Paleomagnetism of Basalts, Leg 34, this volume, for details). Both pillow and massive basalts are represented among the measured samples.

Paleomagnetic directions, after alternating field cleaning, are uniformly steep downwards, with a mean inclination of $+54 \pm 4^\circ$ (standard deviation of the mean). This inclination represents the geomagnetic field at the site during the period of lava eruption. The close grouping of inclinations indicates that eruption of the penetrated sequence took place over a relatively short time, probably less than 1000 yr. The steep inclination contrasts with the centered axial dipole field inclination of 25° for the present latitude of the site. A number of explanations for this difference are viable based on evidence from the basalts alone, including large latitudinal plate motion. However, the cleaned magnetization of the overlying sediments, which represent well the average geomagnetic field shortly after the eruption of the lavas, indicates that negligible latitudinal plate motion has taken place over the last 13 m.y. (see Ade-Hall and Johnson, Paleomagnetism of Sediments, Leg 34, this volume, for details). For this reason the steep basalt inclination is interpreted as a record of a geomagnetic field excursion, rather than evidence for absolute plate motion.

While the fine-grained pillow basalts were little affected by the drilling and recovery procedures, the coarse-grained basalts became strongly remagnetized during this process, assuming inclinations close to vertically upwards. In this state, the coarse-grained massive basalts are as much as two orders of magnitude more strongly magnetized than the pillow basalts. Correction for this drilling-induced magnetization still leaves the massive basalts as the main contributors to the magnetization of the section. A weighted average NRM intensity for the Site 319 section, allowing for the preferential recovery of massive basalts, is $17 \pm 6 \times 10^{-4}$ emu/cm³. This is significantly lower than values used in modeling linear anomaly patterns, but is based on too short a section to be taken as representative of Layer 2 in the area of the site. Induced magnetization contributes negligibly to overall magnetization.

Rock magnetism studies of the Site 319 basalts indicate that the original titanomagnetite had a restricted composition which averaged 0.61 Fe₂TiO₄ 0.39 Fe₃O₄. As a result of the extensive halmyrolysis of the basalts, only a few samples of massive basalt still contain stoichiometric titanomagnetite. The remaining massive basalts and all the pillow basalts now contain cation-deficient titanomagnetite, or titanomaghemite. Permissible replacement of Fe²⁺ by Fe³⁺ is as high as 0.96, a degree of cation deficiency attainable and stable only very close to ambient temperatures. Cation deficiency in titanomagnetite has a strong influence on most of the magnetite properties of the basalts. For example, NRM intensity, when compensated for magnetite abundance and grain size effects, decreases by a factor of 20 as cation deficiency increases from 0 to 0.8. Initial susceptibility and saturation magnetization also decrease sharply with increasing cation deficiency.

CORRELATION OF REFLECTION PROFILE WITH DRILLING RESULTS

The extensive airgun survey conducted on approaching the site and the airgun-sonobuoy profile initiated immediately after stabilization over the positioning beacon suggest a simple structure for the Bauer Deep: a single 0.11-sec thick (2-way), acoustically transparent sedimentary unit with a thin zone of multiple reflectors at its top underlain by a strongly reflecting basement. Due to distortion of the sonobuoy record by rising basement topography along the line of the sonobuoy profile (azimuth 275°), it is not possible to determine the velocity structure of the sediments using standard sonobuoy techniques and the record is not portrayed. (The T²-X² traces of the sediment and basement reflectors are effectively parallel, suggesting, at best, only that the sediment velocities are very slow.)

There is a 0.03-sec. (2-way time) discrepancy between corrected PDR sediment arrival times and the corrected sediment arrival times using the airgun source. The arrival of the PDR signal (14 kHz), 0.03 sec before the airgun signal (80-320 Hz) suggests the presence of a thin 0.03-sec-thick layer, which is acoustically transparent to low frequencies and lies stratigraphically above the 0.11-sec-thick layer. This was confirmed by drilling; the mudline was near the PDR rather than the airgun sea-floor depth (Table 4).

Correlation of the observed reflection structure at Site 319 with the cores recovered and the measured physical properties profile is straightforward. The 0.03-sec sub-bottom reflection interval corresponds to the low-density, low-velocity transition zone between metaliferous clay and nanno ooze at the top of the column. The low acoustic impedance of this unit is consistent with its transparency at low frequencies. The underlying 0.11-sec-thick reflection interval corresponds to the relatively thick, uniform basal nanno ooze unit cored at Site 319.

The site reflection profile-core recovery correlation discussed above is confirmed by computation of reflector depths from the physical properties data. A plot of depth versus averaged inter-core and alternate inter-core reflectivity coefficients, computed from the impedances and the reflectivity relation

$$R = \frac{Z_1 - Z_2}{Z_1 + Z_2}$$

where R = reflectivity and Z_n = acoustic impedance of layer n , indicates the presence of three prominent reflectors, one at the water-sediment interface, one at a sub-bottom depth between 25 and 35 meters, and the strong basement reflector at 110 meters (the PDR, airgun, and basement reflectors, respectively).

Using a total sediment travel time thickness of 0.14 sec and a drilled sediment interval of 110 meters, the mean compressional wave velocity of the sediment column is approximately 1.57 km/sec, in agreement with core velocities measured on ship using the Hamilton frame. The agreement between computed and measured velocities is excellent.

TABLE 4
Site 319 Reflection Intervals From PDR,
Airgun and Sonobuoy Surveys

Subbottom 2 Way Time Interval (sec)	Evidence
0-0.03	PDR, drill recovery
0.03-0.14	Airgun survey, airgun- sonobuoy survey

SUMMARY AND CONCLUSIONS

Site Survey

The survey of Site 319 by *Glomar Challenger* showed that the topography of the Bauer Deep in this area has a northwest-southeast structural grain (Figure 4). This contrasts with the north to north-northeast structural grain of the East Pacific Rise at this latitude. The bathymetric map of the southeastern Pacific by Mammerickx et al. (1975) shows the Galapagos Rise to consist of several northwest-trending ridges which are offset by northeast-trending fracture zones (Figure 2). The survey of the Bauer Deep by the R/V *Yaquina* of Oregon State University, cruise *Yaloc 73-3*, consisting of east-west tracks at 20-nautical mile intervals, achieved poor topographic correlation from track to track, possibly because the topography trends at an acute angle to the track lines. This structural parallelism in the Bauer Deep with the Galapagos Rise suggests that the Bauer Deep is related to spreading from the Galapagos Rise prior to the onset of spreading at the East Pacific Rise. The sharp change in spreading direction from the Galapagos Rise (NE-SW) to the East Pacific Rise (WNW-ESE) may mean that the two ridges never spread at the same time, as might be inferred from the age-depth relation of Sclater et al. (1971), but that spreading from the East Pacific Rise began only after the Galapagos Rise became extinct as suggested by Anderson and Halunen (1974) and others.

The basin in which Site 319 is located contains a thin, relatively undeformed sedimentary sequence overlying a basement surface with at least 50 meters (0.66 sec) of topographic relief (Figure 5) that may be primary volcanic topography. However, the ridges that flank the basin are also covered by sediments up to 50-60 meters in thickness and are strongly linear, suggesting that basin boundaries are controlled by block faulting. The thinner sediment cover on the ridges implies either that the ridges were block faulted prior to the deposition of the youngest sediments in the Bauer Deep, or that bottom currents transported some fine-grained ooze from ridge to basin throughout the time of deposition. The composition of young sediments sampled by piston cores on both ridges and basins reflects the present-day CCD, and no older sediments are known to crop out at the surfaces of ridges or basins; therefore, block faulting could not have taken place prior to deposition of these young sediments, and the bottom current transport hypothesis is more likely. It is logical to conclude that the northwest-trending terrain, presumably controlled by faulting, developed near the rise crest, based on analogies with modern rise crests.

Sediments

The sediments of the Bauer Deep that have high concentrations of metalliferous components are restricted to the surficial few meters deposited during the Quaternary. Yet metalliferous components are present throughout the section. The upper metalliferous sediments were deposited at a rate of 2.3 m/m.y., whereas the underlying nanno ooze of middle and early Miocene age (from about 30 to 110 m below the surface) was deposited at a rate of 28-42 m/m.y., more than an order of magnitude higher. The decrease in metalliferous component concentration downward from the surface is accompanied by an increase in CaCO₃ content as well as an increase in sedimentation rate (at about 28 m depth), indicating that the lower amount of metalliferous components is caused by dilution by calcareous fossils and that the sedimentation rate of metalliferous components remains approximately the same for about the upper two-thirds of the section. The sedimentation rate of CaCO₃ decreases up-section partly because the area subsided below the CCD in the late Pliocene-Pleistocene and also because of decreased productivity. Dissolution effects in calcareous fossils are limited to the uppermost 11 meters (Pliocene and younger), whereas the major change in sedimentation rate of CaCO₃ is around 28 meters.

The bottom 34 meters of sediment have a higher concentration (5%-15%) of metalliferous components than the middle 50 meters (generally less than 5%), although total sedimentation rates in both units are the same. Thus, the accumulation rate of metalliferous components was highest during deposition of the lower part of the core, three or four times higher than for higher parts of the core, suggesting that the accumulation rate for these components is strongly influenced by proximity to an active spreading center, in this case, the extinct Galapagos Rise. However, there is no basal enrichment in metals just above the basalt; highest concentrations are found in beds at 76-85 meters and 95-104 meters.

Also, the metalliferous components (red-brown to yellow-brown, semi-opaque oxides, or RSOs) are different in the upper and lower portions of the core. Dark red to black, opaque to semi-opaque aggregates from 20 to 100 μ in size dominate the upper 26 meters, but are relatively unimportant below. Yellow-red to red-brown semi-opaques, 10 to 15 μ in size, and small yellow flakes are common in the upper and lower parts of the section, rare in the middle. Isotropic yellow spherules are most abundant in the lower 34 meters. Evidently, the RSOs from the upper part of the section were from a new source, or, more likely, the differences are the result either of diagenetic changes, or of differing durations of exposure time to seawater.

A striking feature of the fossil assemblage is the virtual absence of opaline silica, including diatom and radiolarian tests. The few diatoms and rads found are robust types, and all are corroded. Apparently, siliceous organisms were present in the original biota, but depositional or postdepositional conditions promoted the dissolution of silica throughout most of the sedimentary history of the Bauer Deep. Lack of opaline silica and evidence for dissolution of calcareous fossils in sur-

face sediments of the Bauer Deep have also been pointed out by Rosato et al. (in press).

The distribution of *Globoquadrina dehiscens* in the early and middle Miocene and the rarity of keeled *Globorotalia* (probably a warm water indicator) toward the base of the section suggest cooler water conditions than at present. High diversity of the planktonic fauna throughout most of the section suggests that any water temperature change is probably from warm temperate in the Miocene to tropical at present.

Basalt

The igneous rocks represent a suite of rapidly cooled basaltic rocks, probably flows with pillowed and massive portions, which were erupted in a fairly short interval of time (less than 1000 yr). On-shore chemical studies show that the basalts from Site 319, like all those cored during Leg 34, are low-K tholeiites with LIL-element (large-ion-lithophile) abundance patterns typical of those found in basalts on spreading ridges. Within this framework, however, the Leg 34 basalts tend to be relatively fractionated compared to typical MORB (mid-ocean ridge basalts), as indicated, for instance, by high Fe/Mg, relatively oxidized Fe, and relatively low Al_2O_3 (see summary chapter by S. Hart, this volume). Among the basalts from Site 319, this fractionation is expressed mineralogically by the presence of pigeonite and distinctly colored augites and the absence of chromian spinel. On the other hand, the absence of extreme fractionation is indicated by the presence of groundmass olivine, which indicates that the erupted magmas lay on the olivine-plagioclase cotectic or the three-phase olivine-plagioclase-augite cotectic.

Different degrees of fractionation among the Leg 34 basalts permit the recognition of five subgroups, of which two were recovered at Site 319, including the most "primitive" subgroup, which was cored in Hole 319 and in the upper part of the basement at Hole 319A. The lower part of the basalt cored in Hole 319A represents an intermediate subgroup. While major elements would allow derivation of the various subgroups by low-pressure crystal fractionation of a single parental magma, certain trace element concentrations and ratios require different primary magmas from mantle sources of slightly different trace element compositions. The eruption of the lower chemically intermediate magmas at Site 319, followed by the eruption of the upper, more "primitive," but not notably more porphyritic magmas, is difficult to reconcile with successive eruptions from a single, shallow, vertically differentiated magma chamber. Therefore, we must invoke either two or more chambers, of independent primary magmas from different mantle sources, presumably located at different depths below the crest of the ancient Galapagos Rise at the times of magma separation. The rapid (abrupt?) change of magma types in less than 1000 yr should help constrain our choice among the alternative explanations, and similar constraints at many sites will eventually elucidate the mechanics of spreading.

The possible presence of pigeonite, the absence of chromian spinel, and the distinctly colored augites suggest magmas considerably fractionated prior to erup-

tion, but the presence of groundmass olivine indicates that they nonetheless still lay on olivine-plagioclase or the three-phase olivine-plagioclase-augite cotectic.

The Site 319 basalts, despite the common alteration of olivine and mesostasis to smectite, appear unusually fresh from the point of water content, density, and sonic velocity compared to dredge basalts of similar age (15 m.y.). For example, the average water content of 15-m.y. dredge basalts is about 2.5%, compared to 1.0% (total H₂O released above 35°C) for Site 319 basalts. This might suggest that the Site 319 basalts are younger than the age assigned them based on the overlying sediment age. However, K-Ar radiometric ages determined in shore laboratories indicate a probably age of 15-20 m.y., in good agreement with the age of the oldest sediments. The relative freshness of Site 319 basalts may result from the overlying sediments acting as a seal or barrier to exchange with seawater. If this is a generally operable mechanism, however, it becomes difficult to explain why basement densities usually are found to decrease with increasing age of basement, even when covered with considerable thicknesses of sediment.

The average specific gravity of the units cored in Holes 319 and 319A is 2.93, based on 45 gravimetric determinations, and 2.92, based on 94 static GRAPE measurements. These values are comparable to those measured on normal unaltered subaerial basalts, and even the lowest values measured (2.85) are indicative of relatively fresh material. Similarly, the sonic velocities, which average 6.0 km/sec at atmospheric pressure and 6.1 km/sec at in situ pressure (0.5kb) are comparable to those measured on unaltered basalt. The trends of these parameters with depth in the core are relatively insignificant. Water contents are lowest near the surface and tend to increase slightly with depth, whereas density and sonic velocity show no overall trend with depth.

Paleomagnetic measurements on 15 oriented (vertical direction only) mini-cores, after suitable AC demagnetization, yielded rather consistent values for inclination, ranging from +38° to +66° with a mean value of +54±4°. The steep downward inclination of the stable magnetic components of the NRM is in sharp contrast to the present field inclination at the site of -13° and the centered axial dipole field inclination for the latitude of the site of -25°. There are several possible explanations for this difference. (1) The site was originally reversely magnetized while in the Southern Hemisphere or normally magnetized in the Northern Hemisphere. The location during flow extrusion and magnetization would have been ~35°N or S, which would require large plate motions to bring it to its present location. If the site was originally located in the Southern Hemisphere, this being the closest location to the present site, an average rate of motion over 15 m.y. of 20 cm yr⁻¹ is required to bring this segment of oceanic crust to its present position. Since the inclination in basalts at Site 320 is about normal for its present position (-25 ± 9°), and the inclinations in sediments from Site 319 are also approximately normal (-15 ± 6°), an explanation involving large plate motions seems unlikely at this point. (2) The extrusion of the lavas at Holes 319/319A occurred relatively rapidly and froze in a nonrepresentative sam-

ple of the geomagnetic field, either during a period of large secular variations or during a polarity transition. (3) Local tectonic tilting affected the crustal block sampled by Holes 319 and 319A, rotating the inclination by some 30° from its original position. While there is no evidence from the airgun records to indicate any overall tilting of the basement at the site, smaller scale rotation and slumping is difficult to rule out.

The intensity of remanent magnetization was measured on recovered samples and the in situ values estimated by calculation. The in situ intensities are 50% higher than the measured NRM intensities, and both values are in the middle of the large range of values measured on deep-sea basalts and estimated from the magnetic anomalies. At Hole 319, the intensities were highest in the coarser grained rocks and lowest in the finer grained marginal facies. This is in contrast to the previous studies which suggest that rapidly cooled pillows generally show the greatest intensity of magnetization. This obviously has important implications regarding the question of whether the oceanic magnetic anomalies arise dominantly from the upper pillowed surface of Layer 2 or originate from the coarser grained units within the layer.

The anomaly between measured sonic velocities and seismic refraction data should be pointed out. Though some ASPER lines in this part of the Nazca plate have been interpreted in terms of upper basement velocities as high as 6 km/sec, most interpretations of Layer 2 velocities, both on the Nazca plate and elsewhere, suggest much lower velocities. The discrepancy between seismic and laboratory-determined velocities can perhaps be resolved by appealing to a scale effect. Seismic velocities average relatively large crustal paths, including any intercepted joints, shear zones, breccia zones, and unconsolidated pillow zones and interlayered sediments. Laboratory values are generally biased toward samples of high physical integrity, both as a result of the coring process itself and due to the practical necessity of selecting unfragmented samples for measurement. This discrepancy may prove important in the construction of petrologic models for the oceanic crust when such models are based on the correlation of layer velocities with velocities measured in the laboratory on various rock types.

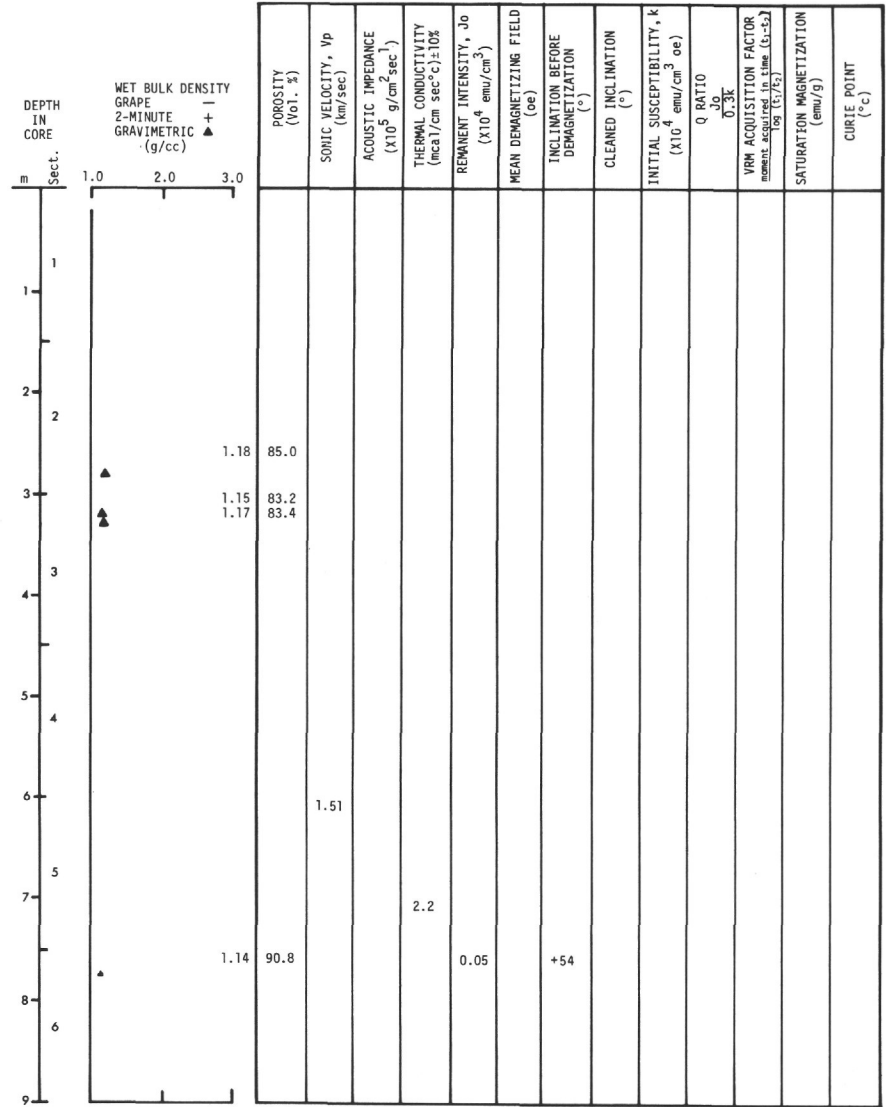
REFERENCES

- Anderson, R.N., and Halunen, J., 1974. Implications of heat flow for metallogenesis in the Bauer Deep: *Nature*, v. 251, p. 473-475.
- Bender, M., Broecker, W., Gornitz, V., Middel, V., Kay, R., Sun, S., and Biscaye, P., 1971. Geochemistry of three cores from the East Pacific Rise: *Earth Planet. Sci. Lett.*, v. 12, p. 425-433.
- Corliss, J.B., 1971. The origin of metal-bearing hydrothermal solutions: *J. Geophys. Res.*, v. 76, p. 8128-8138.
- Corliss, J.B., Graf, J.L., Skinner, B.J., and Hutchinson, R.W., 1972. Rare earth data from iron- and manganese-rich sediments associated with sulfide ore bodies of the Troodos Massif, Cyprus: *Geol. Soc. Am. Abstracts with Programs*, v. 4, p. 476-477.
- Cronan, D.S., van Andel, T.H., Heath, G. R., Dinkelman, M.G., Bennett, R.H., Bukry, D., Charleston, S., Kaneps, A., Rodolfo, K.S., and Yeats, R.S., 1972. Iron-rich basal sediments from the eastern equatorial Pacific: Leg 16, Deep Sea Drilling Project: *Science*, v. 175, p. 61.
- Dasch, E.J., Dymond, J.R., and Heath, G.R., 1971. Isotopic analysis of metalliferous sediment from the East Pacific Rise: *Earth Planet. Sci. Lett.*, v. 13, p. 175-180.
- Dymond, J.R. and Veeh, H.H., in press. Metal accumulation rates in the southeast Pacific and the origin of metalliferous sediments: *Earth Planet. Sci. Lett.*
- Dymond, J.R., Corliss, J.B., Heath, G.R., Field, C.W., Dasch, E.J., and Veeh, H.H., 1973. Origin of metalliferous sediments from the Pacific Ocean: *Geol. Soc. Am. Bull.*, v. 84, p. 3355-3372.
- Eklund, W.A., 1974. A microprobe study of metalliferous sediment components: M.S. thesis, Corvallis, Oregon State University, 77 p.
- Hart, R.A., 1973. A model for chemical exchange in the basalt-sea water system of Oceanic Layer II: *Canadian J. Earth Sci.*, v. 10, p. 799.
- Heath, G.R., Dymond, J.R., and Veeh, H.H., 1973. Metalliferous sediments from the southeast Pacific: the IDOE Nazca Plate Project: Unpublished manuscript.
- Herron, E.M., 1972. Sea floor spreading and Cenozoic history of the East Central Pacific: *Geol. Soc. Am. Bull.*, v. 83, p. 1671-1692.
- Hussong, D.M., Johnson, S.H., Woollard, G.P., and Campbell, J.F., 1972. Crustal structure of the Nazca Plate: *EOS, Trans. Am. Geophys. Union*, v. 53, p. 413.
- Hussong, D.M., Campbell, J.F., Odegard, M.E., Edward, P., and Johnson, S.H., 1973. Structure and tectonic description of the Nazca Plate subduction zone near Peru (abs.): *Program of Science and Man in the Americas Mtg.*, A.A.A.S., Mexico City.
- Johnson, S.H., Connard, G.G., Hussong, D.M., and Ness, G.E., 1973. Crustal structure of the north-central Nazca Plate from seismic refraction: *Geodynamics Conference of I.A.S.P.E.I.*, Lima, Peru.
- Langseth, M.S. and von Herzen, R.P., 1971. Heat flow through the floor of the world oceans: *In Maxwell, A.E. (Ed.), the sea*, v. 4, New York (Wiley-Interscience), p. 299-352.
- Mammerickx, J., Anderson, R.N., Menard, H.W., and Smith, S.M., 1975. Morphology and tectonic evolution of the east central Pacific: *Geol. Soc. Am. Bull.*, v. 86, p. 111-118.
- Mammerickx, J., Smith, S.M., Taylor, I.L., and Chase, T.E., 1971-74. Bathymetry of the South Pacific - in ten sheets: *Scripps Institution of Oceanography, IMR Tech. Rept. Series*.
- Rea, D.K., 1975. Tectonics of the East Pacific Rise, 5° to 12°S: Ph.D. dissertation, Oregon State University, Corvallis, 139 p.
- Rosato, V.J., Kulm, L.D., and Derks, P.S., in press. Surface sediments of the Nazca Plate: *Pacific Sci.*
- Rose, J.C. and Couch, R.W., 1973. Gravity measurements over the Nazca Plate and its boundaries: *Geol. Soc. Am. Cordilleran Section, Portland, Oregon*.
- Salisbury, M.H. and Christensen, N.I., 1973. Progressive weathering of submarine basalt with age: further evidence of sea-floor spreading: *Geology*, v. 1, p. 63-64.
- Sclater, J.G., Anderson, R.N., and Bell, M.L., 1971. Elevation of ridges and evolution of the central East Pacific: *J. Geophys. Res.*, v. 76, p. 2562-2586.
- von der Borch, C.C., Nesteroff, W.D., and Galehouse, J.S., 1971. Iron-rich sediments cored during Leg 8 of the Deep Sea Drilling Project. *In Tracey, J.I., Sutton, G.H., et al., Initial Reports of the Deep Sea Drilling Project, Volume 8: Washington (U.S. Government Printing Office), p. 829-833.*

Site 319 Hole Core 1 Cored Interval: 0.0-9.5 m

AGE	ZONE			FOSSIL CHARACTER			SECTION	METERS	LITHOLOGY	DEFORMATION	LITHO. SAMPLE	LITHOLOGIC DESCRIPTION																																																																																																																																																												
	FORAMS	NANNOS	RADS	FORAMS	NANNOS	RADS							OTHERS																																																																																																																																																											
QUATERNARY	N22-N23							0	Fe			<p>IRON RICH BROWN CLAY, CALCAREOUS BROWN CLAY, and CLAYEY NANNO Ooze</p> <p>Core is moderately deformed (Sec. 1 & 2) and intensely deformed (Sec. 3-6). Major lithologies are divided into two parts. The first, from the top to near the base of Sec. 3, is dark reddish brown (5YR 2.5/2) clay that is rich in semi-opaque and opaque iron oxides (RSO) with some phillipsite and minor carbonate, along with trace amounts of feldspar, pyroxene, phosphatic fish debris, and glass. The second part from the base of Sec. 3 to the bottom of the core is brown (7.5YR 4/4 and 5YR 4/4) nanno-rich (calcareous) brown clay and clayey nanno ooze, iron-bearing to iron-rich, with some dark reddish brown (5YR 2.5/2) beds similar to those in the upper part. The core catcher is mixed calcareous brown clay and nanno ooze.</p> <p><u>Characteristic Smear Slides</u></p> <table border="1"> <tr> <td></td> <td>1-10</td> <td>4-31</td> <td>5-45</td> <td>6-40</td> </tr> <tr> <td>clay</td> <td>60</td> <td>60</td> <td>25</td> <td>70</td> </tr> <tr> <td>RSO</td> <td>20</td> <td>5</td> <td>5</td> <td>15</td> </tr> <tr> <td>nannos</td> <td>5</td> <td>20</td> <td>65</td> <td>5</td> </tr> <tr> <td>micarb</td> <td>3</td> <td>10</td> <td>4</td> <td>5</td> </tr> <tr> <td>phil</td> <td>10</td> <td>5</td> <td>-</td> <td>-</td> </tr> <tr> <td>feld</td> <td>2</td> <td>-</td> <td>-</td> <td>T</td> </tr> <tr> <td>forams</td> <td>-</td> <td>T</td> <td>1</td> <td>-</td> </tr> </table> <p><u>Grain Size</u></p> <table border="1"> <tr> <td></td> <td>1-59</td> <td>2-89</td> <td>3-59</td> <td>4-59</td> <td>5-89</td> <td>6-38</td> </tr> <tr> <td>sand</td> <td>0.1</td> <td>-</td> <td>-</td> <td>0.4</td> <td>0.7</td> <td>-</td> </tr> <tr> <td>silt</td> <td>31.9</td> <td>25.2</td> <td>37.4</td> <td>45.0</td> <td>35.9</td> <td>32.2</td> </tr> <tr> <td>clay</td> <td>67.9</td> <td>74.7</td> <td>62.6</td> <td>54.6</td> <td>63.4</td> <td>67.8</td> </tr> </table> <p><u>Carbon-Carbonate</u></p> <table border="1"> <tr> <td></td> <td>2-20</td> <td>2-40</td> <td>3-30</td> <td>4-87</td> <td>5-20</td> <td>6-60</td> </tr> <tr> <td>t. carb</td> <td>0.2</td> <td>0.1</td> <td>0.1</td> <td>4.6</td> <td>6.7</td> <td>0.4</td> </tr> <tr> <td>o. carb</td> <td>0.1</td> <td>0.2</td> <td>0.2</td> <td>0.1</td> <td>0.1</td> <td>0.2</td> </tr> <tr> <td>CaCO₃</td> <td>-</td> <td>-</td> <td>-</td> <td>37.0</td> <td>55.0</td> <td>2.0</td> </tr> </table> <p><u>Bulk X-ray</u></p> <table border="1"> <tr> <td></td> <td>1-110</td> <td>4-20</td> <td>5-117</td> <td>6-20</td> </tr> <tr> <td>amor</td> <td>82.2</td> <td>68.0</td> <td>53.2</td> <td>83.4</td> </tr> <tr> <td>calc</td> <td>-</td> <td>68.8</td> <td>93.3</td> <td>50.4</td> </tr> <tr> <td>feld</td> <td>21.1</td> <td>-</td> <td>-</td> <td>7.8</td> </tr> <tr> <td>quar</td> <td>0.7</td> <td>0.5</td> <td>0.5</td> <td>0.8</td> </tr> <tr> <td>kaol</td> <td>14.0</td> <td>3.2</td> <td>-</td> <td>6.3</td> </tr> <tr> <td>mica</td> <td>4.8</td> <td>-</td> <td>-</td> <td>-</td> </tr> <tr> <td>chlo</td> <td>-</td> <td>2.2</td> <td>-</td> <td>-</td> </tr> <tr> <td>goet</td> <td>13.8</td> <td>12.4</td> <td>3.5</td> <td>11.6</td> </tr> <tr> <td>phil</td> <td>33.4</td> <td>7.5</td> <td>-</td> <td>9.4</td> </tr> <tr> <td>gyps</td> <td>-</td> <td>-</td> <td>2.7</td> <td>-</td> </tr> <tr> <td>bari</td> <td>12.2</td> <td>5.5</td> <td>-</td> <td>13.7</td> </tr> </table>		1-10	4-31	5-45	6-40	clay	60	60	25	70	RSO	20	5	5	15	nannos	5	20	65	5	micarb	3	10	4	5	phil	10	5	-	-	feld	2	-	-	T	forams	-	T	1	-		1-59	2-89	3-59	4-59	5-89	6-38	sand	0.1	-	-	0.4	0.7	-	silt	31.9	25.2	37.4	45.0	35.9	32.2	clay	67.9	74.7	62.6	54.6	63.4	67.8		2-20	2-40	3-30	4-87	5-20	6-60	t. carb	0.2	0.1	0.1	4.6	6.7	0.4	o. carb	0.1	0.2	0.2	0.1	0.1	0.2	CaCO ₃	-	-	-	37.0	55.0	2.0		1-110	4-20	5-117	6-20	amor	82.2	68.0	53.2	83.4	calc	-	68.8	93.3	50.4	feld	21.1	-	-	7.8	quar	0.7	0.5	0.5	0.8	kaol	14.0	3.2	-	6.3	mica	4.8	-	-	-	chlo	-	2.2	-	-	goet	13.8	12.4	3.5	11.6	phil	33.4	7.5	-	9.4	gyps	-	-	2.7	-	bari	12.2	5.5	-	13.7
									1-10	4-31	5-45		6-40																																																																																																																																																											
								clay	60	60	25		70																																																																																																																																																											
								RSO	20	5	5		15																																																																																																																																																											
								nannos	5	20	65		5																																																																																																																																																											
	micarb	3	10	4	5																																																																																																																																																																			
	phil	10	5	-	-																																																																																																																																																																			
	feld	2	-	-	T																																																																																																																																																																			
	forams	-	T	1	-																																																																																																																																																																			
		1-59	2-89	3-59	4-59	5-89	6-38																																																																																																																																																																	
sand	0.1	-	-	0.4	0.7	-																																																																																																																																																																		
silt	31.9	25.2	37.4	45.0	35.9	32.2																																																																																																																																																																		
clay	67.9	74.7	62.6	54.6	63.4	67.8																																																																																																																																																																		
	2-20	2-40	3-30	4-87	5-20	6-60																																																																																																																																																																		
t. carb	0.2	0.1	0.1	4.6	6.7	0.4																																																																																																																																																																		
o. carb	0.1	0.2	0.2	0.1	0.1	0.2																																																																																																																																																																		
CaCO ₃	-	-	-	37.0	55.0	2.0																																																																																																																																																																		
	1-110	4-20	5-117	6-20																																																																																																																																																																				
amor	82.2	68.0	53.2	83.4																																																																																																																																																																				
calc	-	68.8	93.3	50.4																																																																																																																																																																				
feld	21.1	-	-	7.8																																																																																																																																																																				
quar	0.7	0.5	0.5	0.8																																																																																																																																																																				
kaol	14.0	3.2	-	6.3																																																																																																																																																																				
mica	4.8	-	-	-																																																																																																																																																																				
chlo	-	2.2	-	-																																																																																																																																																																				
goet	13.8	12.4	3.5	11.6																																																																																																																																																																				
phil	33.4	7.5	-	9.4																																																																																																																																																																				
gyps	-	-	2.7	-																																																																																																																																																																				
bari	12.2	5.5	-	13.7																																																																																																																																																																				
LATE MIOGENE/PLOGENE	N20-N21							1	Fe																																																																																																																																																															
								1.0	Fe																																																																																																																																																															
								130	Fe																																																																																																																																																															
								46	Fe																																																																																																																																																															
								75	Fe																																																																																																																																																															
	N19								50	Fe																																																																																																																																																														
									115	Fe																																																																																																																																																														
									24	Fe																																																																																																																																																														
									31	Fe																																																																																																																																																														
									78	Fe																																																																																																																																																														
N12								10	Fe																																																																																																																																																															
								45	Fe																																																																																																																																																															
								120	Fe																																																																																																																																																															
								4	Fe																																																																																																																																																															
								40	Fe																																																																																																																																																															
Core Catcher	CC																																																																																																																																																																							

Explanatory notes in Chapter 2



Site 319 Hole Core 2 Cored Interval: 9.5-19.0 m

AGE	ZONE		FOSSIL CHARACTER					SECTION	METERS	LITHOLOGY	DEFORMATION	LITHO. SAMPLE	LITHOLOGIC DESCRIPTION
	FORAMS	NANNOS	RADS	FORAMS	NANNOS	RADS	OTHERS						
LATE MIOCENE/PLEISTOCENE	N19							0	VOID			CLAY-RICH NANNO Ooze and CALCAREOUS BROWN CLAY	
								0.5				Core is moderately (Sec. 1) to intensely deformed. Color is predominantly dark reddish brown (5YR 3/4 and 5YR 3/3) and dark brown (7.5YR 3/2 and 7.5YR 4/4) with some yellow brown (10YR 4/4 and 10YR 3/3) and dark grayish brown (10YR 3/2). Core catcher is dark reddish brown (5YR 3/3).	
	N12							1				79 10YR 4/4 10YR 3/2 10YR 4/4 130 10YR 7/3	
								2				40 7.4YR 4/4 with mottles of 10YR 7/3 and 5YR 3/3 120 10YR 7/3	
LATE MIOCENE	N19-N18							3				75 5YR 3/4 to 7.5YR 3/2	
								4				Core Catcher	

Explanatory notes in Chapter 2

In Sec. 1 & 2 the darker colors (e.g. 10YR 3/2) are generally iron bearing nanno-rich clays and nanno clays, the predominant intermediate colors (e.g. 10YR 3/3 to 4/4) are clayey nanno ooze and clay-rich nanno ooze, and the minor light patches (10YR 7/3) are clay-bearing nanno ooze.

Characteristic Smear Slides

	1-79	2-120	3-75
clay	55	15	20
RSD	10	3	5
nannos	30	75	65
micarb	4	5	5
phil	1	T	-
forams	-	2	5

Grain Size

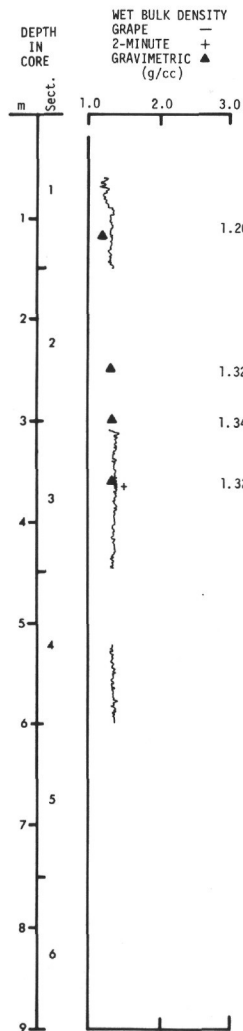
	1-79	2-127	3-38	4-78
sand	0.5	0.7	1.4	0.5
silt	36.7	42.0	37.1	43.0
clay	62.8	57.3	61.6	56.5

Carbon-Carbonate

	1-148	2-12	3-10	4-19
t. carb	7.3	7.9	7.7	7.0
o. carb	0.1	0.1	0.1	0.1
CaCO ₃	60.0	65.0	63.0	58.0

Bulk X-ray

	1-137	2-106	3-80	4-45
amor	46.0	37.9	48.9	45.1
calc	83.1	89.1	85.7	88.3
goet	4.4	2.6	4.7	3.7
mont	10.8	8.3	9.6	8.0
bari	1.6	-	-	-

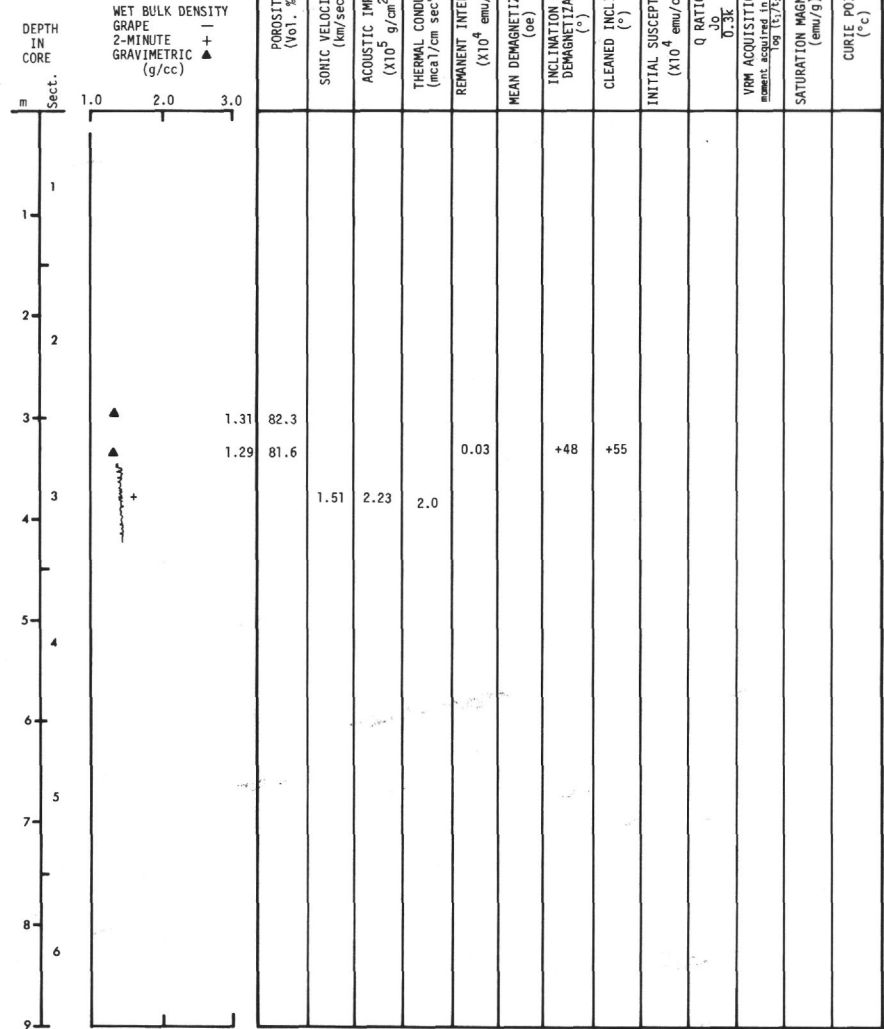


DEPTH IN CORE (m)	DEPTH IN SECT. (m)	WET BULK DENSITY (GRAPE 2-MINUTE GRAVIMETRIC) (g/cc)	POROSIY (Vol. %)	SONIC VELOCITY, Vp (km/sec)	ACOUSTIC IMPEDANCE (X10 ⁵ g/cm ² sec ⁻¹)	THERMAL CONDUCTIVITY (mcal/cm sec ² C) ±10%	REMANENT INTENSITY, J _o (X10 ⁴ emu/cm ³)	MEAN DEMAGNETIZING FIELD (oe)	INCLINATION BEFORE DEMAGNETIZATION (°)	CLEANED INCLINATION (°)	INITIAL SUSCEPTIBILITY, k (X10 ⁴ emu/cm ³ oe)	Q RATIO (J _o /0.3k)	VRM ACQUISITION FACTOR (moment acquired in time (t ₁ -t ₂)/log (t ₁ /t ₂))	SATURATION MAGNETIZATION (emu/g)	CURIE POINT (°C)
1.20	1.20	1.20	78.7												
2.20	2.20	1.32	81.9												
3.20	3.20	1.34	81.7												
3.80	3.80	1.32	82.3	1.51	2.10	1.6									

Site 319 Hole Core 3 Cored Interval: 19.0-28.5 m

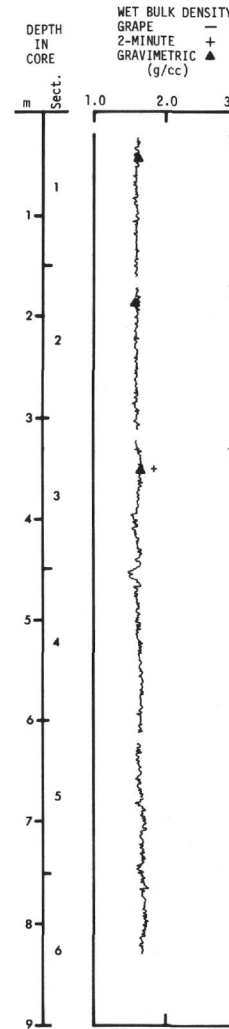
AGE	ZONE		FOSSIL CHARACTER				SECTION METERS	LITHOLOGY	DEFORMATION	LITHO. SAMPLE	LITHOLOGIC DESCRIPTION
	FORAMS	NANNOS	RAIDS	FORAMS	NANNOS	RAIDS					
LATE MIOCENE	N17-N18	Discoaster calcarts		Ag	Cf		0	VOID			CLAY-RICH NANNO OOZE and CALCAREOUS BROWN CLAY Core is intensely deformed. Colors are brown (10YR 4/3), reddish brown (5YR 4/4) and strong brown (7.5YR 5/6). Lithologies include nanno-rich calcareous brown clay that is interbedded with clayey and clay-rich nanno oozes. Oozes predominate. Darker colors correlate with higher amounts of red-brown semi-opaque iron oxides (RSO).
							1.0		130	10YR 4/3	
							2.0		100	5YR 4/4	
MID MIOCENE	N16	N16		Cg	Ag		2.5	mixed 5YR 3/4 5YR 4/4			Characteristic Smear Slides clay 20 50 15 RSO 10 10 10 nannos 60 35 60 micarb 10 5 15 phil - T - forams T - T
							3.0		25	7.5YR 5/6	
							3.5		80		
	N14-N15			Ag	B		Core Catcher		CC	10YR 4/3	Bulk X-ray amor 48.3 38.6 calc 87.4 97.1 goet 3.1 2.9 mont 8.2 - bart 1.4 -

Explanatory notes in Chapter 2



Site 319 Hole Core 4 Cored Interval: 28.5-38.0 m

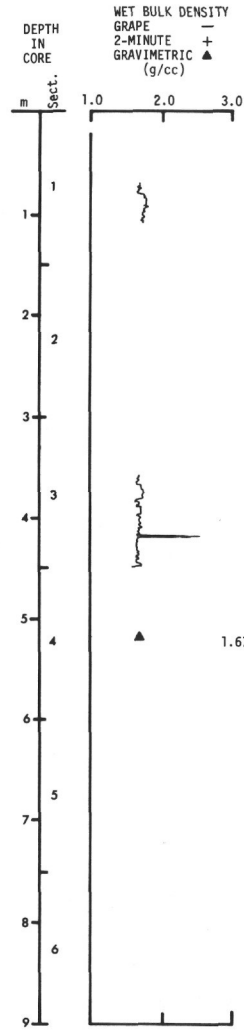
AGE	ZONE		FOSSIL CHARACTER				SECTION METERS	LITHOLOGY	DEFORMATION	LITHO-SAMPLE	LITHOLOGIC DESCRIPTION
	FORAMS	NANNOS	RADS	FORAMS	NANNOS	RADS					
MIDDLE MIOCENE	N14-N15	Discoaster exilis	Af	Ag	-	-	0			10YR 4/4	NANNO Ooze
							0.5			10YR 4/4 and 10YR 3/4 mixed	The entire core is intensely deformed. Dark brown and light brown beds are mixed, creating a "marbly" effect. Core becomes lighter in hue irregularly from top to base, with dark yellowish brown (10YR 3/4 and 10YR 4/4) near the top and light yellowish brown (10YR 6/4) and very pale yellow brown (10YR 7/4) near the base. Colors reflect iron content.
							1.0				
	N13	Discoaster exilis	Af	Ag	-	-	2			10YR 5/4 dominant with some dk brn 7.5YR 4/4	Characteristic Smear Slides
	N12	N16	Discoaster exilis	Af	Ag	-	-	3			10YR 4/4 and 10YR 4/3
							4			10YR 6/4 and 10YR 5/4	Carbon-Carbonate
							5			10YR 8/4	Bulk X-ray
							6			10YR 6/4	
										10YR 7/4	
										10YR 6/4	
										CC	



DEPTH IN CORE (m)	SECTION (Sect.)	POROSIITY (Vol. %)	SONIC VELOCITY, Vp (km/sec)	ACOUSTIC IMPEDANCE (x10 ⁵ g/cm ² sec ⁻¹)	THERMAL CONDUCTIVITY (mca/cm sec-c) ± 10%	REMANENT INTENSITY, J ₀ (x10 ⁶ emu/cm ³)	MEAN DEMAGNETIZING FIELD (oe)	INCLINATION BEFORE DEMAGNETIZATION (°)	CLEANED INCLINATION (°)	INITIAL SUSCEPTIBILITY, k (x10 ⁴ emu/cm ³ oe)	Q RATIO J ₀ / Q _{3K}	IRM ACQUISITION FACTOR (normalized to 100% magnetization in field 100-150 Oe)	SATURATION MAGNETIZATION (emu/g)	CURIE POINT (°C)
1.60	1.60	69.8												
1.56	1.56	70.5												
1.64	1.64	66.8												
1.53	1.53													
2.57	2.57													
2.6	2.6													

Site 319 Hole Core 6 Cored Interval: 47.5-57.0 m

AGE	ZONE		FOSSIL CHARACTER			SECTION METERS	LITHOLOGY	DEFORMATION LITHO. SAMPLE	LITHOLOGIC DESCRIPTION		
	FORAMS	NANNOS	RADS	FORAMS	NANNOS					RADS	OTHERS
MIDDLE MIOCENE	N12	N16	D. exilis	Ae	Ag	0	VOID		NANNO OOZE		
						0.5			Core is intensely deformed and soupy in parts. Section 1, to 77 cm, is a mixture of slumped material and metal flakes from the drill pipe. A similar mixed zone occurs in Section 3 (0-40 cm). Some burrow structures are in Section 4 and a manganese nodule, 5 cm in diameter, is near the base of Section 4. Colors are pred. light yellow brown (10YR 6/4) and very pale brown (10YR 7/4) with streaks of yellow brown (10YR 5/4) in Section 4.		
						1			10YR 6/4 and 10YR 7/4	110	
						1.0			foram-rich zone	10	
						2			Lithologically the entire section is nanno ooze with foram content ranging from 1 to 30%. Foram rich layers were sampled at 1-110, 2-10, and 6-40.		
						2			Characteristic Smear Slides		
			10YR 7/4			1-110 5-20					
						clay 1 1					
						RSO 2 1					
						nannos 70 85					
						micarb 8 4					
						forams 20 10					
						Grain Size					
						1-119 2-26					
						sand 5.0 0.5					
						silt 46.1 44.3					
						clay 48.8 55.2					
						Carbon-Carbonate					
						1-123 3-119 4-17 5-131 6-143					
						t. carb 11.5 11.5 11.5 11.3 11.5					
						o. carb 0.1 - - - -					
						CaCO ₃ 95.0 96.0 95.0 94.0 95.0					
						Bulk X-ray					
						1-84 3-121 4-31 5-120					
						amor 18.4 20.2 25.5 15.2					
						calc 97.7 92.3 94.5 96.8					
						feld - - - 1.0					
						goet 2.3 3.4 4.0 2.2					
						phil - 3.9 1.5 -					
						hema - 0.3 - -					
						← Mn nodule					
						20					
						10YR 7/4					
						40					
						foram-rich zone					
						6					
						Core Catcher					
						CC					

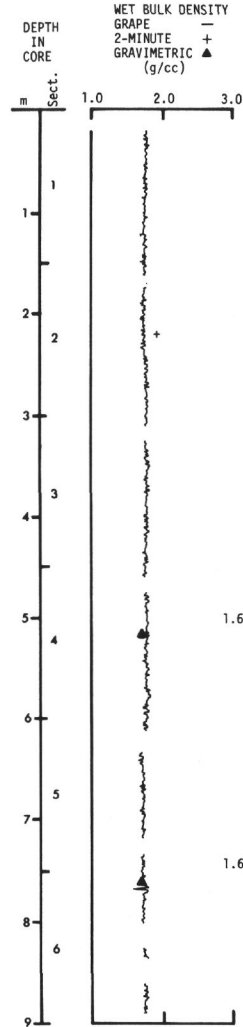


POROSITY (Vol. %)	SONIC VELOCITY, Vp (km/sec)	ACOUSTIC IMPEDANCE (X10 ⁵ g/cm ² sec)	THERMAL CONDUCTIVITY (mcal/cm sec°C) ±10%	REMANENT INTENSITY, Jo (X10 ⁶ emu/cm ²)	MEAN DEMAGNETIZING FIELD (oe)	INCLINATION BEFORE DEMAGNETIZATION (°)	CLEANED INCLINATION (°)	INITIAL SUSCEPTIBILITY, k (X10 ⁴ emu/cm ³ oe)	Q RATIO Jo / 0.3K	IRM ACQUISITION FACTOR (moment acquired in time t ₁ -t ₂ / log(t ₁ /t ₂))	SATURATION MAGNETIZATION (emu/g)	CURIE POINT (°C)
			3.3									
			2.7									
			2.7									
			2.7									
		1.67										
60.4												

Site 319 Hole Core 7 Cored Interval: 57.0-66.5 m

AGE	ZONE		FOSSIL CHARACTER					SECTION METERS	LITHOLOGY	DEFORMATION	LITHO. SAMPLE	LITHOLOGIC DESCRIPTION							
	FORAMS	NANNOS	RADS	FORAMS	NANNOS	RADS	OTHERS												
MIDDLE MIOCENE	MIO-NIT	NNG	D. exilis					0			FORAM-RICH NANNO OOOE Core is intensely deformed except in stiffer parts of Section 3. Light yellow brown (10YR 6/4) and very pale brown (10YR 7/4) nanno ooze, foram-bearing to foram-rich. The red-brown semi-opaques (RSO) are nowhere absent but seldom exceed 1 or 2%. Characteristic Smear Slides 2-75 3-75 clay 5 5 RSO 2 1 nannos 75 70 mtcarb 8 9 forams 10 15 Grain Size 1-79 3-140 4-139 5-135 6-33 sand 1.2 1.2 1.9 1.7 1.2 silt 35.1 38.5 39.3 38.7 38.5 clay 63.8 60.3 58.8 59.6 60.4 Carbon-Carbonate 1-91 2-21 3-31 4-45 5-137 6-30 t. carb 11.2 11.5 11.5 11.4 11.4 11.3 o. carb - - 0.1 - - 0.1 CaCO ₃ 93.0 95.0 95.0 94.0 95.0 94.0 Bulk X-ray 1-101 4-124 5-128 6-44 amor 15.7 17.4 16.3 16.7 calc 98.9 97.7 98.4 98.3 goet 1.1 2.3 1.6 1.7								
								0.5											
								1											
								1.0											
								2											
								3											
								4											
								5											
								6											
								Core Catcher											

Explanatory notes in Chapter 2

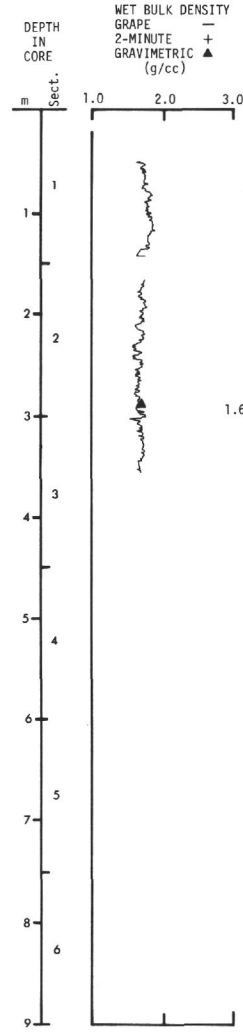


DEPTH IN CORE	SONIC VELOCITY, Vp (km/sec)	ACoustic IMPEDANCE (X10 ⁵ g/cm ² sec ⁻¹)	THERMAL CONDUCTIVITY (mcal/cm sec °C) ± 10%	REMANENT INTENSITY, J ₀ (X10 ⁴ emu/cm ³)	MEAN DEMAGNETIZING FIELD (oe)	INCLINATION BEFORE DEMAGNETIZATION (°)	CLEANED INCLINATION (°)	INITIAL SUSCEPTIBILITY, k (X10 ⁴ emu/cm ³ oe)	Q RATIO J ₀ 0-3K	VRM ACQUISITION FACTOR moment acquired in time (t ₁ -t ₂)/log (t ₁ /t ₂)	SATURATION MAGNETIZATION (emu/g)	CURIE POINT (°C)
1.56	2.75	2.7										
1.69	60.0	2.8										
1.68	61.0	3.1										
		2.8										

Site 319 Hole Core 9 Cored Interval: 76.0-85.5 m

AGE	FOSSIL CHARACTER				SECTION METERS	LITHOLOGY	DEFORMATION	LITHO. SAMPLE	LITHOLOGIC DESCRIPTION																																																																																
	FORAMS	NANNOS	RADS	OTHERS																																																																																					
MIDDLE MIOCENE	N9 NNS	S. heteromorphus	Ae- Ag- B-	-	0	VOID			<p>IRON BEARING NANNO OOZE</p> <p>Entire section is nanno ooze, iron-bearing to iron-rich. Core is moderately deformed in Sec. 1 & 2. Sec. 3 is slightly deformed to 100 cm, below which deformation is extreme. A lag concentration of ooze pellets and forams in Sec. 3, 132 to 141 is probably an artifact of drilling. Yellowish brown (10YR 5/4), dark yellowish brown (10YR 4/4), dark brown (10YR 4/3 and 3/3) colors are darker than Core 8, reflecting large amounts of red-brown semi-opaque iron oxides (RSD).</p> <p><u>Characteristic Smear Slides</u></p> <table border="1"> <tr><td></td><td>1-94</td><td>2-125</td><td>3-97</td></tr> <tr><td>clay</td><td>5</td><td>5</td><td>5</td></tr> <tr><td>RSD</td><td>7</td><td>10</td><td>7</td></tr> <tr><td>nannos</td><td>80</td><td>65</td><td>75</td></tr> <tr><td>micarb</td><td>6</td><td>20</td><td>8</td></tr> <tr><td>forams</td><td>2</td><td>T</td><td>5</td></tr> <tr><td>phil</td><td>T</td><td>T</td><td>T</td></tr> </table> <p><u>Grain Size</u></p> <table border="1"> <tr><td></td><td>1-138</td><td>2-133</td><td>3-88</td></tr> <tr><td>sand</td><td>0.2</td><td>0.2</td><td>0.8</td></tr> <tr><td>silt</td><td>59.6</td><td>59.2</td><td>57.1</td></tr> <tr><td>and 10YR 3/3</td><td>40.2</td><td>40.7</td><td>42.1</td></tr> <tr><td>clay</td><td></td><td></td><td></td></tr> </table> <p><u>Carbon-Carbonate</u></p> <table border="1"> <tr><td></td><td>1-110</td><td>2-130</td><td>3-103</td></tr> <tr><td>t. carb</td><td>11.0</td><td>9.2</td><td>10.3</td></tr> <tr><td>o. carb</td><td>0.1</td><td>0.1</td><td>0.1</td></tr> <tr><td>CaCO₃</td><td>91.0</td><td>76.0</td><td>86.0</td></tr> </table> <p><u>Bulk X-ray</u></p> <table border="1"> <tr><td></td><td>1-89</td><td>2-127</td><td>3-91</td></tr> <tr><td>amor</td><td>22.1</td><td>38.9</td><td>32.8</td></tr> <tr><td>calc</td><td>96.3</td><td>92.2</td><td>94.6</td></tr> <tr><td>goet</td><td>3.7</td><td>7.8</td><td>5.4</td></tr> </table>		1-94	2-125	3-97	clay	5	5	5	RSD	7	10	7	nannos	80	65	75	micarb	6	20	8	forams	2	T	5	phil	T	T	T		1-138	2-133	3-88	sand	0.2	0.2	0.8	silt	59.6	59.2	57.1	and 10YR 3/3	40.2	40.7	42.1	clay					1-110	2-130	3-103	t. carb	11.0	9.2	10.3	o. carb	0.1	0.1	0.1	CaCO ₃	91.0	76.0	86.0		1-89	2-127	3-91	amor	22.1	38.9	32.8	calc	96.3	92.2	94.6	goet	3.7	7.8	5.4
						1-94	2-125	3-97																																																																																	
					clay	5	5	5																																																																																	
					RSD	7	10	7																																																																																	
					nannos	80	65	75																																																																																	
					micarb	6	20	8																																																																																	
					forams	2	T	5																																																																																	
					phil	T	T	T																																																																																	
						1-138	2-133	3-88																																																																																	
					sand	0.2	0.2	0.8																																																																																	
silt	59.6	59.2	57.1																																																																																						
and 10YR 3/3	40.2	40.7	42.1																																																																																						
clay																																																																																									
	1-110	2-130	3-103																																																																																						
t. carb	11.0	9.2	10.3																																																																																						
o. carb	0.1	0.1	0.1																																																																																						
CaCO ₃	91.0	76.0	86.0																																																																																						
	1-89	2-127	3-91																																																																																						
amor	22.1	38.9	32.8																																																																																						
calc	96.3	92.2	94.6																																																																																						
goet	3.7	7.8	5.4																																																																																						
1	0.5				65	10YR 4/3																																																																																			
					94	10YR 3/3																																																																																			
					130	10YR 4/3																																																																																			
					30	10YR 4/3																																																																																			
					80	10YR 5/4																																																																																			
					125	VOID																																																																																			
					30	10YR 3/2																																																																																			
					30	10YR 5/4																																																																																			
					97	10YR 3/3																																																																																			
					CC	10YR 2.5/2																																																																																			
						10YR 4/3																																																																																			
						Core Catcher																																																																																			

Explanatory notes in Chapter 2

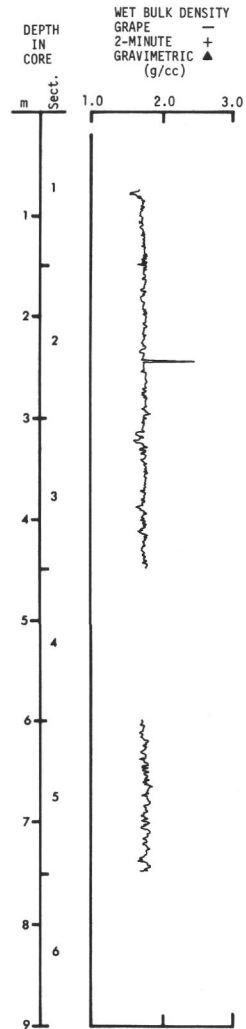


POROSITY (Vol. %)	SONIC VELOCITY, Vp (km/sec)	ACOUSTIC IMPEDANCE (X10 ⁵ g/cm ² sec ²)	THERMAL CONDUCTIVITY (mca/cm sec °C) ±10%	REMANENT INTENSITY, J _o (X10 ⁴ emu/cm ³)	MEAN DEMAGNETIZING FIELD (oe)	INCLINATION BEFORE DEMAGNETIZATION (°)	CLEANED INCLINATION (°)	INITIAL SUSCEPTIBILITY, k (X10 ⁴ emu/cm ³ oe)	Q RATIO J _o /J _o 0.3K	VPM ACQUISITION FACTOR moment acquired in time (t ₁ -t ₂)/log (t ₁ /t ₂)	SATURATION MAGNETIZATION (emu/g)	CURIE POINT (°C)
				2.4								
				2.6								
				2.8								
				3.7								
1.69	59.7											
	1.56			2.5								
				2.3								

Site 319 Hole Core 10 Cored Interval: 85.5-95.0 m

AGE	FOSSIL CHARACTER			SECTION METERS	LITHOLOGY	DEFORMATION	LITHO. SAMPLE	LITHOLOGIC DESCRIPTION		
	FORAMS	NANNOS	RADS							
MIDDLE MIOCENE	N9	S. heteromorphus		0	VOID			IRON-BEARING FORAM-RICH NANNO OOEZ Core is intensely deformed. Dominant colors range through light yellowish brown (10YR 6/4), yellowish brown (10YR 5/4), dark yellowish brown (10YR 4/4) and brown (10YR 4/3).		
				0.5						
				1	Ae-				72	10YR 6/4
				1.0					110	10YR 5/4
				2	Ae-				75	10YR 5/4 with some 10YR 4/3 and 10YR 6/4
				3	Ae- Ag-				78	mixed 10YR 6/6 and 10YR 4/4
				4					91	
				5	Ae- Ag-				75	10YR 5/4
				Core Catcher	Af-	B-			CC	10YR 4/3

Explanatory notes in Chapter 2

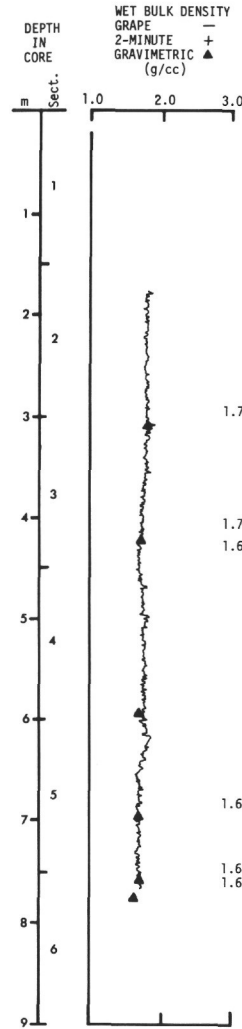


DEPTH IN CORE	POROSIITY (Vol. %)	SORIC VELOCITY, Vp (km/sec)	ACOUSTIC IMPEDANCE (x10 ⁵ g/cm ² sec ⁻¹)	THERMAL CONDUCTIVITY (mca/cm sec ² C)=10%	REMANENT INTENSITY, Jo (x10 ⁴ emu/cm ³)	MEAN DEMAGNETIZING FIELD (oe)	INCLINATION BEFORE DEMAGNETIZATION (°)	CLEANED INCLINATION (°)	INITIAL SUSCEPTIBILITY, k (x10 ⁶ emu/cm ³ oe)	Q RATIO Jo/0.3K	VRM ACQUISITION FACTOR moment acquired in time (t ₁ -5t ₂) log (t ₁ /t ₂)	SATURATION MAGNETIZATION (emu/g)	CURIE POINT (°C)
1.59													
3.6													
4.3													
4.0													
3.6													
2.8													
3.4													
2.8					0.03		-15	+01					
2.7													

Site 319 Hole Core 11 Cored Interval: 95.0-104.5 m

AGE	FOSSIL CHARACTER			SECTION METERS	LITHOLOGY	DEFORMATION	LITHO. SAMPLE	LITHOLOGIC DESCRIPTION
	FORAMS	NANNOS	RADS					
EARLY MIOCENE	NBS	S. heteromorphus	NNS	Ae- Ag- Ag- Ae- Ag- Ae- Ag- Ae- Ag- Ae- Ag-	0			IRON/FORAM-BEARING NANNO OOZE
					0.5	10YR 4/4	Core is slightly deformed, original bedding easily discernible, esp. in Secs. 5 and 6. Colors range through a number of shades of yellow-brown (10YR), from light yellowish brown (10YR), from light yellowish brown (10YR 6/4) to dark brown (10YR 3/3). Intermediate values - 10YR 5/4 and 10YR 4/4 - predominate.	
					1	75 to		
					1.0	10YR 5/4	Entire section is low clay nanno ooze, iron-bearing to iron-rich, and foram-bearing to foram-rich. Darker colors correlate with higher RSD percentages. Burrow-like mottlings present in Sec. 1, 20 to 50 cm, and Sec. 6, 20 to 35 cm.	
					2	10YR 4/3		
					2	75 to		
					2.5	10YR 5/4	Characteristic Smear Slides	
					3	10YR 4/4 grades to	clay 5 5 RSD 5 10 nannos 65 70 micarb 10 15 forams 15 T	
					3	25	Grain Size	
					3	125	1-98 2-41 3-110 4-120 5-106 6-106 sand 0.3 0.2 0.2 0.4 1.4 1.1 silt 57.6 59.2 47.3 51.7 62.3 58.4 clay 42.1 40.7 52.5 47.8 36.3 40.6	
					4	15	Carbon-Carbonate	
					4	32	1-50 2-71 3-100 4-90 5-63 6-90 t. carb 11.0 9.9 9.3 10.4 10.4 10.8 o. carb - 0.1 - 0.1 - CaCO ₃ 91.0 82.0 77.0 86.0 86.0 90.0	
4	90	10YR 6/4						
4	132	10YR 4/4						
5	10YR 5/4	Bulk X-ray						
5	45	1-63 4-100 amor 29.2 26.1 calc 94.2 97.5 goet 5.8 2.5						
5	10YR 4/4							
5	10YR 3/3							
5	10YR 5/3							
5	10YR 3/3							
6	20							
6	70	10YR 5/4						
6	120	10YR 3/3 and 10YR 5/4						
6	CC	10YR 4/4						
			Core Catcher					

Explanatory notes in Chapter 2

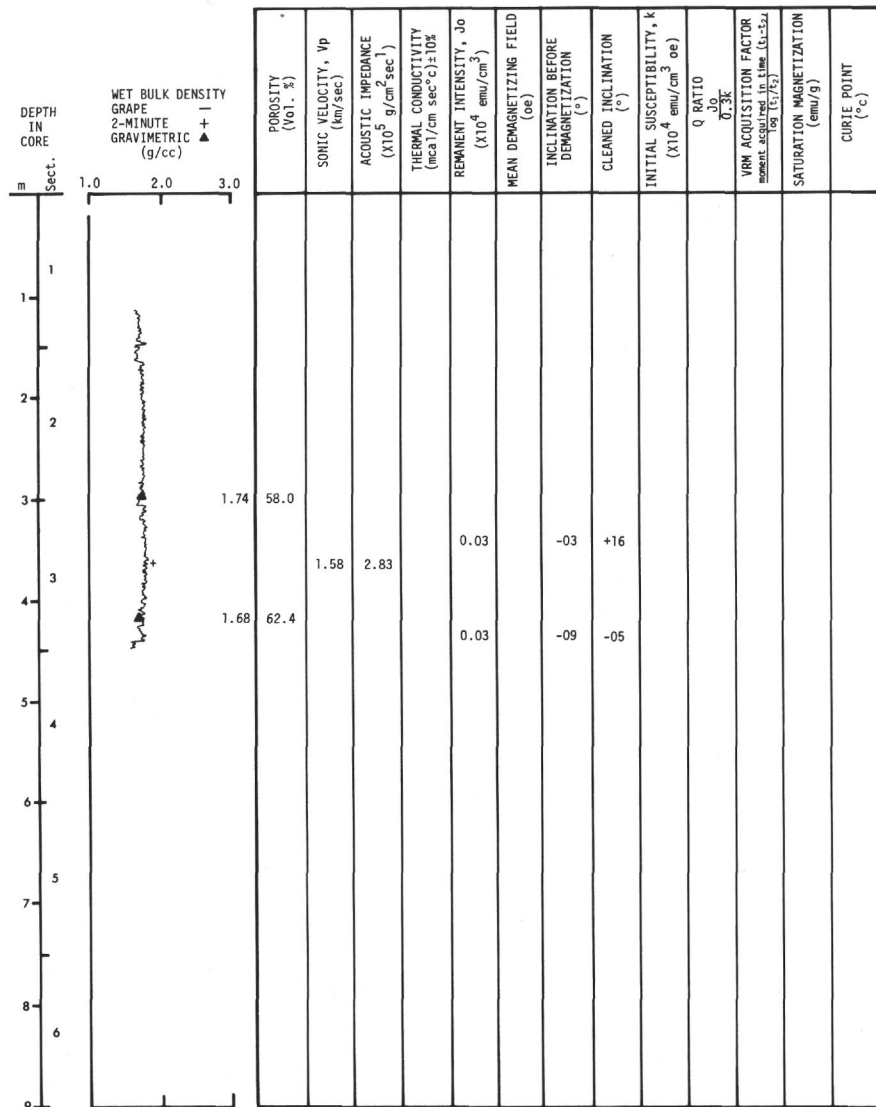


DEPTH IN CORE	WET BULK DENSITY GRAPE 2-MINUTE GRAVIMETRIC (g/cc)	POROSIITY (Vol. %)	SONIC VELOCITY, Vp (km/sec)	ACOUSTIC IMPEDANCE (X10 ⁵ g/cm ² sec ⁻¹)	THERMAL CONDUCTIVITY (mca/cm sec C) ± 10%	REMANENT INTENSITY, J ₀ (X10 ⁴ emu/cm ³)	MEAN DEMAGNETIZING FIELD (oe)	INCLINATION BEFORE DEMAGNETIZATION (°)	CLEANED INCLINATION (°)	INITIAL SUSCEPTIBILITY, k (X10 ⁴ emu/cm ³ oe)	Q RATIO J ₀ 0.3k	VRM ACQUISITION FACTOR moment acquired in time t ₁ -t ₂ log (t ₁ /t ₂)	SATURATION MAGNETIZATION (emu/g)	CURIE POINT (°C)
2.8					2.8									
3.2					3.2									
2.6					2.6									
2.5					2.5									
2.9	1.79	54.1			2.9									
3.0	1.70	64.1			3.0									
2.7	1.67	55.6			2.7									
3.1					3.1									
2.7					2.7									
3.1	1.68	61.9	1.58	2.75	3.1									
3.1	1.68	61.6			3.1									
2.6	1.63	62.3			2.6									
0.01					0.01			+28	+44					
0.04					0.04			+12	+15					

Site 319 Hole Core 12 Cored Interval: 104.5-111.5 m

AGE	ZONE			FOSSIL CHARACTER			SECTION METERS	LITHOLOGY	DEFORMATION	LITHO. SAMPLE	LITHOLOGIC DESCRIPTION
	FORAMS	NANNOS	RADS	FORAMS	NANNOS	RADS					
EARLY MIOCENE							0				IRON-BEARING NANNO OOZE
							0.5	VOID			Core slightly deformed in Sec. 1 and 2, relatively undeformed in Sec. 3. Colors are yellowish brown (10YR 6/4 to 5/4), brown (10YR 5/3) and dark brown (10YR 4/3 to 3/8).
							1.0				10YR 5/4 grading to
							1.30				Entire section is iron-bearing nanno ooze, foram-bearing to foram-rich. The bottom 28 cm of Sec. 3 plus the core catcher is very firm and breaks with angular fracture. There is no apparent enrichment of RSO as compared with Cores 9-11, although this basal unit is only about 1 meter above basalt. Top of basalt placed at about 110 m on basis of drilling.
							2				10YR 6/4
							70				Characteristic Smear Slides
											1-130 3-135
											clay 5 5
											RSO 15 10
											nannos 65 65
										micarb 5 10	
										forams 10 10	
										Minor 10YR 7/8	
										Grain Size	
										1-130 2-60 3-50	
										10YR 5/3 sand 1.7 1.3 2.2	
										and 10YR 3/3 silt 57.4 57.4 60.3	
										10YR 6/4 silt 57.4 57.4 60.3	
										10YR 6/4 clay 41.0 41.3 37.4	
										and 10YR 4/3	
										Carbon-Carbonate	
										1-142 2-85 3-57	
										t. carb 10.9 11.0 11.3	
										o. carb 0.1 0.1 0.1	
										CaCO ₃ 90.0 91.0 93.0	
										Bulk X-ray	
										1-134	
										amor 22.0	
										calc 97.8	
										goet 2.2	
										Core Catcher	
										CC	

Explanatory notes in Chapter 2



SITE 319

Site 319 Hole Core 13 Cored Interval: 111.5-114.5 m

AGE	ZONE			FOSSIL CHARACTER			SECTION METERS	LITHOLOGY	DEFORMATION	LITHO. SAMPLE	LITHOLOGIC DESCRIPTION
	FORAMS	NANNOS	RADS	FORAMS	NANNOS	RADS					
							0	VOID			BASALT Original recovery was 0.8 meter. Styrofoam spacers, each about 2 cm in width, are used to separate core segments that probably are not part of a continuous core sequence. Therefore, the length portrayed is greater than the actual amount recovered. See the accompanying detailed Section description for petrography and interpretations.
							1			57	
										77	
										84	
										97	
										103	
										110	
										126	
										140	

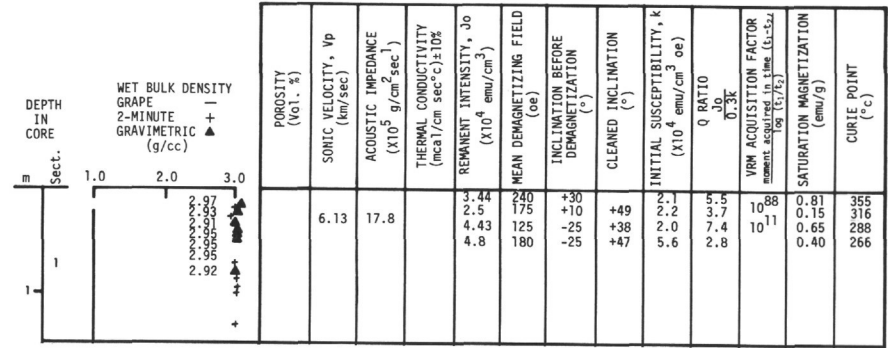
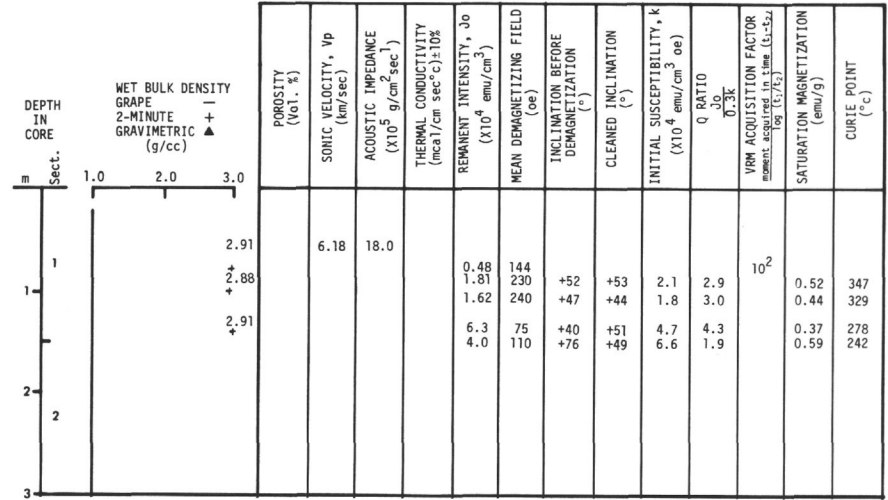
Site 319 Hole Core 14 Cored Interval: 114.5-116.5 m

AGE	ZONE			FOSSIL CHARACTER			SECTION METERS	LITHOLOGY	DEFORMATION	LITHO. SAMPLE	LITHOLOGIC DESCRIPTION
	FORAMS	NANNOS	RADS	FORAMS	NANNOS	RADS					
							0	VOID			BASALT About 0.1 meter was recovered in the core catcher.
								Core Catcher			

Site 319 Hole A Core 1 Cored Interval: 98.0-107.5 m

AGE	ZONE			FOSSIL CHARACTER			SECTION METERS	LITHOLOGY	DEFORMATION	LITHO. SAMPLE	LITHOLOGIC DESCRIPTION
	FORAMS	NANNOS	RADS	FORAMS	NANNOS	RADS					
							0	VOID			BASALT The original recovery was 1.1 meters. Styrofoam spacers, each about 2 cm wide, are used to separate core segments that probably are not part of a continuous core sequence. Therefore, the length portrayed here is greater than the actual amount recovered. See the accompanying Section description for details concerning the petrography and interpretations.
							1			48	
										105	
										110	
										138	

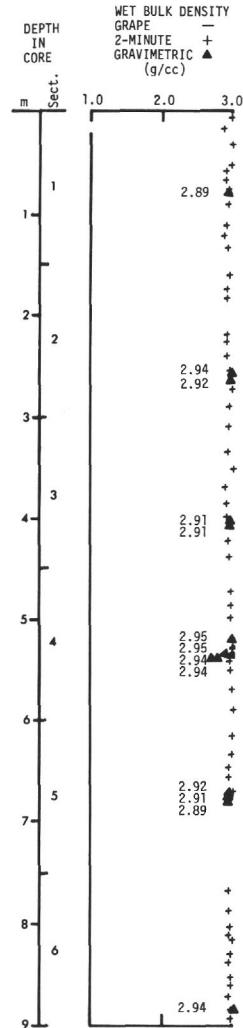
Explanatory notes in Chapter 2



Site 319 Hole A Core 3 Cored Interval: 117.0-126.5 m

AGE	ZONE		FOSSIL CHARACTER			SECTION METERS	LITHOLOGY	DEFORMATION	LITHO. SAMPLE	LITHOLOGIC DESCRIPTION
	FORAMS	NANNOS	RADS	FORAMS	NANNOS					
						0	VOID			<p>BASALT</p> <p>Original recovery was 7.3 meters. Styro-foam spacers, each about 2 cm wide, are used to separate core segments that are not part of a continuous core sequence. Therefore, the length portrayed here is greater than the actual amount recovered. See the detailed descriptions in the accompanying Section descriptions.</p>
						0.5				
						1			78	
						1.0				
							VOID		5	
						2				
						3			106	
							VOID			
						4				
									125	
									140	
							VOID		12	
									33	
									59	
									75	
									90	
									98	
									103	
									115	
									117	
							VOID			
									43	
									115	
									146	

Explanatory notes in Chapter 2



DEPTH IN CORE	SONIC VELOCITY, Vp (km/sec)	ACOUSTIC IMPEDANCE (X10 ⁵ g/cm ² sec)	THERMAL CONDUCTIVITY (mca/cm sec c) ±10%	REMANENT INTENSITY, Jo (X10 ⁴ emu/cm ³)	MEAN DEMAGNETIZING FIELD (oe)	INCLINATION BEFORE DEMAGNETIZATION (°)	CLEANED INCLINATION (°)	INITIAL SUSCEPTIBILITY, k (X10 ⁴ emu/cm ³ oe)	Q RATIO Jo/0.3k	VM ACQUISITION FACTOR moment acquired in time (t1-t2)/log (t1/t2)	SATURATION MAGNETIZATION (emu/g)	CURIE POINT (°C)	
1				4.3		-50	+54	13.0 17.0		10 ⁵⁴			
1				20.3	20	-38	+38	30		0.18		145	
2				17.1	135(T)	-71	+8			0.04		130	
2				11.0	235	-21	+48	3.4 1.4		0.13		250	
3	6.11	17.8		7.52 16.5	280(T) 100	+34 -57	+56	2.0	28	1.1 10 ⁴⁶	0.47	382	
3				25 .03	150	+13 +48	+63 +55	5.0		10 ²³			
3				15.8		-72	+59	16.0 23.0		0.10		165	
4				2.91 2.91	10.8 17	70.0 415(T)	+43 +16	+68 +67	33.1	1.1	15.6	1.02	151
4					18.3	60	+09	-80	33.0 29.0		0.03		145
4	6.21	18.3		2.95 2.95 2.94 2.94									
6					13	175(T)	+23	+66		4.33			
6					25.7		+65	+79		2.9	3.04	145	
5					4.9	315(T)	+12	+74		10 ³⁴			
5				2.92 2.91 2.89	12.5 17.7 19.9	60 55	+26 +39 -34	+36 +85 +61	27.0 29.0 30.3 28.6	0.05		160 147 144	
7								2.4	1.9	2.3	1.05 1.2		
8								2.7					
6								1.4					
9				2.94									

Site 319 Hole A Core 4 Cored Interval: 126.5-128.5 m

AGE	ZONE			FOSSIL CHARACTER			SECTION METERS	LITHOLOGY	DEFORMATION	LITHO. SAMPLE	LITHOLOGIC DESCRIPTION
	FORAMS	NANNOS	RADS	FORAMS	NANNOS	OTHERS					
							0	VOID			BASALT The amount recovered is about 0.6 meters as shown. See the accompanying Section description for detail.
							0.5				
							1.0				

Site 319 Hole A Core 5 Cored Interval: 128.5-138.0 m

AGE	ZONE			FOSSIL CHARACTER			SECTION METERS	LITHOLOGY	DEFORMATION	LITHO. SAMPLE	LITHOLOGIC DESCRIPTION
	FORAMS	NANNOS	RADS	FORAMS	NANNOS	OTHERS					
							0	VOID			BASALT Original recovery was 1.1 meters. Styrofoam spacers make the length shown here greater than the amount recovered. See the accompanying Section description for details.
							0.5				
							1.0				
							1.17				
							1.30				
							1.41				

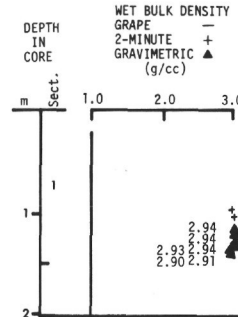
Site 319 Hole A Core 6 Cored Interval: 138.0-147.5 m

AGE	ZONE			FOSSIL CHARACTER			SECTION METERS	LITHOLOGY	DEFORMATION	LITHO. SAMPLE	LITHOLOGIC DESCRIPTION
	FORAMS	NANNOS	RADS	FORAMS	NANNOS	OTHERS					
							0	VOID			BASALT Original recovery was 0.5 meters. Styrofoam spacers make the length shown here greater than the amount recovered. The accompanying Section description gives details of the petrography and interpretations.
							0.5				
							1.0				
							1.09				
							1.41				

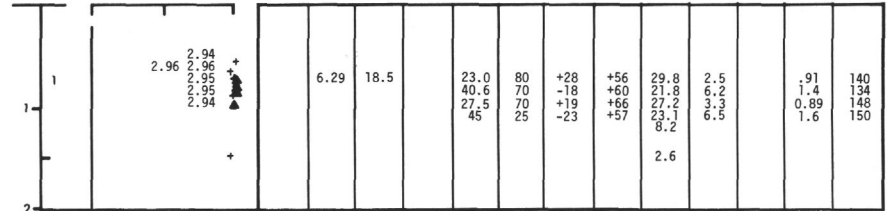
Site 319 Hole A Core 7 Cored Interval: 147.5-157.0 m

AGE	ZONE			FOSSIL CHARACTER			SECTION METERS	LITHOLOGY	DEFORMATION	LITHO. SAMPLE	LITHOLOGIC DESCRIPTION
	FORAMS	NANNOS	RADS	FORAMS	NANNOS	OTHERS					
							0	VOID			BASALT Original recovery was 1.0 meter. Styrofoam spacers make length shown here greater than the amount recovered. See the accompanying Section description for details on petrography and interpretations.
							0.5				
							1.0				
							1.10				
							1.19				
							1.47				

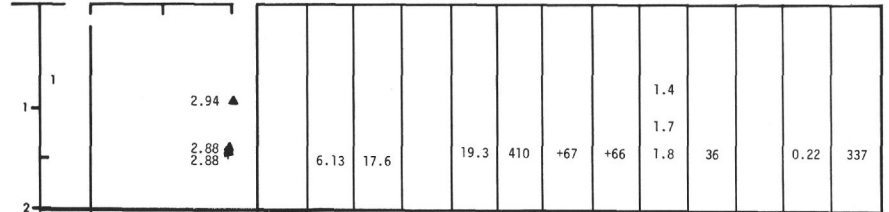
Explanatory notes in Chapter 2



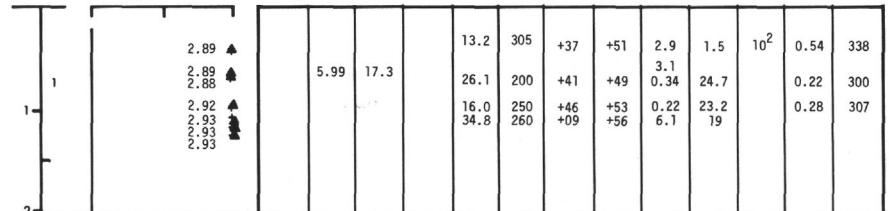
POROSIITY (Vol. %)	SONIC VELOCITY, V_p (km/sec)	ACOUSTIC IMPEDANCE ($\times 10^5$ g/cm ² sec)	THERMAL CONDUCTIVITY (mcal/cm sec ² c) $\pm 10\%$	REMANENT INTENSITY, J_0 ($\times 10^6$ emu/cm ³)	MEAN DEMAGNETIZING FIELD (oe)	INCLINATION BEFORE DEMAGNETIZATION ($^\circ$)	CLEANED INCLINATION ($^\circ$)	INITIAL SUSCEPTIBILITY, k ($\times 10^4$ emu/cm ³ oe)	Q RATIO $\frac{J_0}{0.3k}$	VRM ACQUISITION FACTOR (moment acquired in time 15-5.7 log (17/57))	SATURATION MAGNETIZATION (emu/g)	CURIE POINT ($^\circ$ C)
	6.05	17.5		26.0 24.9 71.8 60.1	70 75 210 10	-6 -22 -53 -56	+64 +63 +64 +58	24.7 28.3 16.7 16.3	3.4 2.8 14 12	2.4	0.97 0.86 1.3 1.5	153 152 181 172



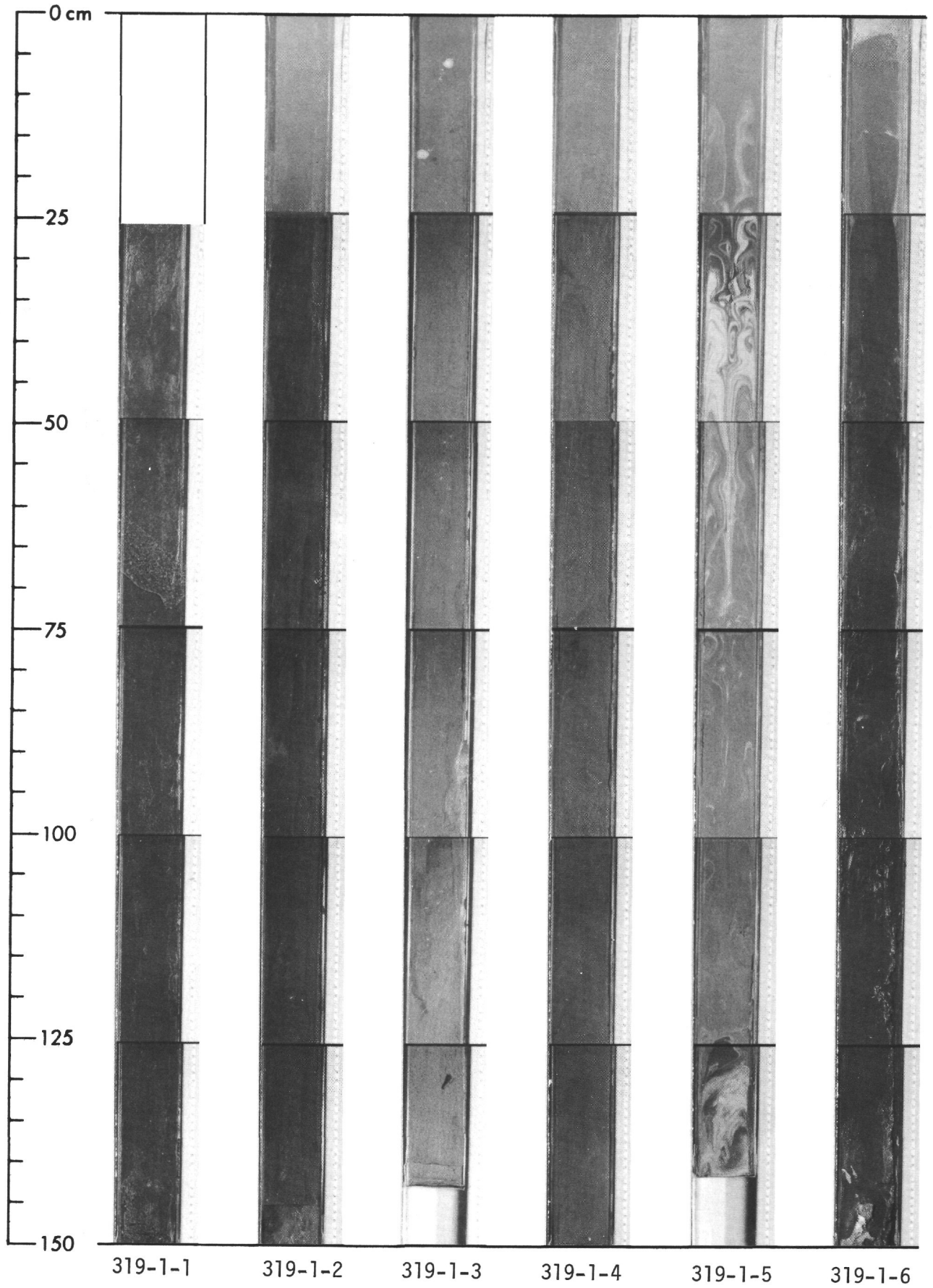
POROSIITY (Vol. %)	SONIC VELOCITY, V_p (km/sec)	ACOUSTIC IMPEDANCE ($\times 10^5$ g/cm ² sec)	THERMAL CONDUCTIVITY (mcal/cm sec ² c) $\pm 10\%$	REMANENT INTENSITY, J_0 ($\times 10^6$ emu/cm ³)	MEAN DEMAGNETIZING FIELD (oe)	INCLINATION BEFORE DEMAGNETIZATION ($^\circ$)	CLEANED INCLINATION ($^\circ$)	INITIAL SUSCEPTIBILITY, k ($\times 10^4$ emu/cm ³ oe)	Q RATIO $\frac{J_0}{0.3k}$	VRM ACQUISITION FACTOR (moment acquired in time 15-5.7 log (17/57))	SATURATION MAGNETIZATION (emu/g)	CURIE POINT ($^\circ$ C)
	6.29	18.5		23.0 40.6 27.5 45	80 70 70 25	+28 -18 +19 -23	+56 +60 +66 +57	29.8 21.8 27.2 23.1 8.2	2.5 6.2 3.3 6.5		.91 1.4 0.89 1.6	140 134 148 150

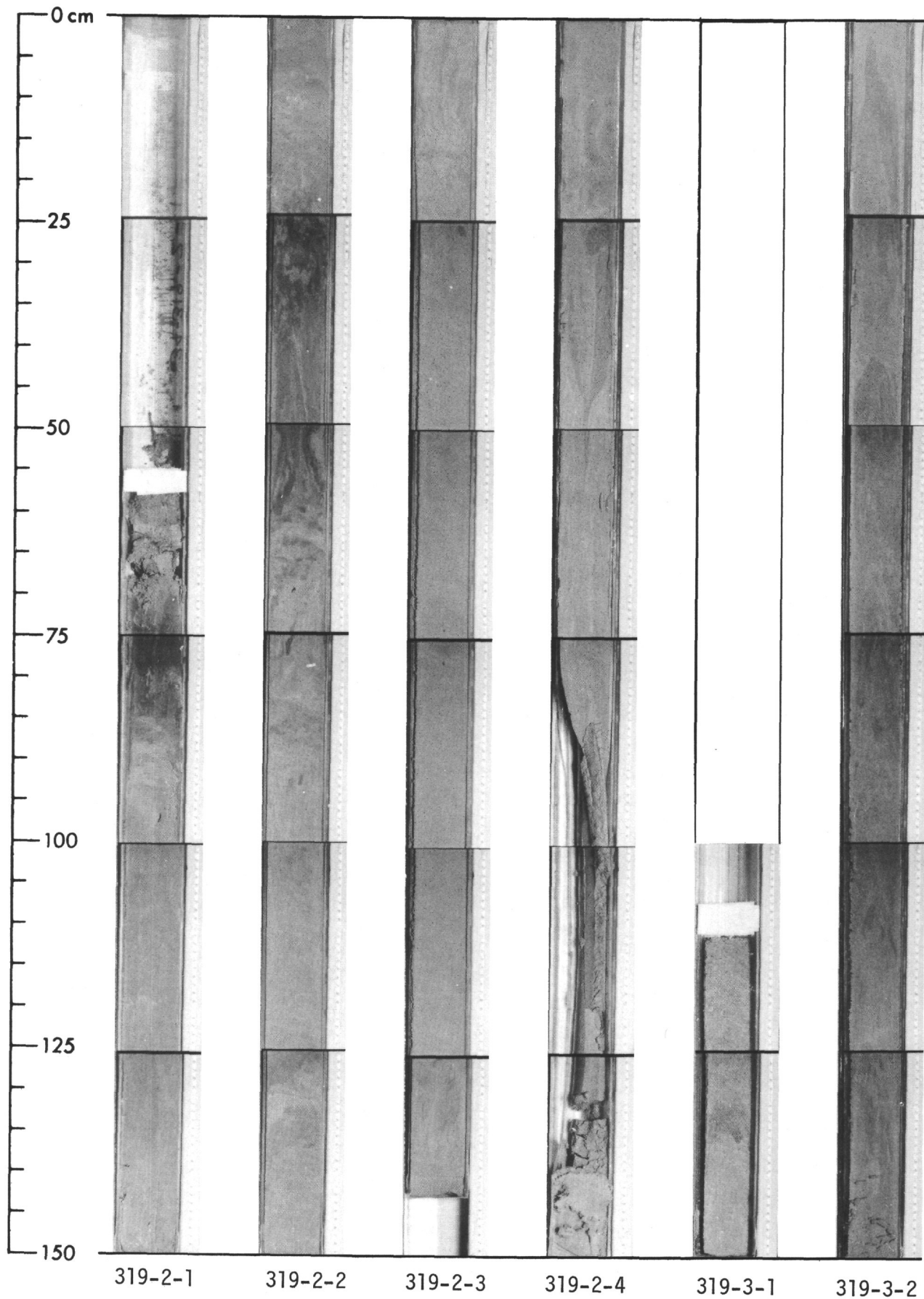


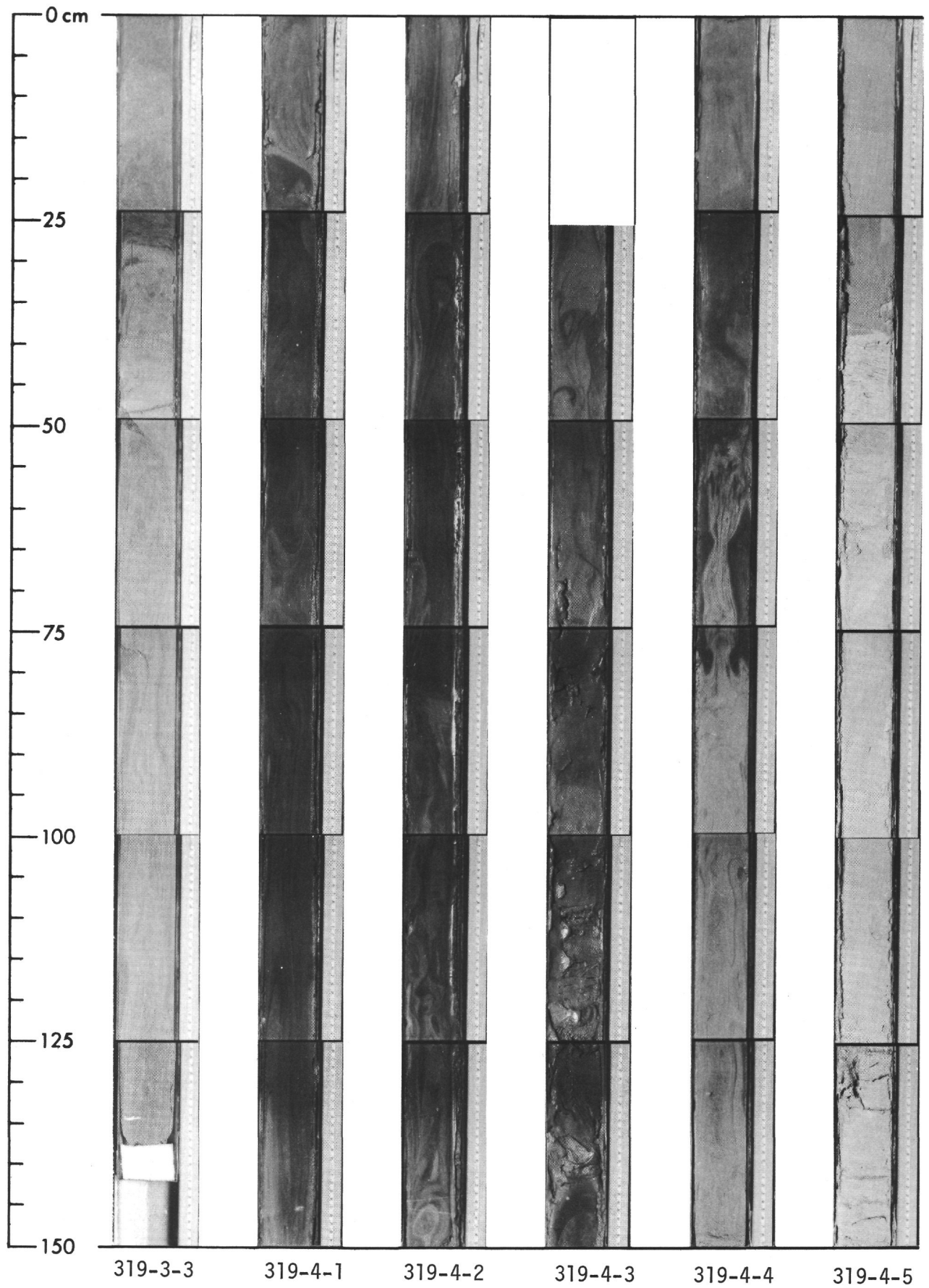
POROSIITY (Vol. %)	SONIC VELOCITY, V_p (km/sec)	ACOUSTIC IMPEDANCE ($\times 10^5$ g/cm ² sec)	THERMAL CONDUCTIVITY (mcal/cm sec ² c) $\pm 10\%$	REMANENT INTENSITY, J_0 ($\times 10^6$ emu/cm ³)	MEAN DEMAGNETIZING FIELD (oe)	INCLINATION BEFORE DEMAGNETIZATION ($^\circ$)	CLEANED INCLINATION ($^\circ$)	INITIAL SUSCEPTIBILITY, k ($\times 10^4$ emu/cm ³ oe)	Q RATIO $\frac{J_0}{0.3k}$	VRM ACQUISITION FACTOR (moment acquired in time 15-5.7 log (17/57))	SATURATION MAGNETIZATION (emu/g)	CURIE POINT ($^\circ$ C)
	6.13	17.6		19.3	410	+67	+66	1.4 1.7 1.8	36		0.22	337

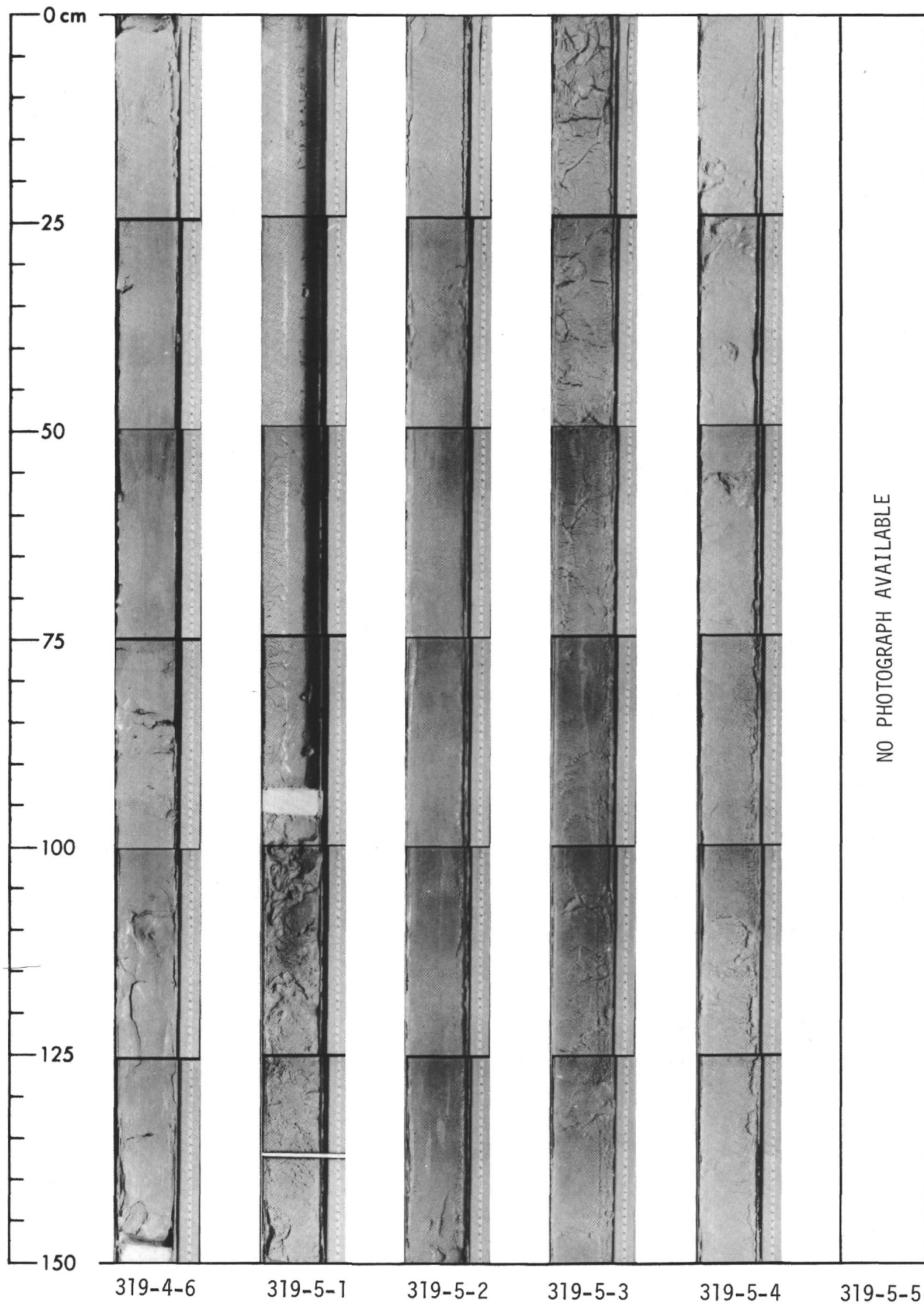


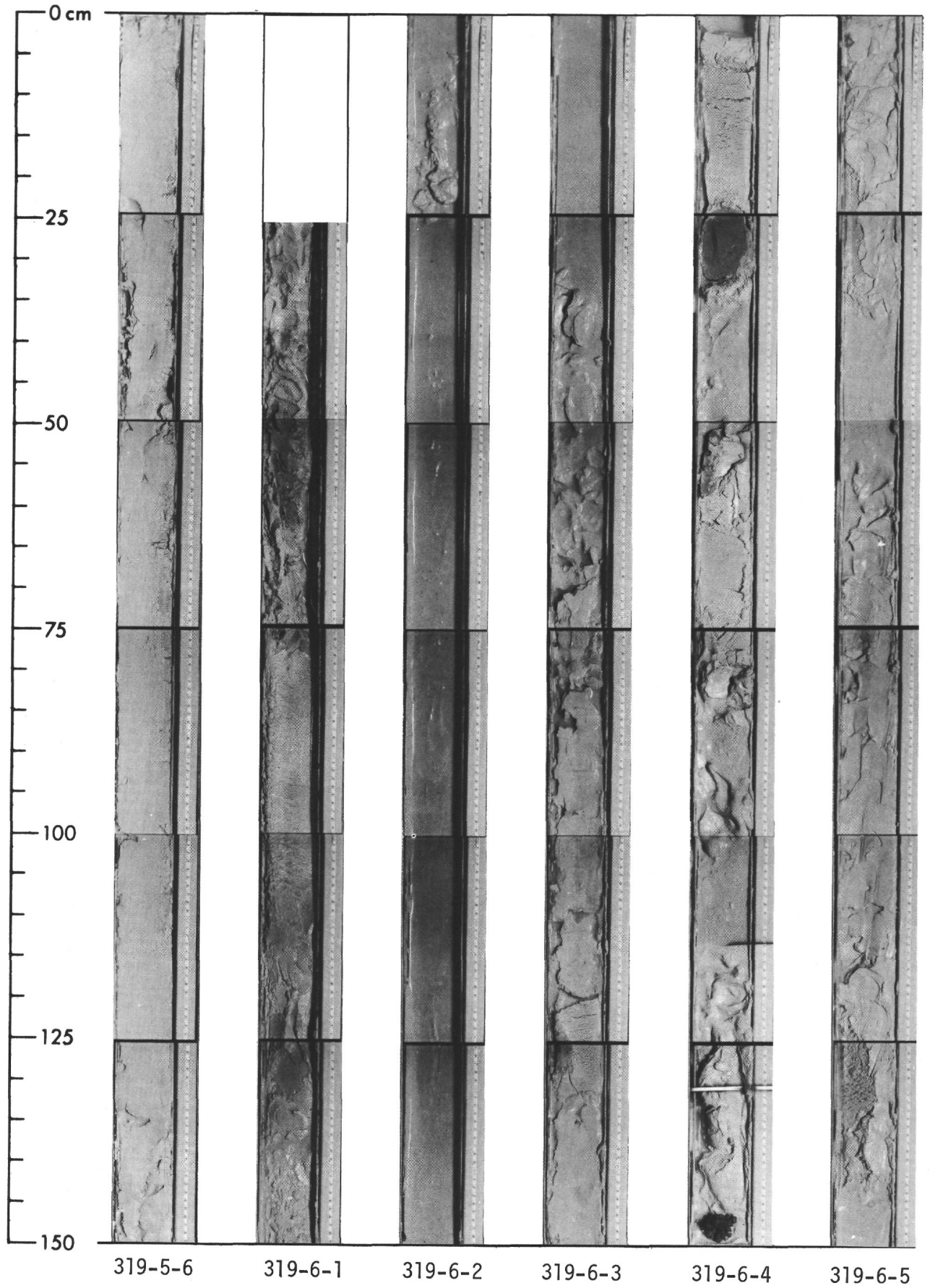
POROSIITY (Vol. %)	SONIC VELOCITY, V_p (km/sec)	ACOUSTIC IMPEDANCE ($\times 10^5$ g/cm ² sec)	THERMAL CONDUCTIVITY (mcal/cm sec ² c) $\pm 10\%$	REMANENT INTENSITY, J_0 ($\times 10^6$ emu/cm ³)	MEAN DEMAGNETIZING FIELD (oe)	INCLINATION BEFORE DEMAGNETIZATION ($^\circ$)	CLEANED INCLINATION ($^\circ$)	INITIAL SUSCEPTIBILITY, k ($\times 10^4$ emu/cm ³ oe)	Q RATIO $\frac{J_0}{0.3k}$	VRM ACQUISITION FACTOR (moment acquired in time 15-5.7 log (17/57))	SATURATION MAGNETIZATION (emu/g)	CURIE POINT ($^\circ$ C)
	5.99	17.3		13.2 26.1 16.0 34.8	305 200 250 260	+37 +41 +46 +09	+51 +49 +53 +56	2.9 3.1 0.34 24.7	1.5 10 ² 0.22 19		0.54 0.22 0.28	338 300 307

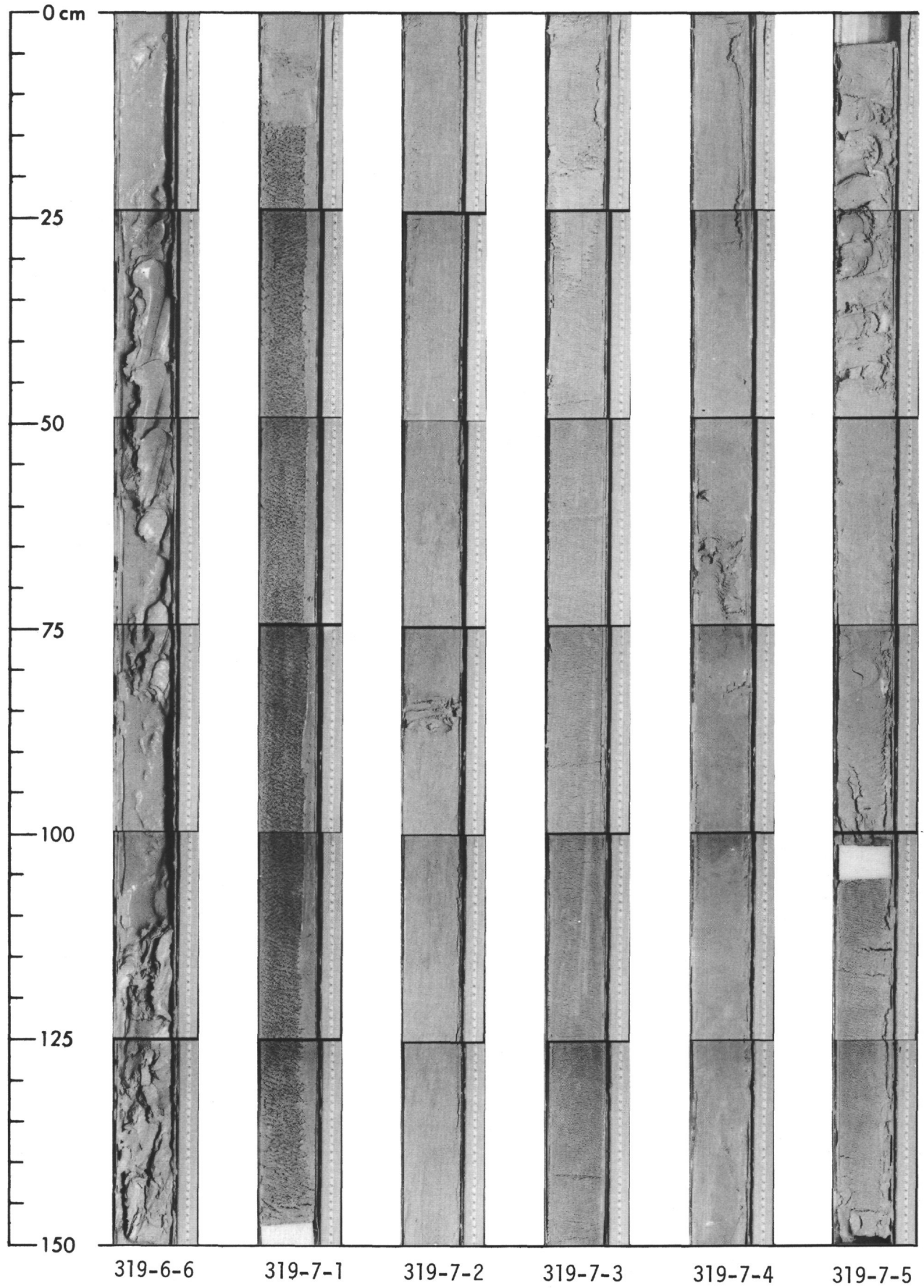


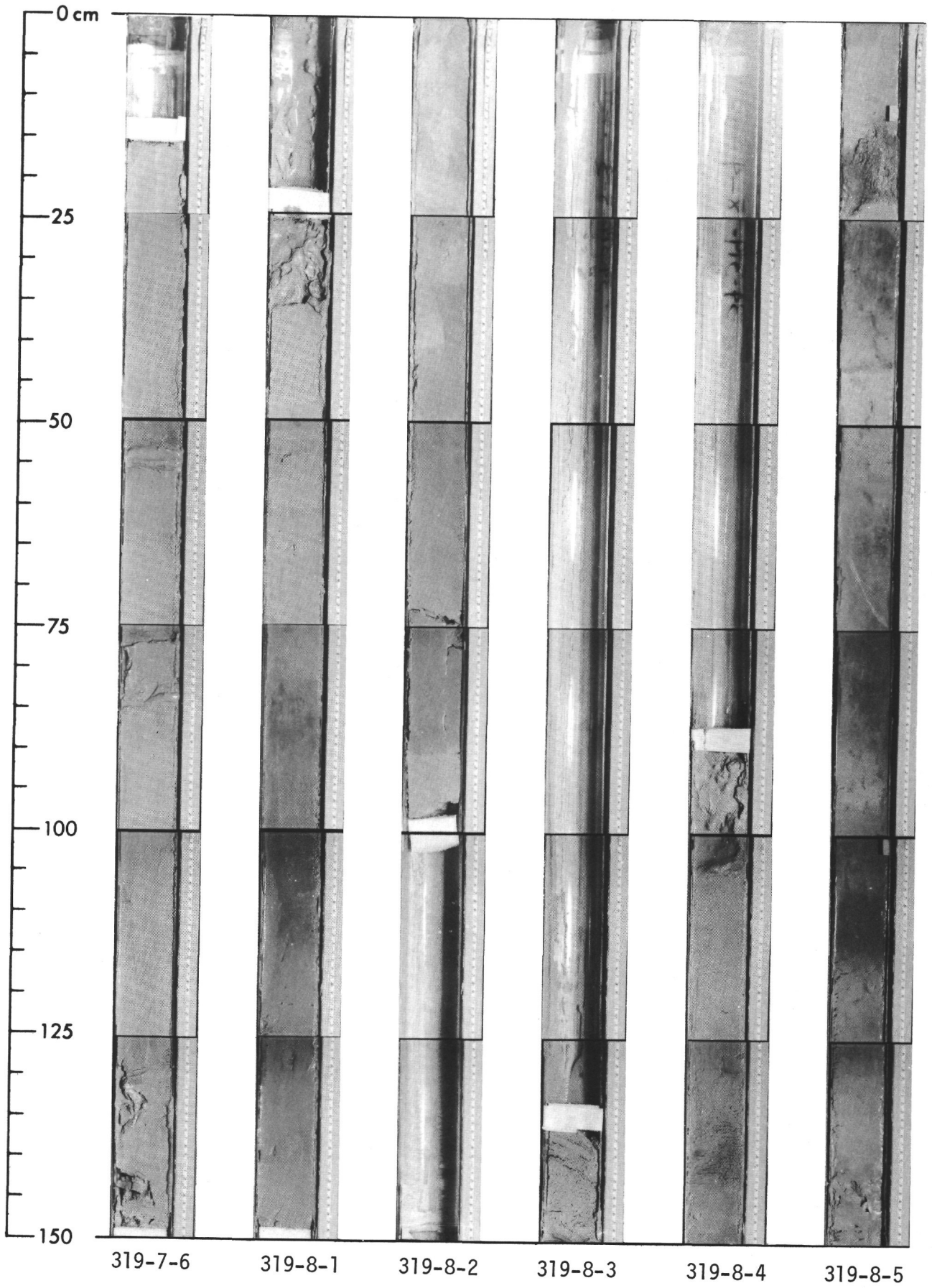


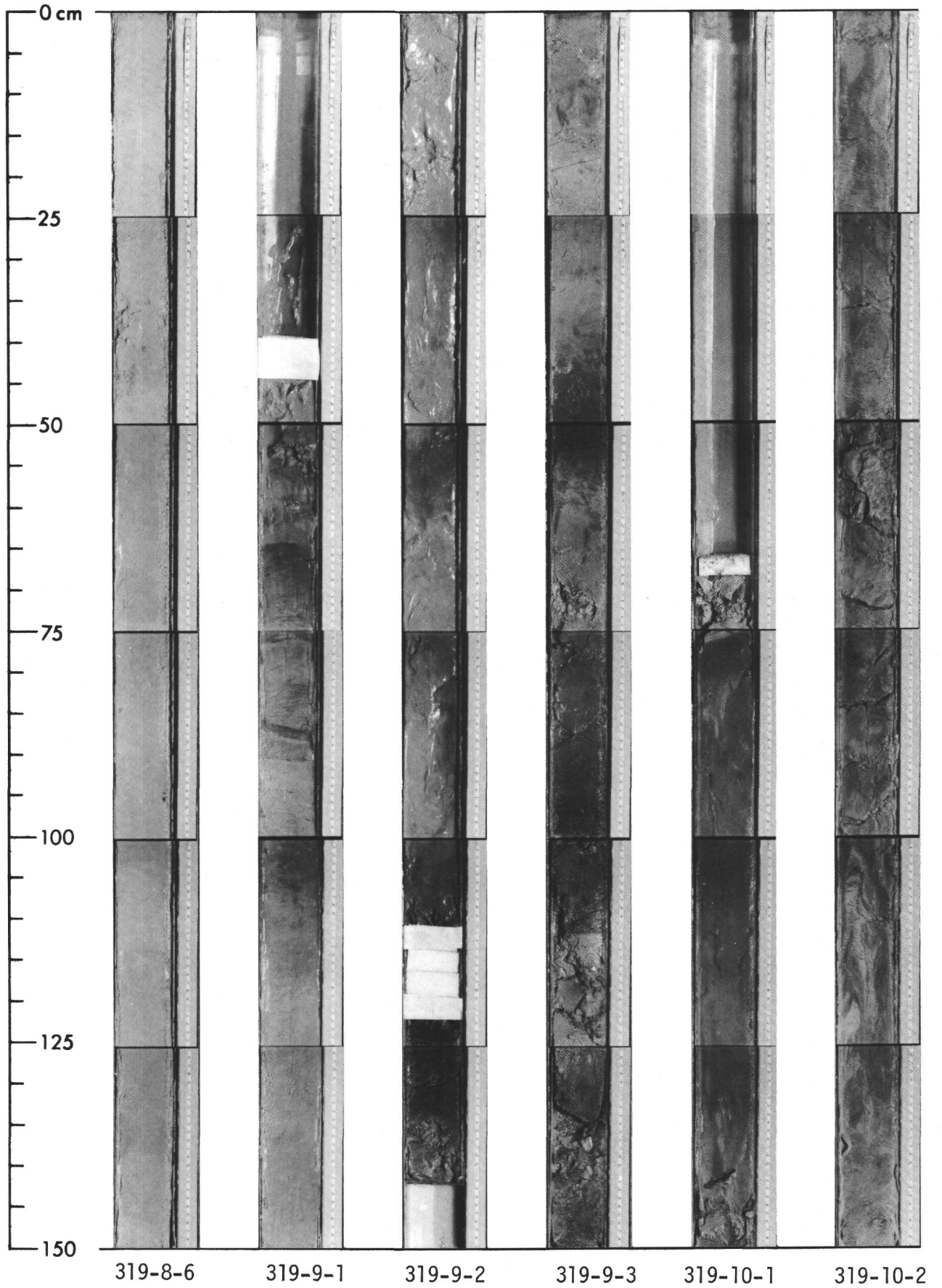


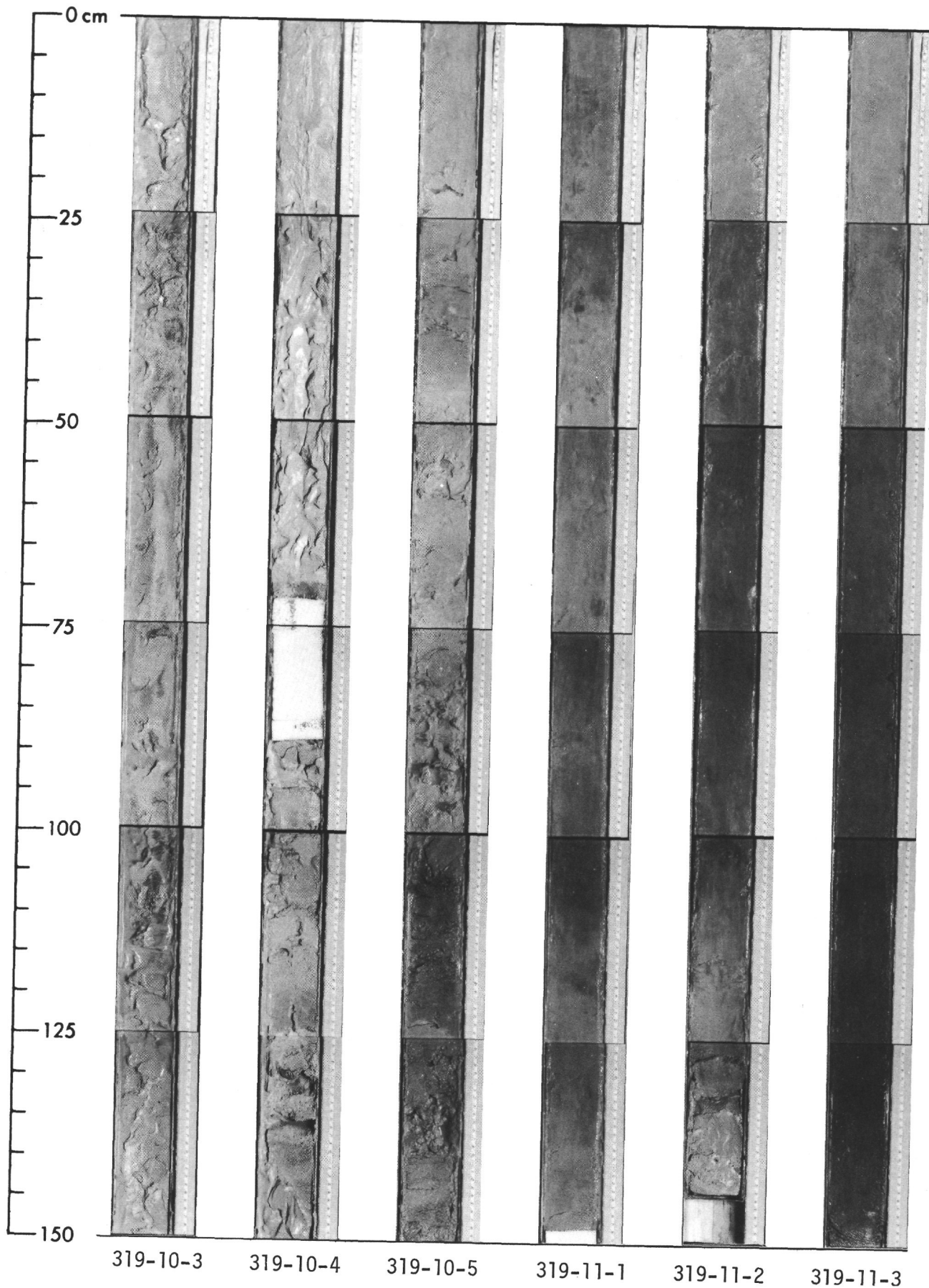


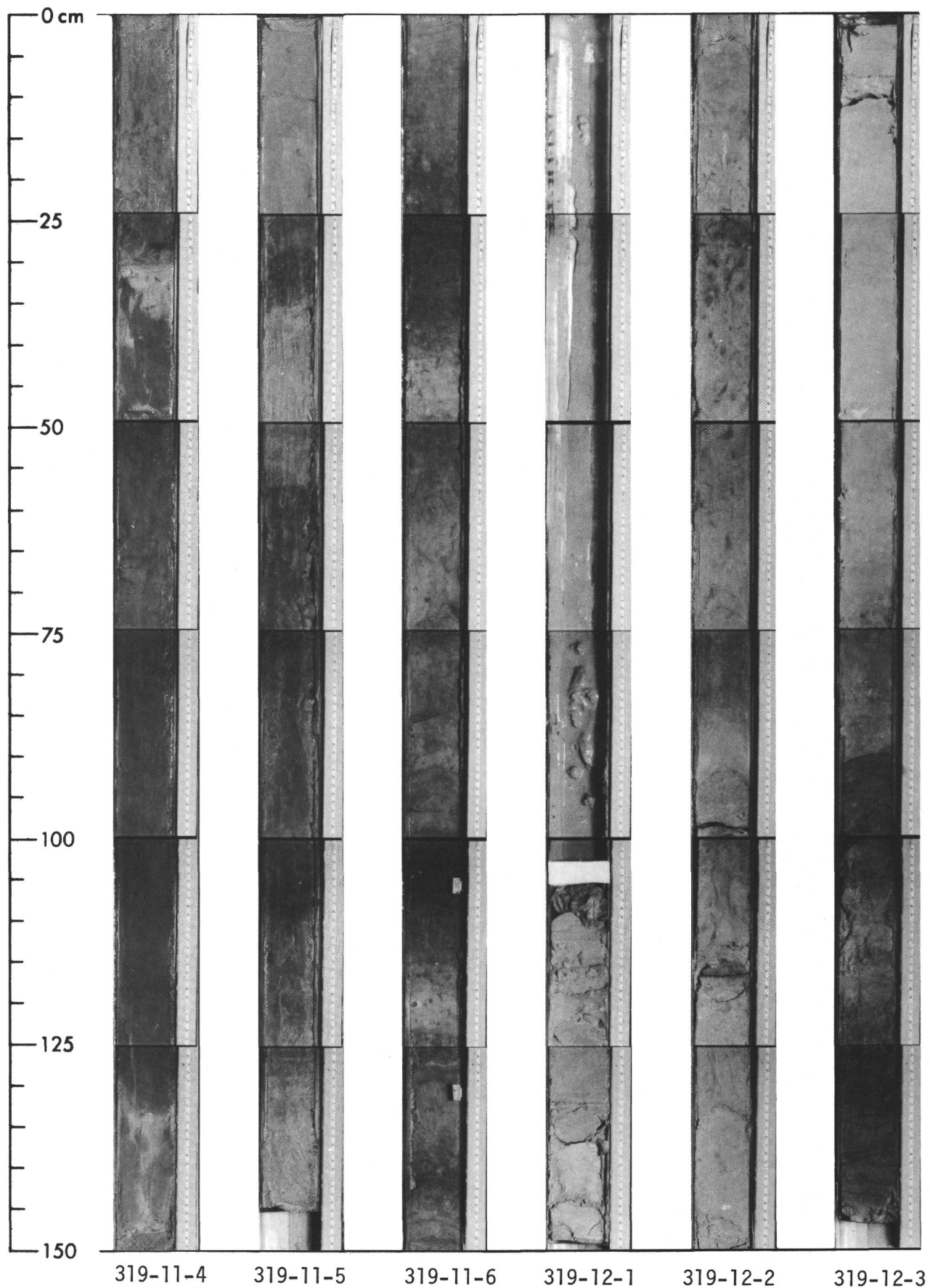


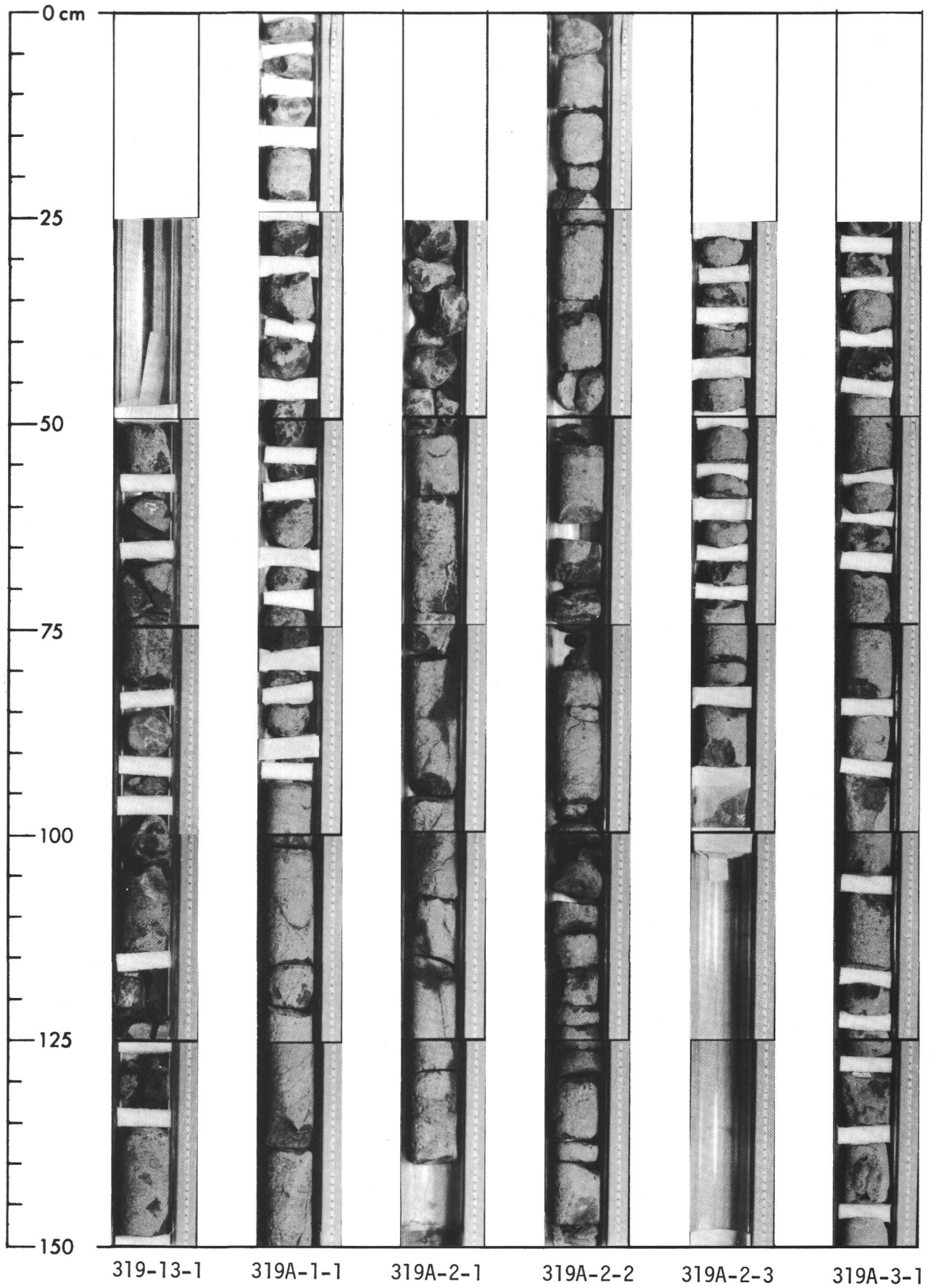


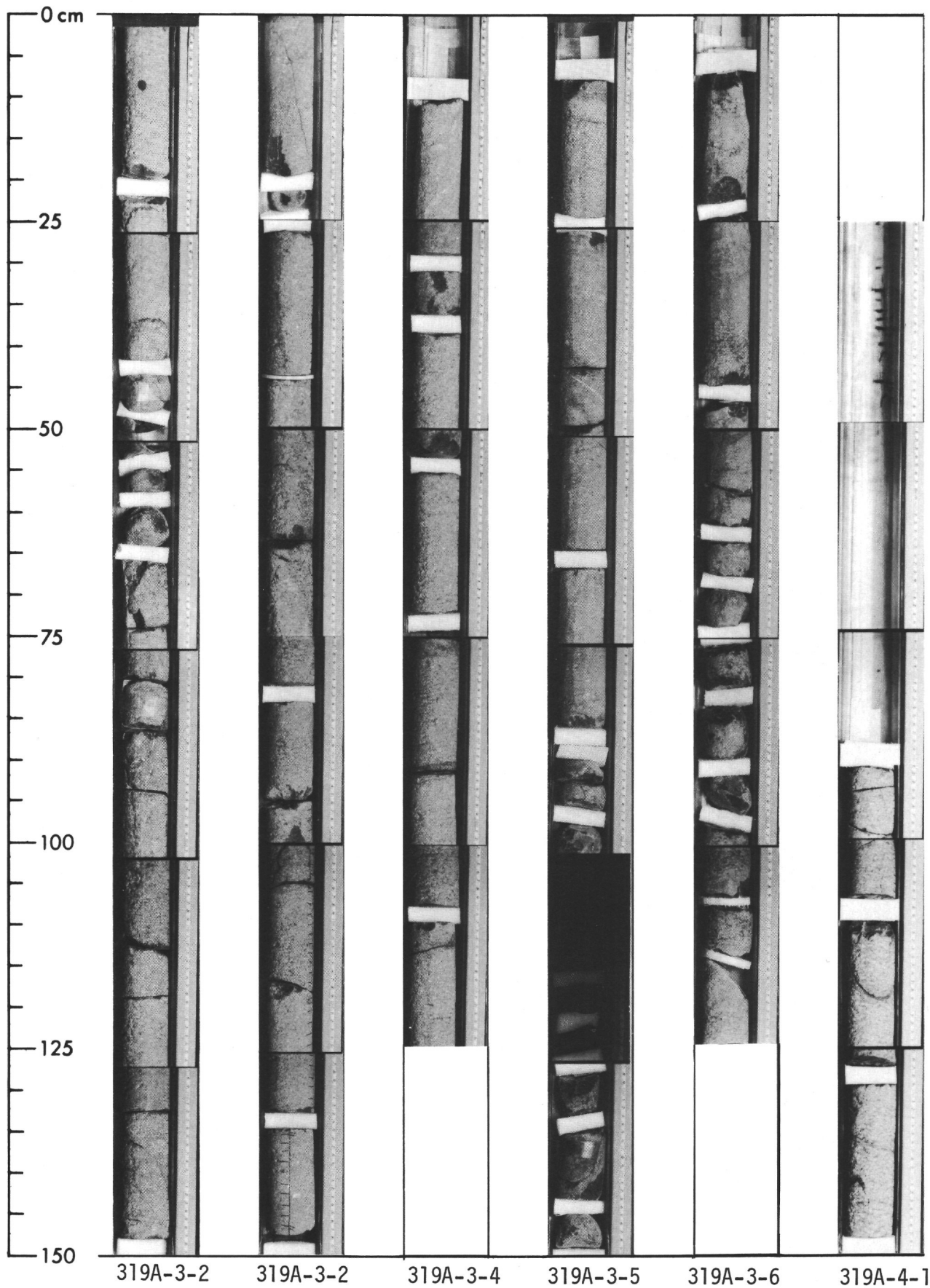


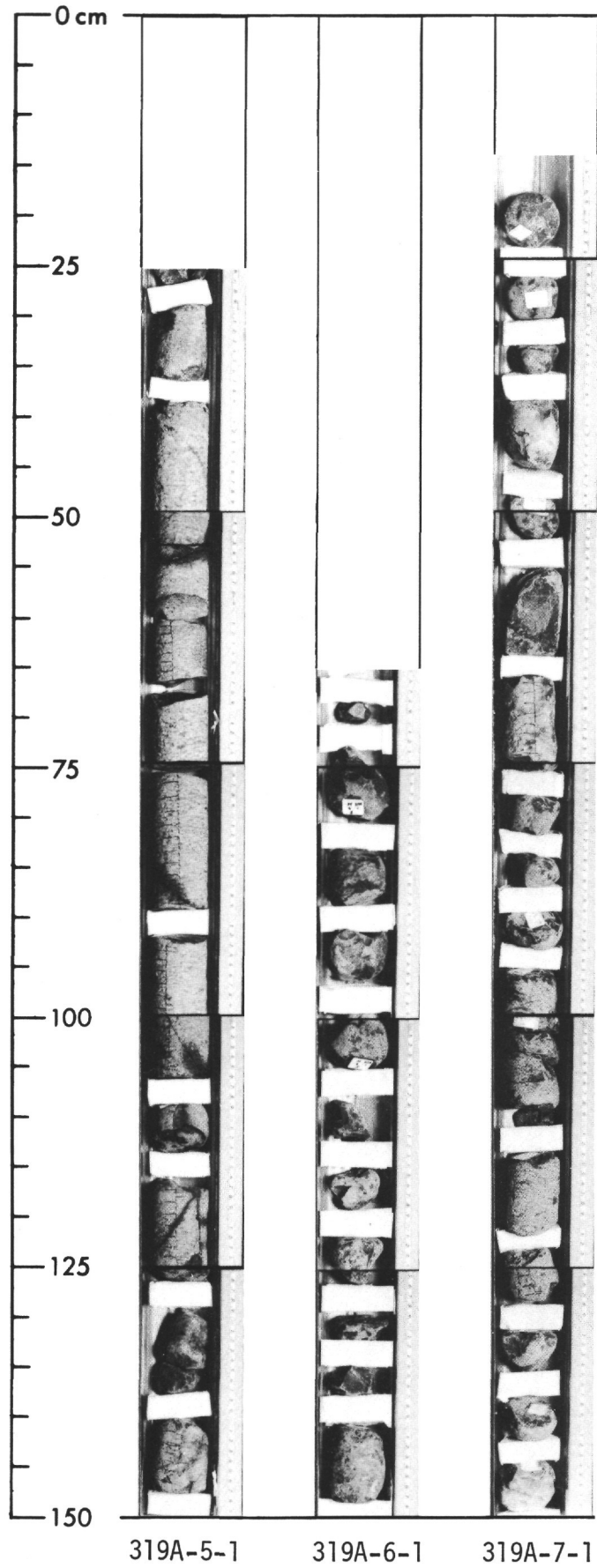






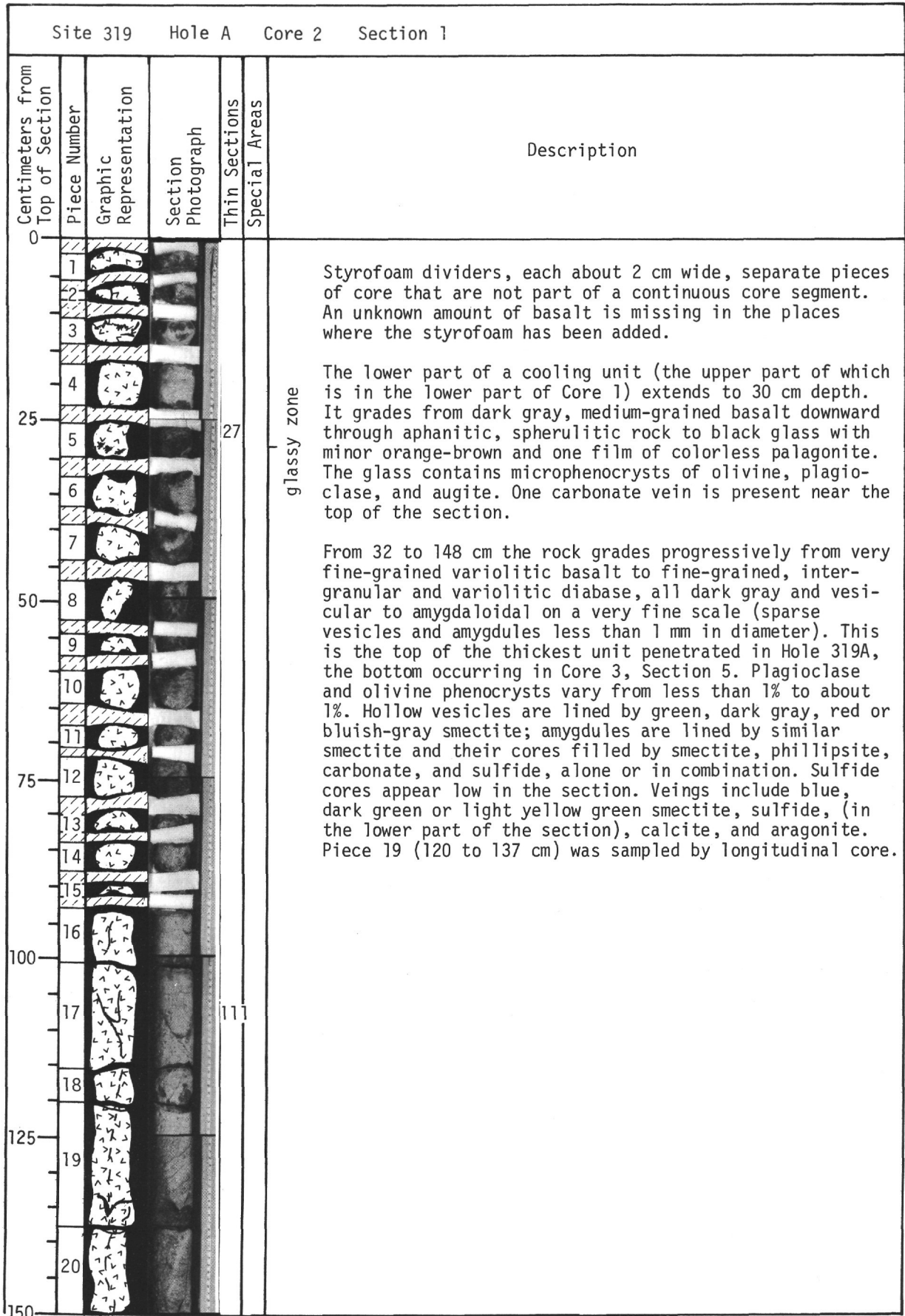






Site 319 Hole Core 13 Section 1				
Centimeters from Top of Section	Piece Number	Graphic Representation	Section Photograph	Description
0				<p>Styrofoam dividers, each about 2 cm wide, separate pieces of core that are not part of a continuous core segment. An unknown amount of basalt is missing in the places where the styrofoam has been added.</p> <p>The boundaries of 3 cooling units occur at about 64 and 131 cm. The uppermost unit grades from fine-grained, spherulitic to finely variolitic, medium gray to dark brownish gray basalt, downward to an incomplete black glassy selvage with minor orange and colorless palagonite. Microphenocrysts (1% or less) include plagioclase and euhedral to skeletal olivine; the olivine commonly is altered to yellow smectite and Fe-oxide. Veins include carbonate and red-brown smectite.</p>
25	VOID			
50	1			<p>The unit from 66 to 126 cm is mainly very fine-grained, dark yellowish gray basalt, varying to aphanitic at the base. Textures are very fine variolitic to intergranular. Microphenocrysts of olivine and plagioclase range from almost none to about 1%, being most abundant at top and bottom. The olivine is almost wholly altered to smectite and minor carbonate; fresh remnants have positive 2V (more magnesian than Fo₈₅). Pyroxene 2V's suggest the presence of some subcalcic augite and possibly pigeonite in addition to the usual augite. Diktytaxitic vugs occur below 83 cm. Veins include calcite, possibly minor aragonite, and yellow, green and brown smectite, Mn-oxide spots and dendrites, and Fe-oxide stains. A thick vertical calcite vein below 97 cm encloses spalls of basalt and appears to have filled an open joint.</p>
57	2			
75	3			<p>The bottom unit (133 to 148 cm) is fine-grained, sparsely microphyric (2.7% plagioclase and altered olivine), medium to dark yellowish gray basalt cut by one calcite vein.</p> <p>All pieces are parts of joint blocks in which sharply bounded, diffusion-controlled color zones reflect bounding joints, most of which lay outside the recovered core. The colors are darker and/or yellower or browner nearer the joints.</p>
77	4			
84	5			<p>glass</p>
97	6			
100	7			<p>veined area</p>
103	8			
110	9			<p>veined area</p>
126	10			
140	11			
150				

Site 319 Hole A Core 1 Section 1							
Centimeters from Top of Section	Piece Number	Graphic Representation	Section Photograph	Thin Sections	Special Areas	Description	
0	1		PHOTO MISSING				<p>Styrofoam dividers, each about 2 cm wide, separate pieces of core that are not part of a continuous core segment. An unknown amount of basalt is missing in the places where the styrofoam has been added.</p> <p>A cooling unit extends from the top of Section 1 to at least 115 and possibly 122 cm. The grain size increases from aphanitic at the top to coarse-grained basalt at 38 cm, remaining coarse-grained to about 98 cm, and decreasing thereafter to fine-grained variolitic (plumose) basalt at the base. The rock varies from dark gray (rarely medium gray), where fresh, to dark brownish or yellowish gray. Microphenocrysts of plagioclase and altered olivine range in abundance from 1% at the top to almost nil through most of the unit, to 1 to 2% below 104 cm, with a suggestion of accumulation in the interval 104 to 107 cm. Olivine is replaced by olive green smectite. Small diktytaxitic vugs appear from 29 to 46 cm and at 109 to 115 cm, and rare large vugs with aragonite occur at 77 to 81 cm. Veins include red, brown, red-brown, yellow-brown, yellow, greenish yellow, green, and blue smectite, calcite Fe-oxide, Mn-oxide, and phillipsite(?). Conical calcite crystals line open joints at 77 to 81 cm.</p> <p>An incomplete cooling unit, whose base is in Section 2, extends from 123 to 148 cm. It is dark gray to dark brownish gray, very fine-grained to coarse-grained, variolitic (plumose), aphyric to microphyric basalt. Plagioclase, augite, and olivine microphenocrysts comprise about 1% of the interval from 137 to 142 cm. The olivine, except for rare remnants, is altered to smectite and/or calcite. Veins are composed of red, brown, red-brown, and greenish brown smectite, Mn-oxide, and minor calcite. Diktytaxitic vugs at 137 to 142 cm contain phillipsite, minor aragonite, and calcite, with traces of Mn-oxide.</p>
	2						
	3						
25	4						
	5						
	6						
50	7				18		
	8						
	9						
	10						
75	11						
	12						
	13						
	14						
	15						
100	16						
	17	BAG		05			
	18			10			
	19						
125	20	BAG					
	21						
	22	BAG		38			
	23						
150							



Site 319 Hole A Core 2 Section 2					
Centimeters from Top of Section	Piece Number	Graphic Representation	Section Photograph	Thin Sections	Special Areas
0					
1	1				
2	2			15	
25	3				
	4				
	5				
50	6				
	7				
	8				
75	9				
	10				
	11				
	12				
100	13				
	14				
	15			114	
125	16		PHOTO MISSING		
	17				
	18				
	19				
	20				
150					

Description

Styrofoam dividers, each about 2 cm wide, separate pieces of core that are not part of a continuous core segment. An unknown amount of basalt is missing in the places where the styrofoam has been added.

This section is uniformly a fine-grained dark brownish-gray diabase (to dark gray) with phenocrysts (mostly or solely of plagioclase) varying in abundance from zero to almost 1%. A 5 mm-long plagioclase phenocryst from the interval 51 to 58 cm is An₇₀₋₇₁ (Tsuboi method). The recovered pieces of core are generally unjointed and un-veined, but their small size and commonly intense brown staining indicate that they are joint blocks, the present surfaces of which were near the natural bounding joints. The freshest rocks were recovered in the interval 110 to 127 cm in which a horizontal brownish alteration zone indicates that the two pieces were separated by a horizontal vein or joint. The few cracks observed are tight and commonly stained by Fe-oxide. The few veins seen, all of which are thin to very thin, are composed of green, yellow, or brown smectite, and carbonate. The carbonate is a mixture of calcite and aragonite in small vein remnants at 65 cm depth. Crossfiber veins of both smectite (interval 1 to 33 cm) and carbonate (interval 145 to 150 cm) are present. At 134 cm, a surface coated by conical calcite and magnesian calcite(?) crystals indicates an open joint; it coincides with especially intense brown alteration.

Site 319 Hole A Core 2 Section 3					
Centimeters from Top of Section	Piece Number	Graphic Representation	Section Photograph	Thin Sections	Special Areas
0					
	1		PHOTO MISSING		<p>Styrofoam dividers, each about 2 cm wide, separate pieces of core that are not part of a continuous core segment. An unknown amount of basalt is missing in the places where the styrofoam has been added.</p> <p>Fine-grained dark brownish gray diabase which, near the bottom of the section at about 84 cm, has coarsened to fine- to medium-grained diabase. Megascopic phenocrysts are sparse. A thin section of medium-grained diabase (86 to 89 cm) indicates ophitic texture with pyroxene up to 1.8 mm in diameter. The pyroxene commonly has a wavy extinction which appears to be due to a complex compositional zoning. Rare plagioclase "phenocrysts" are large among plagioclase grains, but not so large as the enclosing pyroxene oikocrysts. All olivine is pseudomorphed by smectite of relatively large grain size which has second order interference colors (of a type commonly mistakenly identified as chlorite or serpentine). The pseudomorphs occur down to sizes much smaller than average plagioclase and pyroxene sizes (i.e. "groundmass" olivine). The final residue crystallized to a complex of skeletal minerals now in a smectite base.</p> <p>The core pieces are highly altered brownish-gray joint blocks which indicate that Section 3 is from a highly jointed and veined portion of the cooling unit, thus accounting for the poor recovery and small pieces. Veins are composed of brown, red-brown and rarely green smectite, and carbonate. The carbonate definitely includes aragonite in some cases examined in smear slides. Fe-oxide is a common vein constituent which lends a brown to red color. One vein in the interval 38 to 43 cm is composed of stellate arrays of finely prismatic aragonite coated by dark brown opaque material, and set in a base of orange-brown smectite superficially similar to palagonite.</p>
	2				
25	3				
	4				
	5				
	6				
	7				
50	8				
	9				
	10				
	11				
75	12				
	13				
	14			86	
	15	BAG			
100					
		VOID			
125					
150					

Site 319 Hole A Core 3 Section 2						
Centimeters from Top of Section	Piece Number	Graphic Representation	Section Photograph	Thin Sections	Special Areas	Description
0						
1				5		
25	2					
	3					
	4					
50	5					
	6					
	7					
	8					
75	9					
	10					
	11					
100	12					
	13					
125	14					
	15					
150						

Site 319 Hole A Core 3 Section 3						
Centimeters from Top of Section	Piece Number	Graphic Representation	Section Photograph	Thin Sections	Special Areas	Description
0						
1						
25	2					
3						
50						
4						
75						
5						
6						
100						
7						
8						
125						
9						
10						
150						

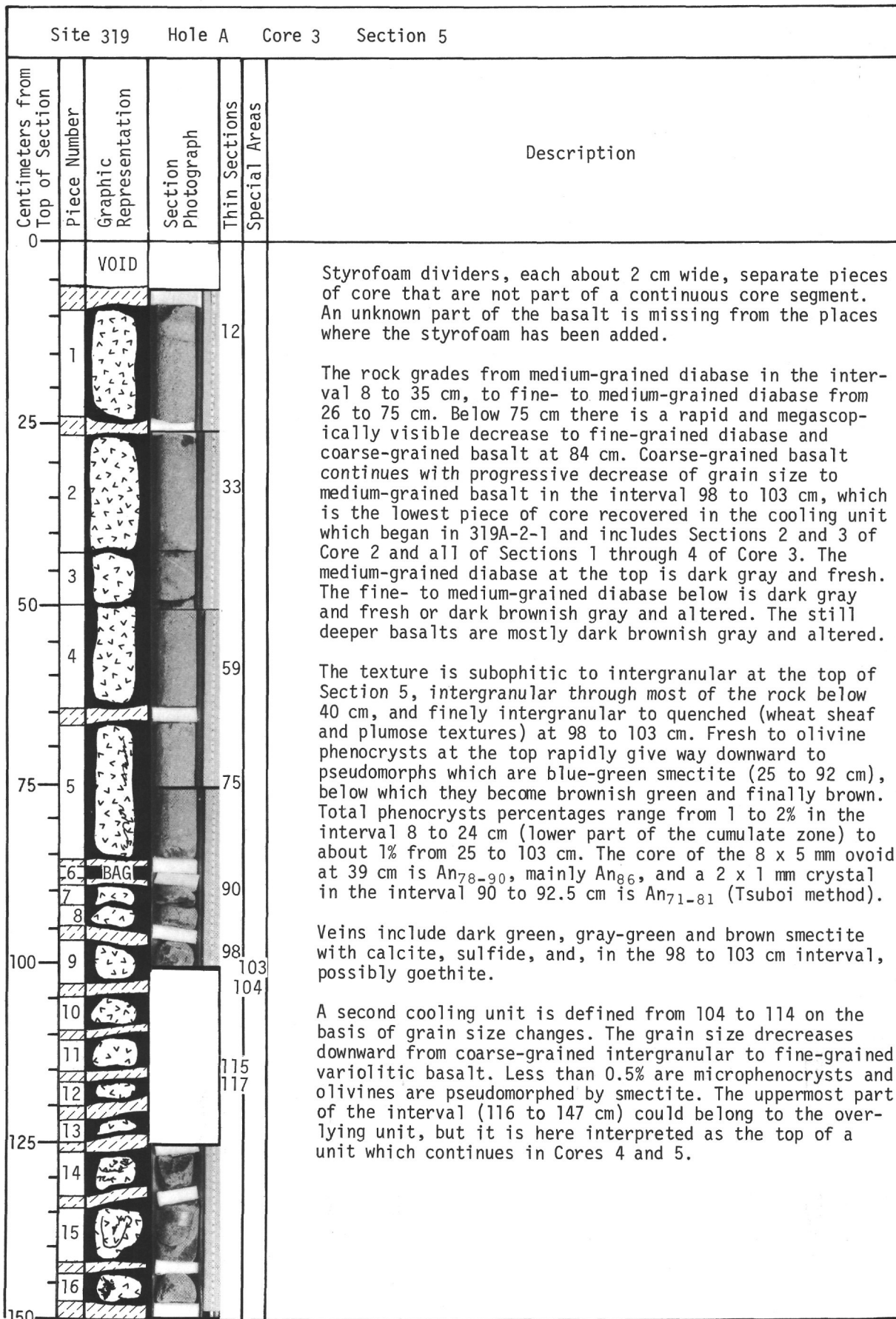
Styrofoam dividers, each about 2 cm wide, separate pieces of core that are not part of a continuous core segment. An unknown amount of basalt is missing from the places where the styrofoam has been added.

Medium-grained diabase like that in Section 2. To a depth of 74 cm there is a mixture of fresh dark gray and altered dark brownish gray rock. The brown altered parts are not related to visible joints or veins, but these presumably lay not far outside the present core which evidently penetrated large blocks bounded by widely spaced joints, thus yielding good core recovery in large pieces which are readily refitted. Below 74 cm the rock is wholly dark gray and fresh.

The abundance of plagioclase phenocrysts varies from almost zero to about 1%, with maximum sizes of 3 x 2 to 6 x 2 mm. The core compositions of two of them (Tsuboi method) are: An₇₆₋₈₈, mainly An₈₀₋₈₆ for a 5 x 3 mm crystal from 49 cm; and An₇₃₋₉₀ for a 6 x 2 mm crystal from 77 cm. Blue-green smectite pseudomorphs after olivine are scattered throughout the section.

Large portions of the core are unjointed and unveined (for instance, 21 to 33 cm and 132 to 146 cm; only one joint is seen in the 25 to 43 cm interval). Observed veins are dark green, blue-green, and brown smectite, and calcite. In at least two places the sharp, diffusion-controlled contacts between altered rock and fresh gray rock crosscut smectite veins, and the veins are brown or green to blue-green in accord with the degree of alteration of the local host rock. This fact demonstrates, as in Core 319-1-1, that the oxidative alteration and staining postdate vein deposition.

Site 319 Hole A Core 3 Section 4						
Centimeters from Top of Section	Piece Number	Graphic Representation	Section Photograph	Thin Sections	Special Areas	Description
0		VOID				<p>Styrofoam dividers, each about 2 cm wide, separate pieces of core that are not part of a continuous core segment. An unknown amount of basalt is missing from the places where the styrofoam has been added.</p> <p>Medium-grained, fresh, gray diabase with perhaps a slight grain size decrease in the interval 132 to 148 cm. The only significant alteration occurs in the bottom 3 cm and in a 1 cm-thick zone on either side of a gently dipping vein at 114 to 116 cm. A lack of correspondence of smectite colors with host rock staining suggests that the staining advanced faster than the oxidation of smectite. Both staining and the locally intense brown color of the vein at the edge of the brown altered zone may be due to high sulfide concentration in the vein prior to alteration.</p> <p>The medium-grained diabase is ophitic, whereas the somewhat finer-grained rock in the interval 132 to 148 cm tends more toward intergranular texture. Both contain well developed "quenched" groundmass with abundant skeletal crystals of plagioclase, amphibole(?), apatite(?), zeolite(?), carbonate, pigeonite(?), and subcalcic augite in an extremely fine-grained smectite base that may have been originally glass. In addition, there are brown ovoid spherulites with microcrystalline radial structures.</p> <p>Plagioclase phenocrysts, up to 5.5 x 3 mm maximum size, increase from less than 0.5% down to 58 cm depth, to 1% in the 60 to 110 cm interval, and 2% from 113 to 148 cm. The 2% represents a definite increase above the normal range of fluctuation of plagioclase phenocryst abundance, which rarely exceeds 1%. The bottom 35 cm appear to be part of a cumulate zone in the sense of an increased volume percentage of phenocrysts, but without development of cumulus textures.</p> <p>In higher sections in Core 3 and in this section, down to about 110 cm, olivine phenocrysts, where present, are pseudomorphed by blue-green smectite. From 110 to 148 cm, they are fresh to largely fresh and light bottle green in color, except in the 3 cm altered brown zone at the bottom.</p> <p>Sparse vugs occur in the interval 35 to 41 cm and are lined by blue-green botryoidal smectite.</p>
25	1					
	2					
50	3					
	4					
75	5					
100	6					
125	7					
150	8					
			PHOTO MISSING			



Site 319 Hole A Core 3 Section 6						
Centimeters from Top of Section	Piece Number	Graphic Representation	Section Photograph	Thin Sections	Special Areas	Description
0		VOID				
1	1					<p>Styrofoam spacers, each about 2 cm wide, separate pieces of core that are not part of a continuous core segment. An unknown amount of basalt is missing from the places where the styrofoam has been added.</p> <p>This section belongs entirely to the cooling unit, the top of which was penetrated in the lower part of 319A-3-5. It coarsens slowly but progressively downward from medium-grained basalt to coarse and very coarse-grained, variolitic to subophitic basalt, and verges on fine-grained subophitic diabase in the lowest part of the section. From 10 to 65 cm and 117 to 149 cm the rocks are mixtures of fresh dark gray and altered dark brownish gray rocks distributed in a manner which indicated that they are pieces of blocks bounded by widely spaced joints.</p> <p>Phenocrysts of olivine and plagioclase form uniformly about 1% from 10 to 130 cm, except in the intervals 95 to 99 cm, with about 2%, and 101 to 116 cm, with 0.5% or fewer. The interval 130 to 149 cm, with about 3 to 4% phenocrysts, appears to be a cumulate zone, and may be complementary to the depleted interval from 101 to 116 cm. The maximum size of plagioclase ranges from 2 x 1.5 to 5 x 3 mm from 10 to 130 cm, and up to 6 x 5 mm in the cumulate zone. A 5.5 x 2.5 mm crystal from the interval 143 to 149 cm has the composition An_{71-82}, mainly An_{73-78} (Tsuboi method). Olivine phenocrysts are commonly replaced by blue-green or dark green smectite, with carbonate in some cases. Fresh olivine from the interval 119 to 130 cm has the composition Fo_{86-87} ($Ny=1.679$ or slightly less).</p> <p>Round vesicles are sometimes filled with green smectite, particularly in the 10 to 49 cm and 111 to 116 cm intervals. Irregular holes up to 8 mm maximum dimension occur in the interval 79 to 93 cm. They are lined by Fe-oxide, tan to brown smectite and calcite.</p> <p>Veins include brown, yellowish brown, greenish brown, red-brown, red, greenish yellow, yellow green, green, and blue green smectite, and carbonate. The various smectite colors occur erratically with depth, varying with the local freshness of the host rock. Where vein carbonate was identified in oils; it was always calcite. A carbonate with high refractive indices, observed in the groundmass of a thin section taken at 145 to 147 cm, may be siderite.</p>
25	2				43	
50	3					
	4					
	5					
75	6					
	7					
	8					
100	9					
	10					
	11				115	
125	12					
	13					
	14				146	
150			PHOTO MISSING			

Site 319 Hole A Core 4 Section 1						
Centimeters from Top of Section	Piece Number	Graphic Representation	Section Photograph	Thin Sections	Special Areas	Description
0						<p>Styrofoam spacers, each about 2 cm wide, separate pieces of core that are not part of a continuous core segment. An unknown amount of basalt is missing from the places where the styrofoam has been added.</p> <p>Fresh, gray, fine-grained diabase was recovered fairly well intact, but subsequently parted into several additional pieces along veins and joints. Recovery appears to have been good. The diabase contains 4 to 5% phenocrysts of olivine and plagioclase and appears to be a continuation of the cumulate zone penetrated in the lower part of 319A-3-6. The olivine is fresh except for green smectite along cracks.</p> <p>Veins are composed of green and brown smectite, Fe-oxide and carbonate. In the interval 111 to 120 cm, a vein of smectite, which dips about 70°m is brown and oxidized in its lower part and green above. A flat-lying green smectite vein which intersects the steep one near the fairly sharp green-brown contact (but on the green side of the contact) is unoxidized and the host diabase adjacent to the oxidized parts of the steep vein shows no brown Fe staining. Evidently, the steep vein was a channel of relatively high permeability for oxidizing solutions. The sharp oxidation front suggests that the oxygen entered by diffusion rather than bulk flow.</p> <p>One vein of green smectite passes next to or through a fresh olivine phenocryst which is altered no more than others more distant from veins. Evidently, the alteration of olivine to green smectite was a diffusion-controlled process that occurred in close proximity to deposition of similar smectite in the doubtlessly more permeable joints without being notably influenced.</p>
25						
50		VOID				
75						
95	1					
98	2					
102	3					
105	4	BAG				
108	5 & 6					
112	7					
118						
125						
145	8					
150						

Site 319 Hole A Core 5 Section 1					
Centimeters from Top of Section	Piece Number	Graphic Representation	Section Photograph	Thin Sections	Special Areas
0					
		VOID	PHOTO MISSING		Styrofoam spacers, each about 2 cm wide, separate pieces of core that are not part of a continuous core segment. An unknown amount of basalt is missing from the places where the styrofoam has been added.
	1				
25	2	BAG			From 17 to 115 cm the rock grades erratically from fine-grained diabase to coarse-grained basalt, below which, from 117 to 138 cm, it grades progressively from coarse- to medium- to fine-grained basalt.
	3				
	4				Phenocrysts vary from less than 0.5% to 2% in abundance in the interval 17 to 127 cm, but are generally about 1%. From 129 to 138 cm, near the boundary of the cooling unit, there are fewer than 0.5% phenocrysts. Plagioclase phenocrysts reach maximum sizes of about 3.5 x 2.5 and 4 x 1 mm down to 42 cm depth. Below that there are scattered ones reaching sizes of 8 x 2, 8 x 4, and 6 x 5 mm down to 108 cm; the large ones may have sunk from higher in the unit. From 108 to 138 cm the largest crystal observed was 4.5 x 2.5 mm and generally they are smaller than 2 x 1 mm. Olivine phenocrysts are wholly replaced by yellow and red smectite in the brownish gray rock from 17 to 24 cm, and partly to wholly by blue-green smectite in the fresh gray rock from 34 to 65 cm. The proportion of fresh olivine increases generally with depth in this interval. From 65 to 108 cm fresh olivine is common. From 108 to 138 cm extensive to complete alteration to smectite is again observed, the smectite being blue-green in the fresh gray rock down to 129 cm (where it may rarely enclose a sulfide grain), and red in the altered brownish gray rock below that. Fresh olivine from the interval 34 to 42 cm has a positive 2V and Ny very near 1.680, indicating a composition of Fo ₈₆₋₈₇ .
50	5				
	6				
	7				
75	8				
	9				Veins and joints are locally uncommon or absent, as in the interval from about 50 to 92 cm. Where present, the veins include yellow, brown, and red smectite and Fe-oxide in altered rock; and green and blue-green smectite and sulfide in fresh rocks. Carbonate occurs in both types of rock and, where identified, is generally aragonite, though calcite may be present as well.
100	10 & 11				
	12 & 13				
125	14	BAG			The deepest interval (141 to 148 cm) is assigned, along with Core 6 and the uppermost part of Core 7, to a sequence of thin flow units discussed more fully under Core 6.
	15				
150					

Site 319 Hole A Core 6 Section 1					
Centimeters from Top of Section	Piece Number	Graphic Representation	Section Photograph	Thin Sections	Special Areas
0					
25		VOID			<p>Styrofoam spacers, each about 2 cm wide, separate pieces of core that are not part of a continuous core segment. An unknown amount of basalt is missing from the places where the styrofoam has been added.</p> <p>The small, highly abraded pieces of core in this section, most of which cannot be confidently oriented as to top and bottom, vary irregularly from aphanitic, through fine- to medium- and coarse-grained basalt. Ten thin sections of holocrystalline rock, eight of them from Core 6 and one each from the lowest interval of 319A-5-1 (141-148 cm) and the highest from 319A-7-1 (18 to 22 cm) show seven reversals of grain size. These data are interpreted to mean that as many as five cooling units, probably pillows, were penetrated with very poor recovery and without any recovery of glassy selvage.</p>
50					<p>The rocks contain 0.5% to 1% phenocrysts, among which the largest plagioclases observed range from 2.5 x 2 up to 4.5 x 4 and 5 x 2.5 mm. Olivine phenocrysts are fresh to partly to wholly altered. In the interval 145 to 147 cm some olivines contain ovoid inclusions of very fine-grained basalt which were probably liquid inclusions trapped by the growing crystals. The alteration products are Fe-oxide and smectites with variable colors which include brown, red, yellow, greenish yellow, and, rarely, dark green to blue. In brown altered rocks, the olivine is converted almost exclusively to earthy red Fe-oxide, rarely with a light colored smectite rim. In the adjacent fresh rock yellow, green or blue smectite pseudomorphs occur.</p>
75	1				77
	2				
	3	SEVERAL PIECES			85
	4				93
100	5				
	6				109
	7				
125	8				
	9				
	10				
150	11				41
					<p>Tiny holes in the piece from the interval 116 to 120 cm contain yellow-tan and blue smectite. Veins include yellow, brown, red, blue and yellowish white smectite, Mn-oxide, Fe-oxide, and carbonate. The Fe-oxide in veins in the interval 122 to 127 cm has an ochre streak and may be goethite. Carbonate veins are uncommon (seen only in the interval 100 to 113 cm), and, where examined in index oils, appear to be calcite. Minor aragonite may be present but that is uncertain.</p>

Site 319 Hole A Core 7 Section 1						
Centimeters from Top of Section	Piece Number	Section Photograph	Graphic Representation	Thin Sections	Special Areas	Description
0						<p>Styrofoam spacers, each about 2 cm wide, separate pieces of core that are not part of a continuous core segment. An unknown amount of basalt is missing from the places where the styrofoam has been added.</p> <p>This core recovered small pieces of fresh, dark gray to altered dark brownish gray basalt that commonly had rotated and cannot be confidently reoriented. They grade in a general but not wholly regular way from medium- to coarse-grained basalt at 18 cm, to coarse-grained basalt from 31 to 47 cm, to coarse- to very coarse-grained basalt in the interval 47 to 141 cm, and finally to very-fine grained basalt in the interval 143 to 148 cm. All the pieces are tentatively assigned to a single cooling unit which seems unlikely in view of the fine grain size.</p> <p>Abundances of olivine and plagioclase phenocrysts are less than 0.5% to 1% from 18 to 51 cm, almost zero to 0.5% from 54 to 110 cm, 2% to 1.5% from 114 to 129 cm, and 1% from 131 to 148 cm. The interval 114 to 129 cm may be a cumulate zone complementary to the relatively depleted zone from 54 to 110 cm, and, if so, supports the idea that Core 7 represents essentially a single cooling unit. Olivine phenocrysts are up to 6 x 4 mm in size, but commonly much smaller. One from the interval 18 to 22 cm is Fo₈₆₋₈₇ (N_y=1.678 with +2V), another from 95 to 110 cm is Fo₈₇₋₈₈ (N_y slightly less than 1.677). Pseudomorphs after olivine are composed of yellow, red, brown, greenish yellow, green, blue-green, yellowish white, and white smectite, Fe-oxide, calcite, and minor aragonite.</p> <p>A vesicle (1.3 mm in diameter) and irregular elongate holes are seen in the interval 38 to 45 cm. The holes contain red smectite linings, and some contain aragonite in addition.</p> <p>Veins are composed of yellow, red, red-brown, brown, orange-brown, blue, greenish-yellow, green and blue-green smectite, Fe-oxide, calcite, aragonite, and phillipsite(?). The green and blue-green smectites occur, along with similarly colored smectite pseudomorphs after olivine, in fresh gray rocks and altered brown rocks.</p>
		VOID				
	1					
25	2					
	3					
	4				44	
50	5					
	6				60	
	7					
75	8					
	9				84	
	10					
100	11-15					
	16				10	
	17				19	
125	18					
	19					
150	20				47	